

**SYNTHESIS AND CHARACTERIZATION OF COMPOSITE
POLYMERIC MEMBRANES FOR PROTON EXCHANGE
MEMBRANE (PEM) FUEL CELL APPLICATIONS**

BY

Mohd. Irfan Ahmad

A Thesis Presented to the
DEANSHIP OF GRADUATE STUDIES

KING FAHD UNIVERSITY OF PETROLEUM & MINERALS

DHAHRAN, SAUDI ARABIA

In Partial Fulfillment of the
Requirements for the Degree of

MASTER OF SCIENCE

In

CHEMICAL ENGINEERING

MARCH, 2005

**KING FAHD UNIVERSITY OF PETROLEUM & MINERALS
DHAHRAN 31261, SAUDI ARABIA**

DEANSHIP OF GRADUATE STUDIES

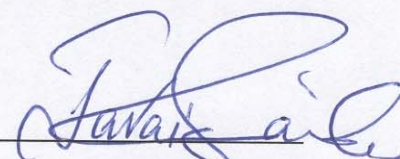
This thesis, written by

Mohd. Irfan Ahmad

Under the direction of his Thesis Advisor and approved by his Thesis Committee, has been presented to and accepted by the Dean of Graduate Studies, in partial fulfillment of the requirements for the degree of

MASTER OF SCIENCE IN CHEMICAL ENGINEERING

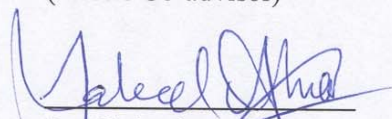
Thesis Committee



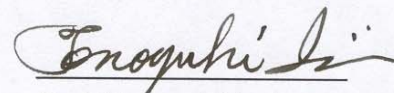
Dr. S. M. Javaid Zaidi
(Thesis Advisor)



Dr. S. U. Rahman
(Thesis Co-advisor)



Dr. Shakeel Ahmad
(Member)



Prof. Tomoyuki Inui
(Member)



Dr. Kevin F. Loughlin
(Member)



Prof. Mohammed B. Amin
(Department Chairman)



Dr. Mohammed A. Al-Ohali
(Dean of Graduate Studies)

5/27/5/05

Date

31-5-2005

ACKNOWLEDGEMENT

In the name of Allah, the most beneficent, the most merciful

All praises are due to Allah (SWT) for his kindest blessings on me and all the members of my family. I feel privileged to glorify his name in sincerest way through this small accomplishment. I ask for his blessings, mercy and forgiveness all the time. I sincerely ask him to accept this meager effort as an act of worship. May the peace and blessings of Allah be upon his dearest prophet, Muhammad (PBUH).

With deep sense of gratitude and reverence, I would like to express my sincere thanks to my thesis advisor, Dr. S. M. Javaid Zaidi for his motivational guidance, help and excellent cooperation in supervising this research work. I am also very grateful to my co-advisor, Dr. S U Rahman for his immense help, continuous inspiration and hours long friendly discussions. I owe special thanks to Dr. Shakeel Ahmad, Research Engineer III and one of my thesis committee member for his continuous guidance & friendly assistance during the course of this work. It is really a privilege to work with him. Special and sincere thanks goes to my learned thesis committee, Prof. Tomoyuki Inui, who is the master of the game called 'catalysis' and Dr. Kevin F. Loughlin, who provided immense help in organizing my work.

I am grateful to chairman of Chemical engineering department Dr. Mohammed B. Amin for his kind help and cooperation. I am also thankful to all faculty and staff members for their kind support and continuous cooperation. The support provided by Chemical Engineering department of King Fahd University of Petroleum & Minerals (KFUPM) is greatly acknowledged. My sincere appreciation goes to CRP, KFUPM-RI for allowing me to work in their excellent laboratories. I would also like to thank the laboratory staffs and technicians of Chemical Engineering department as well as CRP, KFUPM-RI. Special thanks go to Mr. Mahdi, Mr. Mariano, Mr. Mofiz, Mr. K. Alam, Mr. A. Rashid and Mr. Kamal for their help and service during the experimental works.

Finally I would like to thank all my Relatives & friends for their blessings. Yaqoob, Fareed, Mehboob basha, Nafees, Arif bhai, Ashraf Ali, Faiz Azim, Wasif, Shabi hashmi, Ilyas bhai, Ishaq bhai and Nadeem who are like brothers to me, deserve special mention at this juncture. Thanks are also due to my brother in law Ayyub bhai and sister Zeenat with little Sana, Sumaiyah and Sarah who are near to my heart. Special thanks are due to all 903 building friends, specially 44 flat group & all chemical RA's & my room partner.

Last but not least, I humbly offer my sincere thanks to my parents for their constant inspiration and incessant prayers. I owe a lot to my brothers Rizwan bhai (*Bhaiji*), Furkan (*Widhayak*) and Imran with other family members for their unrequited support, encouragement and prayers.

(Mohd. Irfan Ahmad)

*This work is dedicated
to my beloved parents
who taught me to
believe in myself*

CONTENTS

ACKNOWLEDGEMENT	ii
Table of contents	iv
List of Tables	vi
List of Figures	vii
Abstract.....	xi
Abstract (Arabic).....	xii
Chapter 1	1
Introduction.....	1
1.1 Membrane materials	3
1.2. Motivation for current work	4
1.3. Objectives and methodology	5
1.4. Fuel cells: overview.....	8
1.4.1. Brief history of fuel cells	8
1.4.2. About fuel cells.....	8
1.4.3. Why fuel cells?	11
1.4.4. Thermodynamics involved	12
1.4.5. PEM fuel cells applications	14
1.4.6. Fuel cell challenges.....	15
1.5. Zeolites	16
1.5.1. Definition & classification.....	16
1.5.2. Zeolites conductivity	17
1.6. Solid acids: Heteropolyacids	19
1.6.1. Keggin structure of HPAs.....	19
1.6.2. Solid acids conductivity.....	21
1.7. MCM41	22
Chapter 2	24
Literature Review	24
2.1. Composite membranes	25
2.1.1. Modification of Nafion [®] membranes	26
2.1.2. Composite membranes from the inorganic modification of the polymer matrix.....	31
2.1.3. Composite membranes from in-situ hybridization of organic/ inorganic components	36
Chapter 3	42
Experimental Methods	42
3.1. Materials and chemicals	42
3.2. Synthesis of Materials	43
3.2.1. Synthesis of proton conducting powders.....	43
3.2.2. Leaching study of prepared powders.....	45

3.2.2.1. Thermal Leaching:	45
3.2.2.2. Flow Leaching	45
3.3. Membrane preparation	47
3.3.1. Solution casting method	47
3.4. Proton conductivity measurements by impedance spectroscopy	50
3.5. Methods of characterization	52
3.5.1 Atomic absorption spectrophotometry	52
3.5.2. Proton conductivity measurement by impedance spectrometry	52
3.5.3. Water uptake of membranes	53
3.5.4. Fourier transform infra red (FTIR)	54
3.5.5. X-ray diffraction	54
3.5.6. Scanning electron microscopy (SEM)	55
Chapter 4	56
Results and discussion: Solid proton conductors	56
4.1. Development of solid proton conductors	56
4.1.1. Flow Study	56
4.1.2. Proton conductivity through Impedance Spectrometry	62
4.1.3. FTIR Analysis	73
4.1.4. XRD Analysis	80
4.1.5. SEM Technique	87
Chapter 5	92
Results and discussion: Composite polymeric membranes	92
5.1. Composite membranes development	92
5.1.1. Proton conductivity studies	92
5.1.2. Water uptake measurements	110
5.1.3. FTIR Analysis	119
5.1.4. X-Ray Diffraction Analysis	127
5.1.5. Scanning Electron Microscopy	134
Chapter 6	136
Conclusions	136
6.1. Development of proton conducting solids	136
6.2. Development of composite membranes	138
Recommendations	139
APPENDIX A	141
PROTON CONDUCTIVITY MEASUREMENTS	141
APPENDIX B	144
RECIPE FOR PREPARATION OF HETEROPOLYACIDS LOADED SOLID PROTON CONDUCTORS	144
References	146

List of Tables

Table 1-1 Different types of existing fuel cells.....	10
Table 4-1 Amount of tungsten and molybdenum leached out through flow experiments	59
Table 4-2 Flow study data for the amounts of tungsten and molybdenum leached out from TPA and MPA loaded MCM41	59
Table 4-3 Resistances and conductivity values of composite powder samples done and analyzed at ambient conditions.....	63
Table 4-4 Resistances and conductivities values of powder samples with varying percentages of water (weight percent).....	66
Table 4-5 Resistances and conductivity values of composite powder samples analyzed at ambient conditions.....	70
Table 4-6 Proton conductivity values of solid powders synthesized from MCM41 with MPA and TPA for different wt. percentages of water.....	70
Table 5-1 Proton conductivities of the prepared composite membranes at room temperature with the help of Y-zeolite loaded with TPA and MPA into SPEEK	96
Table 5-2 Proton conductivities of the prepared composite membranes at room temperature with the help of MCM41 loaded with TPA and MPA into SPEEK	96
Table 5-3 Proton conductivity values for various composite membranes prepared form Y-zeolite and heteropolyacids at varying temperatures from 20 to 140 °C.....	104
Table 5-4 Proton conductivity values for various composite membranes prepared form MCM41 and heteropolyacids at varying temperatures from 20 to 140 °C.....	104
Table 5-5 water uptake percentages for composite membranes from SPEEK with TPA & MPA loaded Y-zeolite	112
Table 5-6 Water uptake percentages for composite membranes from SPEEK with TPA & MPA loaded MCM41	112

List of Figures

Figure 1-1 Basic description of a PEM Fuel cell operation.....	3
Figure 1-2 Framework structure of Faujasite family Y-zeolite	17
Figure 1-3 Keggin structure of HPA.....	20
Figure 1-4 Schematic representation of $[PW_{12}O_{40}]^{-3}$ anion	21
Figure 1-5 Pore structure of MCM41	23
Figure 2-1 General chemical structure of Nafion [®] membranes.....	27
Figure 2-2 Chemical structure of SPEEK [48]	32
Figure 3-1 Synthesis of solid proton conductors from Y-zeolite and MCM41 with HPAs	44
Figure 3-2 Set-up for flow leaching study	46
Figure 3-3 Conductivity measurement cell.....	51
Figure 4-1 Leaching plots for heteropolyacids loaded Y-zeolite with respect to time	60
Figure 4-2 Leaching plots for heteropolyacids loaded MCM41 with respect to time	61
Figure 4-3 Variation of proton conductivity of Y-zeolite with increasing percentage of TPA.....	64
Figure 4-4 Variation of proton conductivity of Y-zeolite with increasing percentage of MPA.....	64
Figure 4-5 Proton conductivity variation with increasing water content for (a) pure Y-zeolite; (b) Y-zeolite+40% TPA and (c) Y-zeolite+50% TPA.....	68
Figure 4-6 Proton conductivity variation with increasing water content for (a) pure Y-zeolite; (b) Y-zeolite+40% MPA and (c) Y-zeolite+50% MPA.....	68
Figure 4-7 Proton conductivity vs. wt. percentage of water plot for (a) Pure MCM41; (b) MCM41+40 % TPA and (c) MCM41+50 % TPA.	72
Figure 4-8 Proton conductivity vs. wt. percentage of water plot for (a) Pure MCM41; (b) MCM41+40 % MPA and (c) MCM41+50 % MPA.	72

Figure 4-9 FT-IR data comparison for pure Y-zeolite; pure TPA and Y-zeolite+40% TPA.....	76
Figure 4-10 FT-IR data comparison for pure Y-zeolite; pure MPA and Y-zeolite+50%MPA.....	77
Figure 4-11 FT-IR data comparison for pure MCM41; pure TPA and MCM41+40%TPA.....	78
Figure 4-12 FT-IR data comparison for pure MCM41 (top); pure MPA (middle) and MCM41+40%MPA (bottom).	79
Figure 4-13 XRD data comparison for pure Y-zeolite (top); pure TPA (middle) and Y-zeolite+50%TPA (bottom).....	83
Figure 4-14 XRD data comparison for pure Y-zeolite (top); pure MPA (middle) and Y-zeolite+50 % MPA (bottom).....	84
Figure 4-15 XRD plots for pure MCM41 (top); pure TPA (middle) and MCM41+50 % TPA.....	85
Figure 4-16 XRD data comparison for (a) pure MCM41; (b) pure MPA; (c) MCM41+50 % MPA.....	86
Figure 4-17 SEM images of pure Y-zeolite (a), pure TPA (b), pure MPA (c) and pure MCM41 (d).	90
Figure 4-18 SEM images of Y-zeolite+50 % TPA (a), Y-zeolite+50 % MPA (b), MCM41+50 % TPA (c) and MCM41+50 % MPA (d).....	91
Figure 5-1 Proton conductivity comparison of SPEEK+[Y-zeolite+40 % TPA] and SPEEK+[Y-zeolite+50 % TPA] at ambient temperature.	99
Figure 5-2 Proton conductivity comparison of SPEEK+[Y-zeolite+40 % MPA] and SPEEK+[Y-zeolite+50 % MPA] at ambient temperature.	99
Figure 5-3 Proton conductivity comparison of SPEEK+[MCM41+40 % TPA] and SPEEK+[MCM41+50 % TPA] at ambient temperature.....	100
Figure 5-4 Proton conductivity comparison of SPEEK+[MCM41+40 % MPA] and SPEEK+[MCM41+50 % MPA] at ambient temperature.	100
Figure 5-5 Proton conductivity trends of SPEEK with various wt. percentages of BPO ₄ at ambient temperature [48]......	101

Figure 5-6 Proton conductivity plots for SPEEK(60 %)+[Y-zeolite+40 % TPA](40 %) and SPEEK(60 %)+[Y-zeolite+50 % TPA](40 %) at varying temperatures from 20 to 140 °C.	107
Figure 5-7 Proton conductivity plots for SPEEK(60 %)+[Y-zeolite+40 % MPA](40 %) and SPEEK(60 %)+[Y-zeolite+50 % MPA](40 %) at varying temperatures from 20 to 140 °C.	107
Figure 5-8 Proton conductivity plots for SPEEK(60 %)+[MCM41+40 % TPA](40 %) and SPEEK(60 %)+[MCM41+50 % TPA](40 %) at varying temperatures from 20 to 140 °C.	108
Figure 5-9 Proton conductivity plots for SPEEK(60 %)+[MCM41+40 % MPA](40 %) and SPEEK(60 %)+[MCM41+50 % MPA](40 %) at varying temperatures from 20 to 140 °C.	108
Figure 5-10 Proton conductivity plots for SPEEK with 10 and 20 wt. percent of ZrPO ₄ at varying temperatures from 80 to 140 °C [81].	109
Figure 5-11 Water uptake plots for SPEEK+[Y-zeolite+40 % TPA] and SPEEK+[Y-zeolite+50 % TPA]	116
Figure 5-12 Water uptake plots for SPEEK+[Y-zeolite+40 % MPA] and SPEEK+[Y-zeolite+50 % MPA]	116
Figure 5-13 Water uptake plots for SPEEK+[MCM41+40 % TPA] and SPEEK+[MCM41+50 % TPA]	117
Figure 5-14 Water uptake plots for SPEEK+[MCM41+40 % MPA] and SPEEK+[MCM41+50 % MPA]	117
Figure 5-15 Water uptake plots for poly(arylene ether sulfone) (PES) with various percentages of HPA	118
Figure 5-16 Proton conductivity plots with various water uptake percentages for SPEEK with various percentages of BPO ₄	118
Figure 5-17 FTIR data comparison for (a) pure SPEEK; (b) Y-zeolite+50%TPA and (c) SPEEK(60%)+[Y-zeolite+50%TPA](40%).	123
Figure 5-18 FTIR data comparison for (a) pure SPEEK; (b) Y-zeolite+50%MPA and (c) SPEEK(60%)+[Y-zeolite+50%MPA](40%).	124
Figure 5-19 FTIR data comparison for (a) pure SPEEK; (b) MCM41+50%TPA and (c) SPEEK(60%)+[MCM41+50%TPA](40%).	125

Figure 5-20 FTIR data comparison for (a) pure SPEEK; (b) MCM41+50%MPA and (c) SPEEK(60%)+[MCM41+50%MPA](40%).	126
Figure 5-21 XRD data comparison for (a) Pure SPEEK; (b) Y-zeolite+50 % TPA and (c) SPEEK+[Y-zeolite+50 % TPA](30%).	130
Figure 5-22 XRD data comparison for (a) Pure SPEEK; (b) Y-zeolite+50 % MPA and (c) SPEEK+[Y-zeolite+50 % MPA](30%).....	131
Figure 5-23 XRD data comparison for (a) Pure SPEEK; (b) MCM41+50 % TPA and (c) SPEEK+[MCM41+50 % TPA](40%).	132
Figure 5-24 XRD data comparison for (a) Pure SPEEK; (b) MCM41+50 % MPA and (c) SPEEK+[Y-zeolite+50 % MPA](30%).	133
Figure 5-25 SEM images of pure SPEEK (a), SY-T2 (b), SY-M1 (c), SM41-T1 (d) and SM41-M2 (e)	135

Abstract

NAME OF STUDENT	Mohd. Irfan Ahmad
TITLE OF STUDY	Synthesis and Characterization of Composite Polymeric Membranes for Proton Exchange Membranes (PEM) Fuel cell Applications.
MAJOR FIELD	Chemical Engineering
DATE OF DEGREE	March 2005

This thesis presents the synthesis and characterization of novel composite membranes for medium temperature proton exchange membrane (PEM) fuel cells. Novel solid proton conductors have been prepared and characterized prior to the development of composite membranes. Two sole new classes of solid proton conductors are prepared from the incorporation of heteropolyacids onto Y-zeolite and MCM41 separately. Proton conductivities of solids are measured using impedance spectroscopy (IS) technique. These solids are also characterized using FTIR, XRD and SEM techniques.

Composite membranes are prepared by blending various weight percentages of these solid proton conductors into sulfonated polyether ether ketone (SPEEK) polymer matrix. Proton conductivities as well as water uptakes were measured for the prepared membranes. The membranes are found to be highly proton conductive at room temperature and demonstrate appreciably high values at high temperatures (up to 140 °C). Highest conductivities of the order of 10^{-2} S/cm are measured for these composite membranes. The prepared composite membranes are also characterized using FTIR, XRD and SEM techniques. Characterization techniques confirmed uniform loading of solid inorganic material into the polymer matrix. Hence, these proposed membranes have the potential to be considered as candidates for medium temperature fuel cell applications.

Master of Science
King Fahd University of Petroleum & Minerals
Dhahran, Saudi Arabia
March 2005

ملخص الرسالة

اسم الطالب:	محمد عرفان أحمد
عنوان الرسالة:	تصنيع ووصف خصائص أغشية بوليمرية مركبة لتطبيقات خلية الوقود ذات أغشية التبادل البروتوني (PEM).
التخصص:	هندسة كيميائية
تاريخ التخرج:	مارس / 2005م

تعرض هذه الرسالة تصنيع ووصف أغشية مركبة جديدة لخلايا الوقود ذات غشاء التبادل البروتوني عند درجات حرارة متوسطة. تم تحضير ووصف موصلات بروتونية صلبة جديدة قبل إنشاء الأغشية المركبة. تم تحضير فنتان جديدتان مفردتان من الموصلات البروتونية الصلبة من خلال دمج أحماض مبلمرة غير متجانسة بمركب زيولايت-Y و مركب MCM-41 ، كل على حدة. تم قياس الموصلات البروتونية للمواد الصلبة باستخدام تقنية مطياف المعاوقة الظاهرية. أيضا تم وصف خصائص هذه المواد الصلبة باستخدام تقنيات مطياف الأشعة تحت الحمراء (FTIR)، حيود أشعة اكس (XRD) ومجهر المسح الالكتروني (SEM).

تم تحضير الأغشية المركبة بواسطة مزج نسب وزنية مختلفة من هذه الموصلات البروتونية الصلبة مع بوليمر سلفونات بولي ايثر ايثر كيتون (SPEEK). تم قياس الموصلية البروتونية إضافة إلى مقدار امتصاص الماء للأغشية المحضرة. وجد أن الأغشية تكون موصلة بشكل كبير للبروتون عند درجة حرارة الغرفة، كما أنها أظهرت قيما عالية للموصلية بشكل ملفت عند درجات حرارة عالية (تصل إلى 140 درجة مئوية). أعلى موصليات من الدرجة (10^{-2} S/cm) تم قياسها لهذه الأغشية المركبة. أيضا تم وصف الأغشية المركبة المحضرة باستخدام تقنيات مطياف الأشعة تحت الحمراء (FTIR)، حيود أشعة اكس (XRD) ومجهر المسح الالكتروني (SEM). تقنيات الوصف أكدت وجود امتصاص منتظم للمادة الصلبة غير العضوية في البوليمر. لذلك فان هذه الأغشية المقدمة تمتلك إمكانية اعتبارها مرشحة لتطبيقات خلية الوقود عند درجة حرارة متوسطة.

ماجستير في العلوم
جامعة الملك فهد للبترول والمعادن
الظهران، المملكة العربية السعودية
مارس 2005

Introduction

Fuel cells are seen by many commentators as a solution to a whole range of environmental challenges, such as global warming and harmful levels of local pollutants, for instance those from cars in the urban environment. Fuel cells may also be able to provide economic benefits due to their high efficiency. Because of their potential to reduce the environmental impact and geopolitical consequences of the use of fossil fuels, fuel cells have emerged as tantalizing alternatives to combustion engines. Like a combustion engine, a fuel cell uses chemical fuel as its energy source; but like a battery, the chemical energy is directly converted to electrical energy, without an often messy and relatively inefficient combustion step [1-3]

Fuel cells are electrochemical devices that convert chemical energy of the reactants directly into electricity and heat with high efficiency. Electrochemical processes in fuel cells are not governed by Carnot's law and therefore their operation is simple and more efficient as compared to internal combustion (IC) engines. Furthermore, contrary to IC engines, the efficiency of fuel cells is not strongly dependent on operating power. High efficiency makes fuel cells an attractive option for a wide range of applications, including road vehicle power sources, distributed electricity and heat production, and even portable and mobile systems, such as consumer electronics, laptop computers, video cameras etc.

The fuel cell was invented in the first half of the 19th century, and many fundamental technological breakthroughs have been achieved during the past two decades. Presently fuel cell technology is maturing towards commercialization, but work still needs to be done in many fields [1]. For commercial applications, component materials need to be developed and optimized to improve performance and to lower the costs. Long-term testing has to be done to obtain information on fuel cell performance. Furthermore, as fuel cell research moves on from laboratory-scale single cell studies to the development of application-ready stacks, new in situ measurement methods are needed for characterization and diagnostics.

Recent improvements in fuel cell technology have sparked renewed and widespread interest in fuel cells for transportation and stationary applications [1]. One of the most important constituents of these fuel cells is the polymer electrolyte membrane which allows protons to pass through it but not the electrons. Fuel cells currently use PFI Nafion[®] membranes which exhibit a number of shortcomings to use them with optimum efficiency. This thesis is focused on the development and characterization of novel composite membranes for direct methanol fuel cells. The membrane functions twofold, it acts as the electrolyte which provides ionic communication between the anode and the cathode and also it serves as a separator for the two reactant gases. Optimized proton and water transport properties of the membrane and proper water management are crucial for efficient fuel cell operation. Dehydration of the membrane reduces proton conductivity and excess of water can lead to flooding of the electrodes, both conditions may result in poor cell performance. A typical schematic diagram of proton exchange membrane fuel cell is given below:

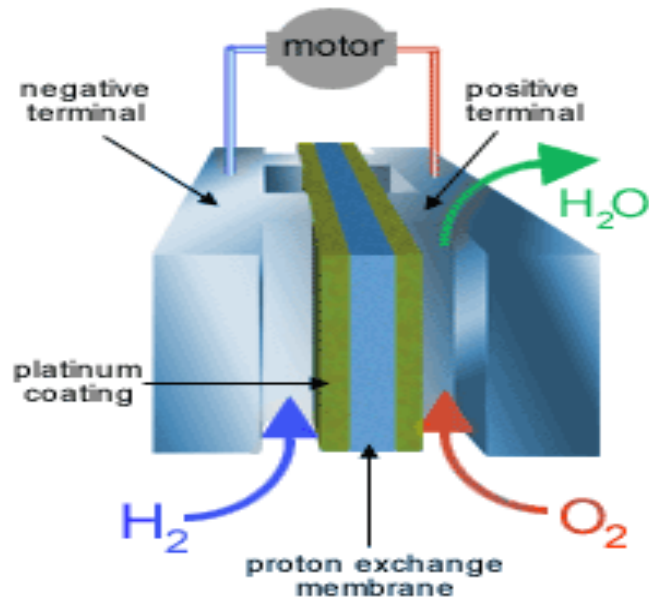


Figure 1-1 Basic description of a PEM Fuel cell operation

1.1 Membrane materials

Ever since the invention of ion exchange membranes as electrolyte for fuel cells in the 1950s, the challenge was on to find the ideal membrane material to withstand the harsh fuel cell operating environment. Since then numerous attempts have been made to optimize the membrane properties for application in fuel cells. The desired properties for use as a proton conductor in DMFC essentially include the following [4]:

1. Chemical and electrochemical stability in the cell operating environment (high resistance to oxidation, reduction and hydrolysis)
2. Mechanical strength and stability in the cell operating environment.
3. Chemical properties compatible with the bonding requirements of the membrane electrode assembly (MEA).

4. Extremely low permeability to reactant gases to minimize coulombic inefficiency.
5. High water transport to maintain uniform water content and to prevent localized drying.
6. High proton conductivity to support high currents with minimal resistive losses and zero electronic conductivity.
7. And last but not least is the production costs compatible with the application.

1.2. Motivation for current work

Until now PFI Nafion[®] membranes have been widely used and considered as most efficient proton exchange membrane for fuel cell. A literature search on Nafion[®] over the period 1990-2002 resulted in more than 1000 references [5]. However, Nafion[®] membranes have several problems, which act as an obstruction for its large scale commercialization. One of the most important of these factors is their cost. These membranes are very expensive and are in the range of 700-800 US \$/m². Another serious problem of Nafion[®] membrane is methanol crossover from anode to cathode area due to both diffusion and electro-osmotic drag. The diffusion coefficient for methanol in Nafion[®] is in the order 10⁻⁵ cm²/s [6]. This value is too high for long term use because it results in considerably decreased output voltage of the DMFC, brings down its performance and service life, besides the fuel loss. In addition, there is a problem of water balance in the anode area, associated with membrane dehydration during proton transportation, reducing its conductivity drastically to very low values. The polymer structure of Nafion[®] is not crosslinked, which reduces its stability in water methanol mixtures at elevated temperature. So, Nafion[®] membrane is not stable at temperature higher than 80 °C as it loses its water of hydration, hence, it cannot be

considered for use in high temperature fuel cell at 160-200 °C. Compositing the solid conducting material in a polymer matrix is one of the approaches suggested in the literature to improve the conductivity as well as the methanol permeation of the membranes.

Due to the above-mentioned limitations of the Nafion[®] membranes, researchers switched their attention towards the development of alternate membranes and since then many significant studies have been reported in the literature. In a recent study, Zaidi et al. reported the preparation of composite membranes with the help of sulfonated polyether ether ketone (SPEEK) polymer, which has been studied for their electrochemical properties such as conductivity and morphology and subjected to other membrane characterizations [7]. But thermal stability and glass transitions behavior as a result of adding the composite components into SPEEK polymers were not studied extensively. Since then extensive research is going on to find a suitable replacement for commercial Nafion[®] membranes for use in fuel cells. This work is a stepping stone towards the current quest in the field of membrane development.

1.3. Objectives and methodology

Although different types of composite membranes development have been reported, they still do not conform to the ideal membrane characteristics desired for the application in fuel cell systems. So still a lot of work needs to be done in this fast emerging field of fuel cell membranes. In the current work, a new series of composite membranes have been developed which are made up of

- (a) Heteropolyacids (namely tungstophosphoric acid & molybdophosphoric acid) loaded Y-zeolite blended with sulfonated polyether ether ketone (SPEEK) polymer and
- (b) Heteropolyacids loaded MCM41, blended with the sulfonated polyether ether ketone (SPEEK) polymer.

This novel idea is based on the fact that zeolites have very large pores as is the case with the MCM41. These two materials have uniform pore sizes and high thermal stability. Actually if we are able to insert some highly conductive materials (which in our case are heteropolyacids) into the pores of these porous materials then the resulting material will have a high conductivity. This highly conductive material will then be blended with the sulfonated polyether ether ketone to get the composite membrane. The conductivity of zeolites is well known and is of the order of 10^{-5} S/cm [8]. Although MCM41 does not have any significant conductivity, its highly stable structure at high temperatures provides a strong basis to use it as a base component in the composite membranes. Since currently used membranes in fuel cells are not stable at high temperature, it is expected that MCM41 will provide sufficient stability to the membrane at relatively high temperatures. In addition its large and uniform pore sizes are ideal for heteropolyacid incorporation.

Heteropolyacids which have been used in the loading of Y-zeolite and MCM41 have very high conductivity, typically of the order of 0.1-0.2 S/cm. Although there are some other conductive solid materials available which have been used in preparing membranes, e.g. zirconium phosphate and boron phosphate etc., but heteropolyacids, with keggin-type

structure are unique and more promising over other inorganic conducting materials. The keggin structure demonstrates activity as in both acidic and redox forms. In addition, they include heteropolyanions $XM_{12}O_{40}^{\xi-8}$ where X is the central atom (P, Si etc.), ξ is its oxidation state and M is the metal ion (Mo, W, V etc.). The keggin anion is the primary structural unit and consists of 12-edge sharing octahedra MO_6 , grouped into four M_3O_{13} units, surrounding a central tetrahedron XO_4 . There are four different types of oxygen atom present in the keggin anion unit $[PW_{12}O_{40}]^{-3}$:

- (1) Four O_i (internal oxygen connecting P and W)
- (2) 12 O_e (edge-sharing oxygen connecting W atoms)
- (3) 12 O_c (corner sharing oxygen connecting W_3O_{13} units)
- (4) 12 O_t (terminal oxygen at the vertex)

The idea proposed here is based on the high conductivities of heteropolyacids and high thermal and structural stability of Y-zeolite & MCM41. The incorporation of heteropolyacids into the structures of Y-zeolite and MCM41 has been applied successfully to prepare the catalysts for liquid phase reactions [9]. Since it is desirable for composite membrane to have high proton conductivity and thermal stability at high operating temperatures, the findings of this thesis should be proved pivotal to the development of composite membranes for medium temperature as well as direct methanol fuel cells.

1.4. Fuel cells: overview

1.4.1. Brief history of fuel cells

Although fuel cells are only now beginning to gain commercial significance, the concept was first suggested as long ago as 1839. W. R. Grove was working on water electrolysis and reasoned that the reverse process should generate electricity. However, attempts to create a working fuel cell did not meet with any great success until Bacon developed a H₂/O₂ fuel cell with a potassium hydroxide electrolyte and nickel electrodes in the 1930s [10]. This led to the demonstration of a first industrial prototype in 1953.

NASA's interest in fuel cells as power sources for space applications gave another impetus to their development. Polymer electrolyte membrane fuel cells (PEMFCs) were used in the American GEMINI space program and alkaline fuel cells in the APOLLO missions. Their success in these programs motivated much further research, but high costs and problems in long term testing remained major obstacles. A breakthrough for PEMFCs came when Dupont de Nemours developed membranes of superior stability. Environmental concerns and progress in the technology reawakened interest and today high temperature fuel cells are being tested for stationary applications by the US military, and PEMFCs are used in buses in Chicago and Vancouver, in car prototypes, and in submarines [11].

1.4.2. About fuel cells

"A SHOCK WAS GIVEN WHICH COULD BE FELT BY FIVE PERSONS JOINING HANDS, AND WHICH WHEN TAKEN BY A SINGLE PERSON WAS PAINFUL"

Sir William Grove (1839)

Fuel cells are electrochemical devices that convert the chemical energy of the reactants directly into electricity and heat, without combustion as an intermediate step. There are similarities between fuel cells and primary batteries. Both systems have two electrodes separated by an electrolyte and electrical energy can be withdrawn from the cell reaction. Unlike batteries, in a fuel cell the fuel is supplied from an external source and it operates as long as it is supplied with fuel and oxidant. In addition, battery performance deteriorates when the charge level drops, whereas fuel cell operates at constant level as long as fuel is supplied. The six most common fuel cell types are

1. Polymer Electrolyte Membrane Fuel Cells (PEMFC)
2. Direct Methanol Fuel cells (DMFC),
3. Alkaline Fuel Cells (AFC),
4. Phosphoric Acid Fuel Cells (PAFC),
5. Molten Carbonate Fuel Cells (MCFC) and
6. Solid Oxide Fuel Cells (SOFC).

Direct Methanol Fuel Cell (DMFC), is the cell which is similar to PEMFC, except it uses methanol as the fuel directly on the anode instead of hydrogen or hydrogen rich gas. A detailed classification based on the electrolyte used is given as [\[12\]](#).

Table 1-1 Different types of existing fuel cells

Electrolyte	Temperature	Advantages	Disadvantages	Status
Alkaline	70-200 °C	High current & power densities, high efficiency	CO ₂ intolerance	Extensive field Testing
Proton Exchange Membrane	80-110 °C	High current & power densities, long operating Life	CO intolerance, water management noble catalyst	Field testing (kilowatt Scale) including prototype vehicles
Phosphoric acid	150-210 °C	Technologically well advanced	Relatively low efficiency, limited lifetime noble catalyst	Commercially Available
Molten Carbonate	550-650 °C	High efficiency, internal fuel processing, high grade waste heat	Electrolyte Instability, short operating life	Field testing (2 MW scale)
Solid oxide ceramic	1000-1100 °C	Internal fuel processing, high grade waste heat, long operating life, potential inexpensive	High operating temperature, limited thermodynamic efficiency, relatively low ionic conductivity	Laboratory testing (kilowatt scale)

Direct methanol fuel cell (DMFC) is gaining worldwide attention because it uses liquid fuel directly at anode, thus avoiding the need for reformer. DMFC is found to be handy in small scale applications. Consumer electronics is one of the pioneer field in which DMFC is used now quite frequently. Since DMFC uses conventional perfluorinated (PFI) membranes which are plagued by serious problem of methanol permeation through them, an alternative membrane is required with desired characteristics to complement the drawbacks incurred by membranes already in use.

1.4.3. Why fuel cells?

Fuel cells have several highly attractive characteristics. The efficiency of a fuel cell can be higher than the conventional energy conversion processes and the performance remains good even at partial loads. The only waste product is minute amounts of flue gases from oxidized fuel. Normally, the fuel is hydrogen and consequently, the product is water. Carbon dioxide may be present as well; if a hydrocarbon fuel is used. Fuel reformation adds the benefit of fuel flexibility, but multi-fuel reformer technology is still in early development stage [1].

Furthermore, the lack of moving parts in the energy converter and modular design make the maintenance easy and improves system reliability. High availability and endurance has been demonstrated with low temperature units and as a proof of endurance, it can be mentioned that no fuel cell power source in NASA's programs has yet failed. Due to the modular design and rapid response to load changes, fuel cell technology can be used in a wide range of applications, from portable electronics power sources to megawatt-scale power plants.

The operation of a fuel cell is silent compared to combustion engines due to the lack of moving parts. High power density makes them unique in operation. Low emission levels and low maintenance requirement, provides extra flexibility that is superior to many of the conventional energy production methods. Efficient and clean energy production processes are very interesting and of foremost importance due to the concern for the environment and earth's limited resources. In addition, fuel cells are expected to be economically viable once mass production begins, at least in the fields of distributed power generation and remote systems [1, 10].

1.4.4. Thermodynamics involved

A fuel cell is an energy conversion device that transforms the chemical energy of the reactants into electrical energy and heat. The fuel is not burnt in this process but oxidized electrochemically which fundamentally distinguishes fuel cells from heat engines. A heat engine works via the combustion of the fuel to generate heat which is subsequently transformed into mechanical work; heat is supplied at the higher temperature T_1 and rejected at the lower temperature T_2 . The laws of thermodynamics imply that the thermal efficiency of the heat engine η_{HE} , defined as the ratio of mechanical work produced to the amount of heat initially supplied at T_1 is constrained according to

$$\eta_{HE} \leq 1 - \frac{T_2}{T_1} \quad (4)$$

This relation is known as the Carnot limit. Since T_2 is always greater than zero, and T_1 is finite, the efficiency of heat engine can never be unity. Fuel cells do not suffer from this fundamental restriction because their operation does not require heat input. The maximum work that can be done by a fuel cell is given by the change in the Gibbs free energy, $-\Delta G$, in the oxidation reaction of fuel [1,10,12]. The energy content of the fuel cell is expressed in terms of its heating value which is the change in enthalpy, ΔH ; the efficiency of the fuel cell is therefore:

$$\eta_{FC} \leq \frac{\Delta G}{\Delta H} \quad (5)$$

which is not restricted by the Carnot limit. A hydrogen/oxygen fuel cell operating at 100 °C has a theoretical efficiency of 91 % based on the lower heating value (LHV) of hydrogen. In practice the efficiencies of both technologies i.e. the IC engines and the fuel cells, are much below their theoretical limits. In some of the current (non-optimized) fuel cell power generation systems, the overall system efficiency may be only 40 %. What makes the internal combustion engine inferior is not so much the Carnot limit but materials limitations that prevent it from operating at a temperature as high as the flame temperature of hydrogen. The operation of fuel cell is schematically represented in [Figure 1-1](#). It can be considered as the inverse of electrolysis. The fuel, molecular hydrogen, enters through the porous anode and reaches the electrode electrolyte interface, where it adsorbs on the surface of a catalyst and enters the electrolyte in ionized form, H^+ . After traversing through the electrolyte, oxidation takes place at the cathode and the product water is removed. The whole process requires an external electrical connection of the two electrodes to allow the electrons

involved in the reactions to pass from one side to the other. The electrical energy is dissipated in the external circuit [15].

1.4.5. PEM fuel cells applications

PEM Fuel cells are attractive option for a wide range of applications, including vehicle, power sources, distributed power and heat production, and even portable and mobile systems. At this moment automotive industry is the largest investor in the PEM fuel cell development. Many manufacturers have announced their commitment to introduce commercial fuel cell cars in near future.

Development of fuel cell engines for vehicles is catalyzed by striving for better efficiency and low emission vehicles. Most of the prototypes introduced so far operate directly on compressed hydrogen, but it is widely believed that first fuel cell powered passenger car will utilize on-board reforming. This will lower pollution emissions compared to internal combustion engines due to higher energy conversion efficiency. In addition, the only byproduct of the fuel reformation is carbon dioxide and there are virtually no sulfur or nitrogen oxide emissions. Direct hydrogen fuel cells cars do not produce polluting emissions. Stationary power generation applications include both large scale utility plants and smaller scale systems for distributed electricity and heat generation in buildings and individual homes. Fuel cells are already an alternative for power generation in areas where there is no existing power grid or the power supply is often unreliable [1,10].

New applications are emerging in the field of portable power generation, where fuel cell systems may offer benefits compared to primary and rechargeable batteries in portable electronics. Major drawbacks of batteries are limited capacity and slow recharging. With a suitable hydrogen storage method, fuel cell systems are quicker in operation and will achieve higher power and energy densities.

1.4.6. Fuel cell challenges

Although great improvements in fuel cell design and components have been made in the past 10 years, there remain several problems to overcome if fuel cells are to be a viable commercial alternative to internal combustion engines. A major hurdle is the fuel, which is mostly hydrogen. PEMFCs run best on very pure hydrogen. Hydrogen obtained from hydrocarbons tends to contain small amounts of CO, which have disastrous effects on the efficiency of anode reaction. Moreover, the onboard storage of hydrogen is problematic, whilst alternatives such as the on-board reformation of methanol complicate the system and reduce the efficiency.

The simpler DMFC, where methanol is used as a fuel instead of hydrogen, suffers from the poor kinetics of methanol oxidation reaction at low temperatures and from a high methanol permeation rate through the membrane. Finally, the overall cost of the fuel cell with its platinum based catalyst and problems with the currently used membranes, like methanol permeation, high temperature stability and high costs of membranes are an obstacle in the commercialization of fuel cells.

1.5. Zeolites

1.5.1. Definition & classification

Zeolites are well defined class of crystalline naturally occurring aluminosilicate minerals. They have three-dimensional structures arising from a framework of $[\text{SiO}_4]^{4-}$ and $[\text{AlO}_4]^{5-}$ coordination polyhedra linked by all their corners. The frameworks generally are very open and contain channels and cavities in which are located cations and water molecules [16]. The cations often have a high degree of mobility giving rise to facile ion exchange and the water molecules are readily lost and regained, especially for hydrophilic zeolites; this accounts for the well known desiccant properties of zeolites. A general formula for the chemical composition may be expressed as:



where M represents extraframework cation. The exchange of silicon for aluminum in the framework results in a net negative charge which must be compensated by extraframework cations. In general, these may be any alkali, alkaline-earth or rare earth cations as well as organic cations such as the tetramethylammonium ion. Water molecules are located in channels and cavities, as are the neutralizing cations. The framework structure of the faujasite zeolite family is shown below:

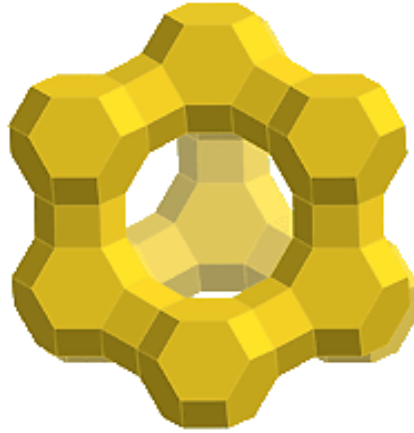


Figure 1-2 Framework structure of Faujasite family Y-zeolite

Zeolites may be classified on the basis of structural differences, one of them being based on the size of the pore openings. Depending on the structure, the size of the pores is in the range 3 to 8 Å. Apertures are bonded by oxygen atoms of connected tetrahedral. In general these rings involve 6, 8, 10 or 12 oxygen atoms. However, other factors are involved in determining the final pore size, which include the location, size and coordination of the extraframework cations [17].

1.5.2. Zeolites conductivity

Although there are a large number of zeolites present naturally as well as synthesized manually however, there are two important types of zeolites which are used very frequently. One is ZSM-5 and other is zeolite X and Y. From the conductivity point of view, the ZSM-5 family of zeolites has not been investigated in detail. Very few studies throw some light on the conductivity of this family of zeolite. From the conductivity point of view, the conductivity of zeolites primarily depends on the degree of hydration. Adsorbed water plays

an important role in conduction, bridging particles of zeolites and assisting the ion hopping process. It influences interactions between cations and the negative framework and provides additional charge carriers (H^+ , OH^-). As far as the conductivities is concerned, electrical properties of zeolites were studied at relative humidity (RH) varying from 0 to 100 %. However, DMFC application involves a direct contact of the material with liquid water. Besides, conductivity measurements at RH= 0-100 % often lack precision since the equilibration of the compressed porous pellet in a water vapor is going on slowly and may sometimes take several days [8].

Zeolite X and Y belong to the faujasite-type structure and differ from zeolites with ZSM-5 structure by much bigger void space which amounts to about 50 vol. % of the dehydrated crystal. One major difference between zeolite X and Y is that zeolite Y has high Si/Al ratio compared to zeolite X. This could provide better conditions for ion transport within zeolite framework. A further important factor which can lead to higher conductivity of this type of materials is their more favorable chemical composition because they have much lower silicon to aluminum ratio and consequently a higher concentration of exchange ions. [Zaidi et al.](#) studied the conductivities of a series of zeolites, prepared by ion exchange from Na-Y.

Li-Y, Na-Y, K-Y, Rb-Y, Cs-Y, H-Y

The conductivity of the above zeolites decreased in the order: Li-Y, Na-Y, K-Y, Rb-Y, and Cs-Y. The ammonium form of Y-Zeolite had conductivity at 100 % RH which was lower than that of Li-, Na- and K forms and higher than for Rb- and Cs-Y. Zeolite H-Y had the lowest conductivity both in water and at 100 % RH. The conductivity in water of the rest of the studied series varied only slightly close to 5×10^{-4} S/cm [8].

To summarize the conductivities of zeolites, the literature suggests that there are very diverse trends as far as the conductivities of the zeolites are concerned. The highest conductivity among all studied zeolites was found for clinoptilolite. Conductivity of clinoptilolite even in the protonic form exceeded all other zeolites. Zeolites A and L had lower conductivity than clinoptilolite, chabazite and mordenite. Natural mordenite, which has a less perfect structure and more impurities than synthesized specimens, also showed higher conductivity. Mordenite dealumination brought about a decrease in conductivity both in natural and in synthetic forms. The same trend is reported for ZSM-5 and Y-Zeolite. The H-forms of all the materials exhibited the poorest conductivity [8].

1.6. Solid acids: Heteropolyacids

Heteropolyacids (HPA) possess the highest protonic conductivity among inorganic solids at temperatures near ambient. This was first discovered in 1980 for dodecamolybdophosphoric acid, $\text{H}_3\text{PMo}_{12}\text{O}_{40}\cdot 29\text{H}_2\text{O}$ (MPA) [18]. Since then heteropolyacids have been considered for potential use as solid electrolytes applicable to fuel cells.

1.6.1. Keggin structure of HPAs

Keggin structures are a particular type of heteropolyoxometalate, a class of inorganic metal-oxygen cluster compounds containing more than one type of metal atom. Although there are several other known heteropolyoxometalates, the general term “heteropolyoxometalate”, as well as the general terms “heteropolyanion” and “heteropolyacid” (HPA) are often used in

the literature to describe specifically keggin-type heteropolyoxometalates [18]. The keggin structure of the heteropolyacid is as shown in the figure below:

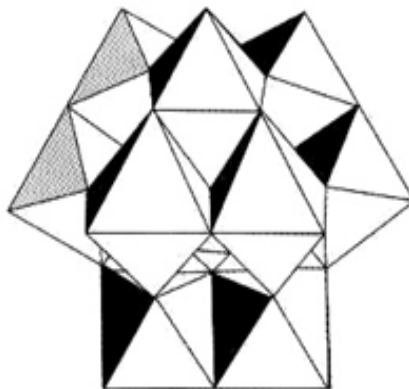


Figure 1-3 Keggin structure of HPA

HPAs are polyoxometalates incorporating anions having metal oxygen octahedral as basic structural units. Among a variety of HPAs those belonging to the so called keggin series, as molybdophosphoric acid (MPA) and tungstophosphoric acid (TPA) are most important as most stable and more easily available. Keggin structures demonstrate activity as both acid and redox catalysts. They include heteropolyanions $\text{XM}_{12}\text{O}_{40}^{\xi-8}$ where X is the central atom (P, Si etc.), ξ is its oxidation state and M is the metal ion (Mo, W, V etc.). The keggin anion is the primary structural unit and consists of 12-edge sharing octahedra MO_6 , grouped into four M_3O_{13} units, surrounding a central tetrahedron XO_4 [8]. The schematic representation of $[\text{PW}_{12}\text{O}_{40}]^{-3}$ anion is shown below:

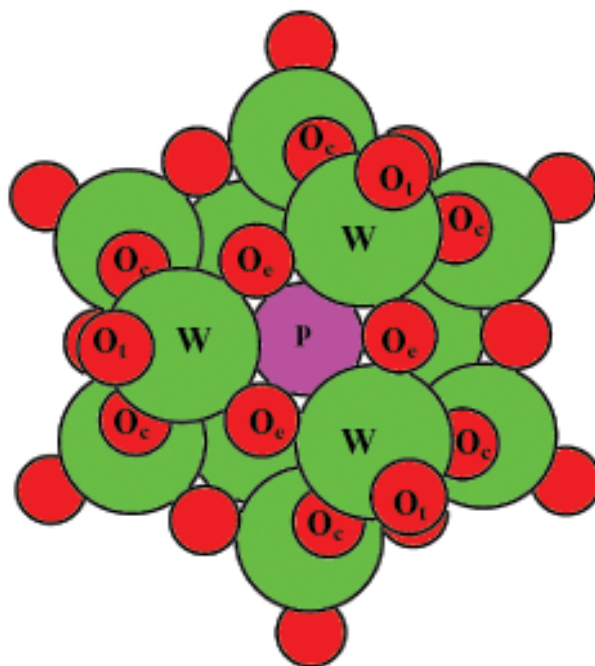


Figure 1-4 Schematic representation of $[PW_{12}O_{40}]^{-3}$ anion

1.6.2. Solid acids conductivity

On the basis available literature it can be concluded that heteropolyacids rank among the best low temperature solid protonic conductors and therefore, deserve consideration as a component of the composite fuel cell membrane [18]. Zaidi et al. reported that heteropolyacids possess high conductivities only in saturated water vapor. The sample conditioned in dry air showed conductivity lower by more than two orders of magnitude. The solid acids were water soluble and could not be used directly in fuel cell applications [8]. The electrical conductivity of one solid acid named boron orthophosphate has been studied and reported by Zaidi et al. [19]. Electrical impedance studies of the ammonium salt of 12-tungstophosphoric acid in the presence of liquid water has been studied and reported by Kaliaguine et al. [20]. They reported that conductivity in water increased appreciably as

compared to dry acid and consequently inferred that water plays a decisive role in conductivity measurements.

Chandra and Lakshmi prepared and characterized proton conducting composites of heteropolyacids hydrates (phosphomolybdic acid and phosphotungstic acids) dispersed with insulating Al_2O_3 . The bulk electrical conductivity was found to be dependent upon the composition, temperature and the relative humidity [21]. In an extension to the above work the same group studied the ion transport in above prepared proton conducting composites from volta cell e.m.f. and complex impedance spectroscopy. The ionic conductivity peaked at two concentrations of Al_2O_3 indicating two percolations for proton conduction [22].

1.7. MCM41

Since the development of MCM41, MCM-48, and MCM-50, which is designated as M41S by Mobil in 1992, mesoporous materials permit new possibilities for the application as catalyst for bulky molecules, support for various transition metal compounds, and as host lattice for nanometer sized materials. MCM41 exhibits a hexagonal array of one dimensional uniform mesopores [23]. The high thermal and hydrothermal stability, uniform diameter and shape of the pores over micrometer length scale, as well as, the prospect of tuning the pore aperture make MCM41 of interest to heterogeneous catalysis and molecular separation. The most important potential applications are the separation of proteins, the selective adsorption of large molecules from the effluents and the processing of tar sand and high distillates of crude oils to valuable low boiling products [24].

While zeolites have a limited pore diameter, the pore size in MCM41 materials can be controlled from 1.5 nm to 10 nm by the hydrophobic alkyl chain length of ionic surfactants. MCM41 exhibits catalytic activity for macromolecular reaction because of the larger surface area ($>1000 \text{ m}^2/\text{gm}$) and tunable pore sizes and pore volumes ($>1.0 \text{ cm}^3/\text{gm}$) and narrow pore size distributions and high sorption capacity [25]. Structure of MCM41 is shown below:

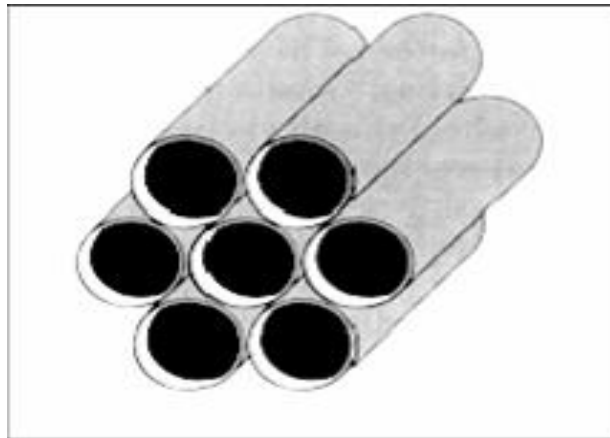


Figure 1-5 Pore structure of MCM41

Literature Review

This chapter addresses the development of composite polymer electrolyte membrane for direct methanol fuel cells (DMFCs), which are considered as one of the most promising alternative power sources especially for sub-megawatt scale applications [1,26,29,31].

Direct methanol fuel cells (DMFCs) working at low and intermediate temperatures (up to 150 °C) and employing solid proton electrolytes have been postulated as suitable systems for transportation. DMFCs utilize liquid fuel to deliver continuous power. They have higher utilization efficiencies and intrinsically lower polluting emissions with respect to internal combustion engines. Since transportation represents a significant portion of world energy consumption and contributes considerably to atmospheric pollution, the development of an appropriate fuel cell system is an important issue from both economical and environmental points of view. In order to be competitive within the transport market, the DMFC must be reasonably cheap and capable of delivering high power densities. At present there are a few challenging problems to the development of such systems. These mainly consists of finding i) suitable electrolyte membranes which have high ionic conductivity, low cost and low methanol cross-over ii) electrocatalysts which can effectively enhance the electrode kinetics of methanol oxidation and iii) methanol tolerant electrocatalysts with high activity for oxygen reduction [30,31]. Due to

these limitations of DMFCs, search for the suitable electrolyte membrane is on full swing. Since it is very difficult for a single material to possess all the requirements of a desired membrane, composite membrane technology is gaining momentum day by day. A brief description of the literature review on the approaches used for the preparation of composite membranes is presented below.

2.1. Composite membranes

The term "composite membrane" applies to a membrane made up of two or more materials. Actually the mixing or blending of two or more than two relatively compatible materials paves the way for optimization of individual material properties. Another term used precisely for composite membrane is "synergetic" composite membrane. A synergetic composite membrane may be defined as one in which a mixed membrane is more effective for at least one property (water uptake, protonic conductivity, methanol permeation etc.) than either material of the composite system alone [31]. The known properties of right materials merged together can solve the existing problem for search of suitable composite membranes.

Until now, perfluorosulfonic acid (PFSA) membranes are used in DMFCs due to the unavailability of suitable composite membrane with all the desired properties. Largest commercial membrane for fuel cell applications, Nafion[®] falls into PFSA category. But recently researchers have come up with some better composite membranes, and some composite membranes have been successfully demonstrated for their use in DMFC. At

present, there are mainly three approaches by which composite membranes have been developed.

- a) Chemical or physical modification of Nafion[®] membrane.
- b) Chemically or physically compositing the polymer matrix with an inorganic solid proton conducting material.
- c) In-situ hybridization of the organic and inorganic components.

Each of the above-mentioned approaches will be discussed in brief complementing with current literature available. As mentioned above, until now Nafion[®] membranes are widely used and considered as most efficient proton exchange membrane for DMFC. However, these membranes are plagued by serious problems such as low thermal stability, high methanol permeation and high cost. Hence to overcome these problems people primarily tried to modify Nafion[®] membrane itself. Apparently some of the stated problems were improved a lot but cost of these membranes still remains a big problem.

2.1.1. Modification of Nafion[®] membranes

Presently Nafion[®] membranes are used commercially in different types of polymer electrolyte fuel cells including DMFCs. Since there are already some problems existing with the Nafion[®] membranes for use in DMFCs as well as in H₂ operated fuel cells, researchers have tried to modify Nafion[®] with different inorganic and organic materials. The chemical structure of Nafion[®] membrane is shown below:

Compositing Nafion[®] polymer with various inorganic materials has been a hot area among various researchers. Composite Nafion[®] membranes with zirconium phosphate for direct methanol fuel cell applications at high temperature has been reported and tested for some of the existing problems. Composite membranes thus prepared at operating temperatures upto about 150 °C with dry oxidant, under mild preheating conditions (85 °C) showed better performance in DMFC. The typical cell resistances of 0.08 Ω-cm² were observed under cell operation at 140-150 °C [6,33,34]. Composite membranes of Nafion[®] with silicon oxide for use in fuel cell operating at 80-140 °C were also reported in literature. All the composite membranes prepared had a silicon oxide content of less than or equal to 10 wt %. The silicon oxide content improved the water retention of the composite membranes, increasing proton conductivity at elevated temperatures. Thermal and mechanical stability of composite membranes were also improved as compared to unmodified Nafion[®] membranes [35-37]. Further, hybrid Nafion-silica membranes doped with heteropolyacids for application in direct methanol fuel cells have been reported recently. Nafion-silica composite membranes doped with phosphotungstic and silicotungstic acids showed better performances at higher temperatures for DMFC operations (about 145 °C). Composite membranes thus prepared showed significant enhancement in the operating range of a direct methanol fuel cell as well as the kinetics of methanol oxidation was improved due to high temperature operation [38].

Heteropolyacids (HPAs) due to their high proton conductivities and mesoporous materials e.g. zeolites due to their high thermally & mechanically stable structures drew attention of many people to be used as one of the promising candidates in composite membrane

technology. In a recent study, Savadogo and Tazi has prepared and studied Nafion[®] composite membranes with the help of Nafion[®] and heteropolyacids. Heteropolyacids used in this study were silicotungstic acid, phosphotungstic acid and phosphomolybdic acid. The ionic conductivities of composite membranes were found to be higher than those of pure Nafion[®] membranes. The composite membrane prepared from Nafion[®] and silicotungstic acid was found to be most conductive of all other membranes prepared [39]. In another recent study, Ramani et al., has prepared and investigated Nafion[®]/HPA composite membranes for high temperature and low relative humidity fuel cell operation. The decomposition temperature of the composite membrane was extended to 150 °C, permitting more stringent operating conditions. The protonic conductivities of the composite membranes at 120 °C and 35 % RH were of the order of the 0.015 S/cm. These membranes have been evaluated at high temperatures and low relative humidities in an operating fuel cell [37,40].

Nafion[®] composite membranes with zeolite have also been reported recently by some groups. Tricoli and Nanetti [41] has proposed a novel zeolite-Nafion[®] composite membrane as ion conducting material. Composite membranes from zeolite fillers embedded in Nafion[®] were made by evaporating the solvents from a suspension of small zeolite crystals in a Nafion[®] solution. The zeolites used in this study were chabazite and clinoptilolite. They reported that the presence of zeolite fillers in the membranes caused notable changes in conductivity, methanol permeability and selectivity with respect to pure Nafion[®] [41]. In another interesting study, Holmberg et al., has synthesized and characterized zeolite-Y nanocrystals for Nafion[®]-zeolite-Y composite proton exchange membranes. The composite

membranes were found to be more hydrophilic and proton conductive than the base unmodified membranes at high temperatures. The composite membranes were also found better candidate for the methanol permeation as compared to the base Nafion[®] membrane [42].

Compositing Nafion[®] polymer with other polymeric materials has also been the center of attraction for some researchers. In this category of Nafion[®] modification people have come up with numerous studies, but here only the important ones will be discussed. In one such study, poly (1-methylpyrrole) has been impregnated with commercial Nafion[®] membrane by in-situ polymerization. A decrease of more than 90 % in the permeability of the membranes to methanol is reported, although the ionic resistance of such heavily loaded membranes became too high for high power fuel cells. At lower poly (1-methylpyrrole) loadings, a decrease in methanol permeability by as much as 50 % could be realized without a significant increase in ionic resistance [43]. Nafion[®]/PTFE composite membranes for fuel cell applications have also been reported with some improved features. In this study, porous polytetrafluoroethylene (PTFE) membranes were used as support material for Nafion[®]/PTFE composite membranes. The composite membranes were synthesized by impregnating porous PTFE membranes with a self made Nafion[®] solution. Resulting membranes were found to be mechanically and thermally stable. The composite membranes thus prepared were also cost effective [44,45].

Composite membranes with polybenzimidazole (PBI) are also reported in direct methanol fuel cells. Since polybenzimidazole polymer is not proton conductive in its native state, so it

was sulfonated prior to blending with Nafion[®] polymer. The composite membrane thus prepared showed a higher protonic conductivity of 0.032 S/cm as compared to Nafion[®] itself which is 0.07 S/cm. The methanol permeability of the composite membrane was found to be 0.82×10^{-6} cm²/s as compared to Nafion[®] which is around 2.21×10^{-6} cm²/s [46]. Addressing the problem of methanol permeation as a dominating one, a composite membrane of Nafion[®] with polyvinyl alcohol (PVA) for direct methanol fuel cell has been reported. It is concluded that at the weight ratio of 1:1 in PVA and Nafion[®], the thin film coated Nafion[®] membrane exhibited low methanol crossover and the membrane protonic conductivity could be improved by the sulfonation treatment [47].

2.1.2. Composite membranes from the inorganic modification of the polymer matrix

The approach of making composite membranes from the inorganic modification of the polymer matrix for direct methanol fuel cells has not been explored by most of the researchers. But the approach has gained momentum recently due to the exemplary success achieved by some people working on this approach. Different polymers have been used in this approach with many different inorganic materials. One of these important polymers which has drawn the attention of everyone is sulfonated polyether ether ketone (SPEEK) polymer. Sulfonated polyether ether ketone (SPEEK) polymer falls into the category named aromatic sulfonic acid. The properties of the membranes of this category are more suitable for use in DMFC. Advantages include low methanol permeation, high conductivity and very good mechanical properties. Good mechanical stability provides the membrane enough

flexibility, thus making the membrane thin enough to decrease the resistance offered by the thickness of the membranes [8,48,49].

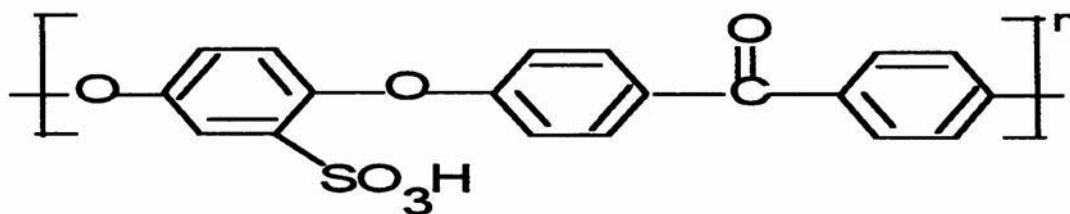


Figure 2-2 Chemical structure of SPEEK [48]

SPEEK polymer is supposed to be a noble substitute to Nafion[®] membranes as far as its use in DMFC is concerned. SPEEK polymer does have the caliber to be a potential substitute to Nafion[®] membranes but only with modification to certain properties. Mainly these properties include protonic conductivity of SPEEK membranes as compared to Nafion[®] membranes; otherwise SPEEK has comparable methanol permeation, high temperature stability and low cost as compared to commercial Nafion[®] membranes [8]. Electrochemical properties of a series of composite membranes prepared by incorporation of boron phosphate into polymeric matrix of sulfonated polyether ether ketone (SPEEK) were studied. The proton conductivity of the composites was found to be higher than the pure SPEEK polymer. The mechanical stability was also in the satisfactory range for use in DMFC at moderately high temperatures [19].

SPEEK polymer was blended with the polyetherimide (PEI) polymer and then doped with HCl and H₃PO₄ to get more appropriate solution to the DMFC problem. Results with these

membranes were of mixed success. The doping of HCl was found to be more significant than that of H₃PO₄ [7]. Though water retention properties of membranes enhanced substantially as compared to the pure SPEEK polymer membranes which were found to be main reason for enhanced conductivities of membranes, still several factors were to be taken into account in order to declare them suitable for use in fuel cells. With boron phosphate and polyetherimide (PEI), the protonic conductivity increased moderately but with the incorporation of heteropolyacids into the SPEEK structure increased the protonic conductivity noticeably. The room temperature protonic conductivities of the order of 10⁻² S/cm were reported while with the same composite membrane and at high temperatures around 100 °C the conductivity values raised upto 10⁻¹ s/cm. The composite membranes were found to be thermally stable upto 250 °C [8,27]. While the results with the boron phosphate were encouraging but certainly not the stepping stone in the quest of more appropriate candidate for medium temperature fuel cells, researchers went on to explore other materials to optimize the composite membrane properties.

Zirconium oxide modified sulfonated polyether ether ketone (SPEEK) membranes for direct methanol fuel cell applications have been proposed recently. In this work it is reported that organic-inorganic composite membranes based on polyether ether ketone showed promising performance at low, moderate and high temperature operated DMFC. The zirconium oxide modification affected its water swelling, chemical and mechanical stability, methanol and water permeations and, finally proton conductivity. Depending on the amount of the inorganic component in the membrane, a good balance between high proton conductivity, good chemical stability and low methanol permeability could be reached [50,51].

Layer silicates (clay) such as laponite and montmorillonite (MMT) have also been studied to get composite membranes for DMFC applications. Composite polymer membranes are prepared by embedding layered silicates (laponite and montmorillonite) into sulfonated polyether ether ketone (SPEEK) membranes for fuel cell applications. Sulfonation of the polymer increased membrane hydrophilicity to give good proton conductivity. Layered silicates incorporated into SPEEK polymer membranes helped to reduce swelling significantly in hot water; they also helped to decrease the methanol permeation through the composite membranes. In fact, methanol crossover was reduced without an alarming reduction in the proton conductivity [52].

As far as low permeabilities to methanol is concerned, new organic-inorganic composite membranes based on sulfonated polyetherketone (SPEK) and sulfonated polyether ether ketone (SPEEK) were synthesized for application in direct methanol fuel cell. Composite membranes were synthesized with SiO_2 , TiO_2 and ZrO_2 . The permeabilities were decreased by inorganic zirconia modification. The modification of SPEK and SPEEK with ZrO_2 reduced the methanol flux by 60-fold, But on the other hand there was a big compromise on conductivity which was reduced by 13-fold, while modification of PEK and SPEEK with silane (SiO_2) led to a 40-fold decrease of the water permeability without a large decrease of the protonic conductivity [53]. With some encouraging results of the modification of PEK with SiO_2 , TiO_2 and ZrO_2 , modification of PEK with heteropolyacid further yielded some notable results. Actually the composite membranes were prepared using an organic matrix of SPEK, different heteropolyacids and an inorganic network of ZrO_2 and $\text{RSiO}_{3/2}$. The

bleeding out of the heteropolyacid from the membranes was also measured in addition to the water and methanol permeation and protonic conductivity tests. The presence of ZrO_2 decreased the water and methanol permeability and reduced the bleeding out of heteropolyacid. High conductivities values were obtained with membranes containing tungstophosphoric acid (TPA) [54].

Apart from SPEEK polymer some other polymer materials have also been used in order to get the appropriate candidate material for DMFC applications. Sulfonated poly(arylene ether sulfone) polymer has been incorporated with heteropolyacid (HPA). The composite membrane showed good bleeding out of heteropolyacids into the poly(arylene ether sulfone) polymer matrix. Composite membranes thus prepared showed excellent thermal stability (about $300\text{ }^\circ\text{C}$). The composite membranes displayed good proton conductivities especially at elevated temperatures ($130\text{ }^\circ\text{C}$). Infrared and dynamic thermo-gravimetric data showed that the composite membrane had much higher water retention from $100\text{-}280\text{ }^\circ\text{C}$ than the pure sulfonated copolymer. These results also suggested that the incorporation of HPA into these proton conducting copolymers should be good candidate for elevated temperature operation of DMFC [55]. Heteropolyacids come handy in the manufacture of composite membranes due to their uniquely very high proton conductivity and thermally stable structure. Novel composite membranes based on poly (vinyl alcohol) (PVA) with embedded phosphotungstic acid were prepared and measured for their protonic conductivity and methanol permeation. A marginal conductivity of the order of $6.27\times 10^{-3}\text{ S/cm}$ was obtained while the values of methanol permeation were found to be in the range of 1.28×10^{-7} and

4.54×10^{-7} cm²/s. From the values for methanol permeation obtained, these composite membranes had the potential to use them in direct methanol fuel cell [56].

Composite membranes with the help of polybenzimidazole (PBI) polymer have also been reported. As polybenzimidazole (PBI) polymer is not proton conductive in its native state, so PBI is used with some preprocessing to make it proton conductive. Polybenzimidazole doped with phosphoric acid has been used to prepare the composite membranes. The PBI composite contained inorganic proton conductors including zirconium phosphate, phosphotungstic acid and silicotungstic acid. The conductivity of the phosphoric acid doped PBI and PBI composites membranes was found to be dependent on the acid doping level, relative humidity (RH) and temperature [31,57]. Apart from the direct incorporation of one component into another, a new synthetic route to synthesize organic/inorganic nanocomposites hybrid polymer membrane using SiO₂ and polymer such as modified polybenzimidazole (PBI), polyethylene oxides, polypropylene oxide, polyvinylidene fluoride etc., the composite membranes was prepared through sol-gel processes. The methanol permeation through the membranes decreased significantly and membranes showed excellent proton conductivity [58].

2.1.3. Composite membranes from in-situ hybridization of organic/inorganic components

The approach of getting composite membranes from in-situ hybridization of inorganic and organic materials has also been a hot field among various researchers. Hybrid membranes incorporating an inorganic and organic component are receiving much attention as

promising solid electrolytes for fuel cells. Recent progresses in membranes for medium and high temperature fuel cells include not only the synthesis of new functionalized proton conducting polymers or their modification by acid or base-doping, but also associations of polymers (polymer blends), better understanding and control of polymer microstructure, the development of composite systems incorporating a micro- or macro-reinforcement, and hybrid membranes containing inorganic component in addition to the polymer matrix. The presence of an inorganic proton conducting component can contribute to the overall conductivity of a composite or hybrid system, such that a polymer of more moderate extent of sulfonation, conductivity, and limited swelling characteristics can be used [59].

Different hybrid membranes with the help of inorganic/organic or organic/organic components have been reported in literature with some exciting results. Hybrid polyaryls ether ketone membranes with the help of zirconium phosphate and modified silica have been prepared and characterized for fuel cell applications. The preparation and characterization included their performance in a hydrogen-oxygen fuel cell. The examples were chosen to illustrate the in-situ formation of inorganic particles, either on a prepared membrane, or in a polymer solution. SPEEK modified silica and SPEEK zirconium phosphate membranes provided power densities of 0.62 W/cm² at 100 °C. In all cases, the presence of the inorganic particles led to an increase in proton conductivity of the polymer membrane, without any harm to its flexibility [59,60].

Sulfonated polyether ether ketone (SPEEK) has been used as polymer matrix for hybrid membrane formation with inorganic proton conductors. In almost all of the cases studied,

the presence of the inorganic particles led to an increase in conductivity of the polymer membrane, and was found to be without detriment to the membrane flexibility [61]. Apart from being the major component in the blended membranes, SPEEK has also been investigated as an additive in the membrane formation and performance. Sulfonated polyether ether ketone, a strong polyelectrolyte, was investigated as an additive in polysulfone (PSU)/SPEEK/N-methyl-2-pyrrolidone (NMP) systems. The effect of SPEEK in the charged membrane formation was investigated through thermodynamic and viscosity studies. Charged membranes prepared from 20 wt. % PSU solutions with the ratio of SPEEK/PSU in the range of 0.005-0.05, substantially increased permeability, porosity and greatly reduced the fouling tendency compared to the base PSU membrane [62].

Functionalization of the utility polymer has been one important aspect in hybrid membrane manufacture. Functionalization not only enhances the structural flexibility of the candidate polymer but also upgrades some of the inherent specific properties e. g. proton conductivity, which in turn makes the candidate polymer best suitable to use as a hybrid membrane constituent. So prior to make hybrid membranes directly researchers initiated with the functionalization of candidate polymers like polyether ether ketone and polybenzimidazole. Sulfonation of SPEEK enhances its proton conductivity significantly while polybenzimidazole (PBI) polymer also shows significant improvement in the protonic conductivity after its complexation with acids [59,63]. Some other newly synthesized materials are also been reported for hybrid membrane manufacture. Zirconium carboxybutylphosphonate was synthesized to prepare inorganic/organic composite membranes based on polybenzimidazole (PBI). The membrane thus prepared showed

promising performance and relatively high protonic conductivities under the given conditions. Membranes were also highly thermally stable [64].

Nafion[®]-silicon oxide (SiO₂)/ phosphotungstic acid (PWA) and Nafion[®]/silicon oxide composite membranes have also been proposed for high temperature fuel cell operation. The composite membranes were prepared by well known recasting technique. High water uptake hence the high proton conductivities were reported for the membrane prepared. The highest conductivity value for these composite membranes was found of the order of pure Nafion[®] membranes at high temperatures and 100 % relative humidity (RH), however, it was found to be much lower at low relative humidity (RH) [65]. A series of organic/inorganic composite materials based on polyethylene glycol (PEG)/silicon oxide (SiO₂) for use as electrolytic membrane in direct methanol fuel cell (DMFC) have been synthesized through sol-gel processes. Acidic moieties of 4-dodecylbenzene sulfonic acid (DBSA) were doped into the network structure at different levels to provide the hybrid membrane with proton conducting behavior. An increasing trend of proton conductivity with increasing DBSA doping was obtained, while presence of SiO₂ framework in the nanocomposites hybrid membrane provided the enhanced thermal stability. Some of the hybrid membranes exhibited low methanol permeability without sacrificing their conductivities significantly and were thus proposed to be potentially useful in DMFC [66].

Blending of two organic components to get a hybrid membrane has always been a point of attraction for almost all researchers. Basically the flexibility of playing with the microstructure of the organic polymer candidates and easy handling has paved the way to

explore a suitable hybrid membrane. As in one study, novel acid-base polymer blends have been characterized for application in membrane fuel cells. The membranes synthesized are composed of SPEEK Victrex or polyether sulfone (PES) as well as sulfonated polysulfone (sPSU) Udel[®] as the acidic compounds, and of PSU CELAZOLE[®], or poly (ethyleneimine) PEI (Aldrich) as the basic compounds. The membrane showed good proton conductivities and excellent thermal stabilities. Two synthesized membranes were also tested in a hydrogen fuel cell and showed good performance [67]. In another contribution, different types of acid-base composite membranes have been prepared and characterized for their use in DMFC at high temperatures. In this study, sulfonated polyetherketone and sulfonated polysulfone is used as acidic blend components, while PSU(NH₂)₂, poly (4-vinylpyridine), and polybenzimidazole are used as basic components [68].

Multilayered polyphosphazene membranes have been suggested as new series of hybrid membranes with improved protonic conductivity and low methanol permeation. For membrane synthesis, phosphazenes polymer was used, in which the polyphosphazene was sulfonated, blended with an uncharged polymer, and then crosslinked. Poly[bis(3-methylphenoxy)phosphazene] has also been reported a promising material for fuel cell applications. Polymer crosslinking was carried out by use of UV light and photo initiator. The results showed that there was a significant decrease in methanol crossover (the methanol flux was about 10 times lower than Nafion[®] 117) [69]. Membranes from polybenzimidazole/sulfonated polysulfone have been studied and compared with homopolymer membranes made from sulfonated polysulfone, blends of polyether sulfone with sulfonated polysulfone and Nafion[®] 117. Also an improved behavior of these

membranes towards methanol permeation was observed [70]. In another study, blended membranes were prepared by the blending of SPEEK and polyether sulfone. The transport properties of membranes with SPEEK content in the range of 50-80 wt. % were found to be comparable to those known for commercial ion exchange membranes [71].

Novel methanol barrier polymer electrolyte membrane for direct methanol fuel cells were proposed and characterized. These novel hybrid membranes were prepared from polyvinyl alcohol (PVA)-blend-polystyrene sulphonic acid (PSSA). The effects of curing temperature, methanol concentration and membrane composition on the ionic conductivity and the methanol permeability of the membranes were also investigated [72]. In an interesting study, a new proton exchange membrane from the sulfonation of poly (phthalazinone ether ketone) has been synthesized. Membrane performances were directly related to the degree of sulfonation (DS). Proton conductivity increased with degree of sulfonation and temperature up to 95 °C, reaching up to 10^{-2} S/cm [73]. Both high protonic conductivity and low methanol cross over is required from the membrane for the application in direct methanol fuel cell. Considering these facts as prime concerns, composite multi-layered membranes for direct methanol fuel cells have been synthesized. Composite membranes were synthesized with the help of polyvinyl alcohol membrane loaded with mordenite or tin mordenite. It was observed that single layer of these materials had poor mechanical strength with noticeable cracks and also with poor conductivity, but some encouraging results were obtained when they sandwiched these layers and membranes were prepared with many layers of the polyvinyl alcohol and tin mordenite [74].

Experimental Methods

The experimental procedures performed in this work are described systematically here. The materials which have been synthesized prior to using them in casting composite membranes have been described with their preparation procedure. All of the experimental procedures used in this work are described in this chapter.

3.1. Materials and chemicals

Sulfonic polyether ether ketone (SPEEK) polymer with ion exchange capacity (IEC) of 1.6 meq/gm was bought from Fumatech Inc. Germany. Both the heteropolyacids used in this study, tungstophosphoric acid (TPA) and molybdophosphoric acid (MPA) were supplied by Fluka Chemicals and used as received. Solvents used for casting membranes namely dimethylacetamide (DMAc) 99% grade, dimethylsulfoxide (DMSO) 99% grade and dimethylformamide (DMF) 99% grade were purchased from Aldrich Chemicals company. Y-zeolite used in this work was procured from CATAL, UK while MCM41 used was prepared in Centre for Refining & Petrochemicals (CRP) lab of Research Institute (RI) at KFUPM using already established procedure [75]. Y-zeolite used was dried at 250 °C while silica/alumina ratio for the MCM41 used was 15.

3.2. Synthesis of Materials

3.2.1. Synthesis of proton conducting powders

All of the synthesized powders used in this thesis project were prepared according to the standard procedures mentioned in literature [9]. Similar procedures were followed for the loading of heteropolyacids onto Y-zeolite and MCM41. Four different types of materials were synthesized, namely tungstophosphoric acid (TPA) loaded onto Y-zeolite & MCM41 and molybdophosphoric acid (MPA) loaded onto Y-zeolite & MCM41 (Appendix B). All of the samples were prepared in weight percentages of heteropolyacids and USY-zeolite and MCM41. In all four cases the percentage loading of the two heteropolyacids were varied from 20-50 %.

In order to establish the procedure by which strong HPA and Y-zeolite interaction would be achieved, three procedures were adopted to impregnate HPAs on Y-zeolite. A predetermined amount of TPA was dissolved in distilled water and few drops of dilute HCl were added in order to avoid hydrolysis of TPA. Then required amount of Y-zeolite was added to make a suspension. The suspension was stirred, and evaporated at 80 °C until dryness. Then the solid was ground to fine particles and dried at 200 °C for 6 hours in air flowing oven.

The second procedure involved over night soaking of the suspension at room temperature before evaporating at 80 °C following the same procedure mentioned above. In the third instance, the suspension was homogenized using ultrasonic gun in pulsating mode of operation for 30 minutes. After that the suspension was stirred and evaporated at 80 °C

until dryness following further drying at 200 °C as mentioned in the first procedure. The solids were then finely ground and collected for further characterization.

The resulting materials were evaluated by washing the HPA supported Y-zeolite with hot water at 80 °C in a beaker for one hour and then analyzing the washing by atomic absorption spectroscopy for tungsten. The results of AAS analysis showed minimum amount of the TPA was leached out in the case of samples prepared by ultrasonic treatment. This procedure was followed to prepare other samples with different loadings and also using MPA supported Y-zeolite. Exactly same procedure was followed to load various weight percentages of heteropolyacids onto MCM41.

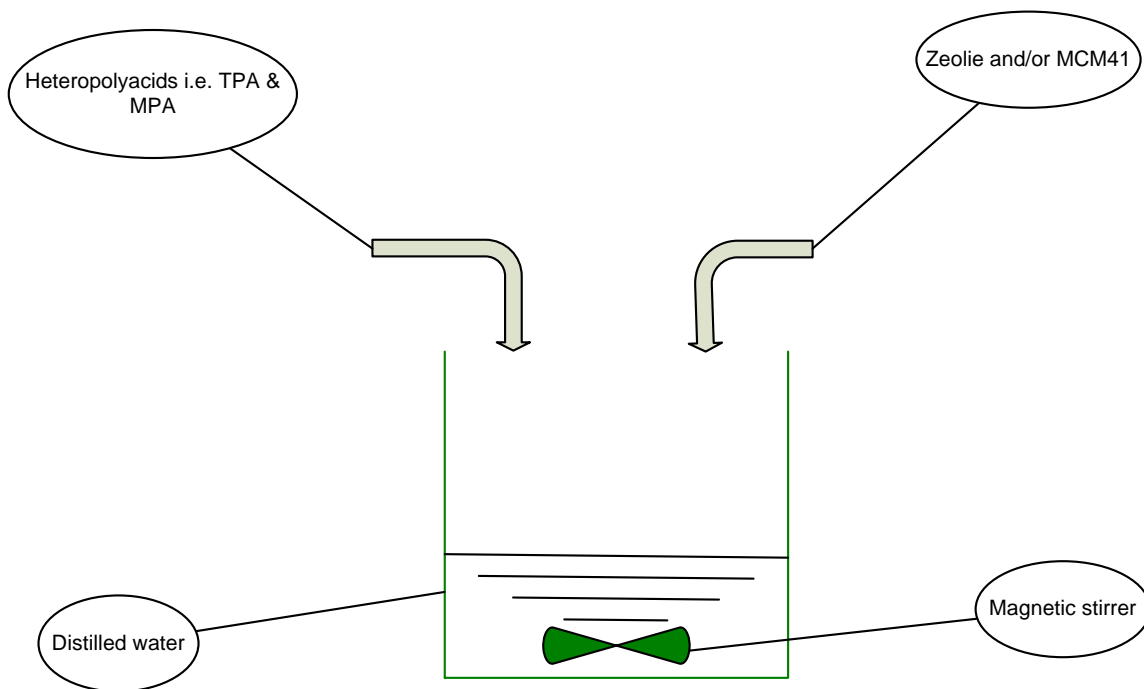


Figure 3-1 Synthesis of solid proton conductors from Y-zeolite and MCM41 with HPAs

3.2.2. Leaching study of prepared powders

The leaching experiments were performed on the prepared powder sample to ensure the loading of heteropolyacids into zeolite and/or MCM41 structures. Two types of leaching studies were performed to establish the fact of HPA retention on zeolite and/or MCM41. Thermal as well as flow leaching were performed in order to ensure that the material will be stable under real practical situations.

3.2.2.1. Thermal Leaching:

The main purpose of thermal leaching was to ensure the retention of HPAs into zeolites and/or MCM41 at high operating temperatures which is quite possible in practical operations. Predetermined quantity of the synthesized material was mixed with 50 ml of distilled water and continuously stirred and heated at 80 °C for one hour. Contents were then filtered into a standard graduated 250 ml flask and the solution was diluted to 250 ml with the help of distilled water. The solution was then analyzed with the help of atomic absorption spectrophotometer for the amount of tungsten and/or molybdenum leached out. The amounts of metals i.e. tungsten and molybdenum leached out were found to be negligible.

3.2.2.2. Flow Leaching

Leaching study was carried out on some selected samples in order to ensure negligible HPA leaching out from loaded Y-zeolite. The leaching study was carried out in a flow apparatus. The flow apparatus consisted of a simple U-tube, one end of the U-tube was

connected to distilled water supply, while the other end was connected to the conical flask to collect the distilled water passed through the solid powder in the midst of U-tube. The prepared powder was put at the bottom of the tube and both ends of the tube were packed with glass wool. The U-tube was then immersed into a beaker with an oil bath, which was heated and maintained at 80 °C throughout the experiment. The distilled water thus passed through the solid synthesized powders was collected and analyzed for molybdenum and tungsten metals respectively with the help of atomic absorption spectrophotometer (AAS) and inductively coupled plasma (ICP) techniques. The water used here was distilled twice.

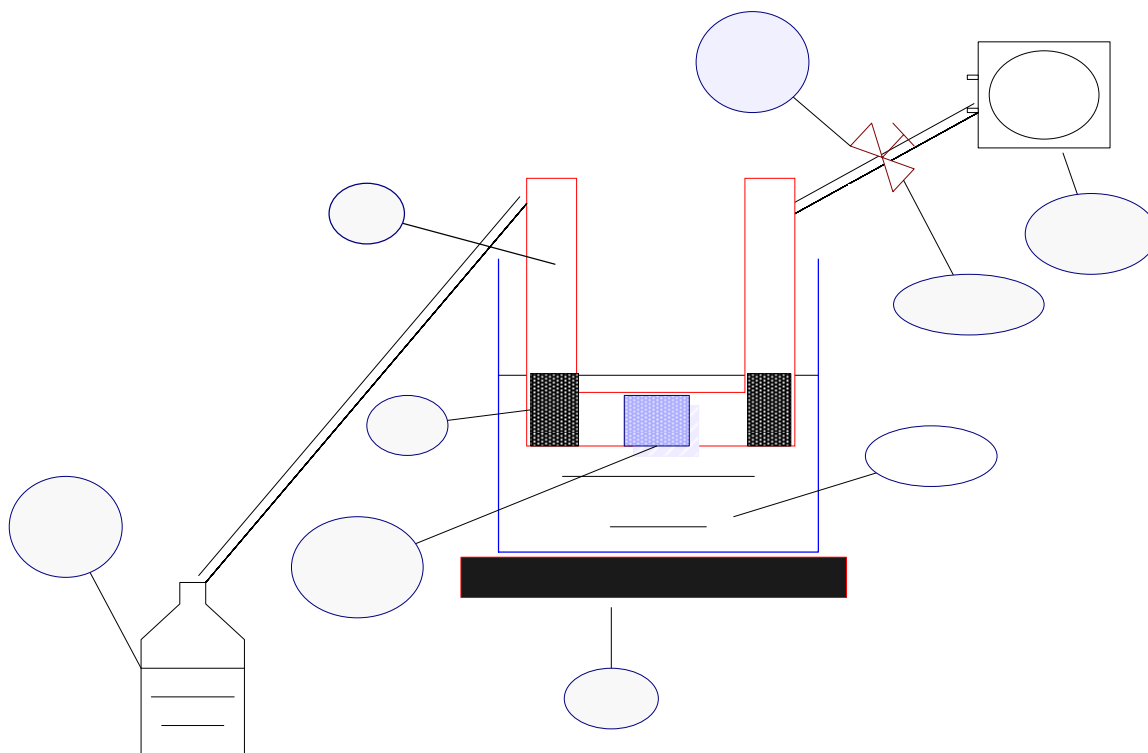


Figure 3-2 Set-up for flow leaching study

3.3. Membrane preparation

The polymer membranes can be prepared from their dilute polymer solutions by several techniques. Currently, phase inversion and solution casting techniques are two most important techniques that are being used. Actually, phase inversion technique is used when the membrane to be prepared is of porous nature, while dense membranes are prepared using solution casting technique. Since only dense membranes are prepared in this work, so solution casting technique was followed throughout the work.

3.3.1. Solution casting method

Both pure polymer and composite membranes were prepared by this method. The pure polymer membrane can be prepared easily by the casting technique as compared to the composite membranes. In the case of pure membranes, the polymer was first dissolved in dimethylacetamide (DMAc) and the polymer solution was heated at 60-140 °C to evaporate the solvent. The starting concentration of the casting solution was around 3-5 wt. % polymer which was gradually increased to approximately 30-40 wt. % after evaporation. The polymer solution was then poured onto a glass plate and spread using the casting knife. In case of composite membranes, the solid proton conducting powder (heteropolyacids loaded Y-zeolite or heteropolyacids loaded MCM41) was added to the polymer solution. The resulting suspension stirred under heating was cast onto the glass plate after solvent evaporation.

However, some intricacies were encountered in preparing homogeneous and reproducible thickness of solid/polymer composite membranes by casting technique. The difficulties in the preparation of composite membranes containing a powder inorganic solid into the polymer are: 1) generally inorganic solid proton conducting powders cannot be dissolved in any organic solvent and have poor affinity towards aromatic polymers; 2) solid conducting powders have higher density than most polymers and their solutions. Therefore it is difficult to disperse solid conducting particles homogeneously in a polymer solution. Setting of the powdered conducting particles may occur during preparation of membranes resulting in an inhomogeneous solid powder suspension in the polymer phase. This inhomogeneity will affect the performance of the membranes. Also, in the case of high loading of the solid powder in the polymer, the particle may agglomerate which results in the formation of defects and irregularities of the dried membranes.

At the laboratory scale it is very difficult to prepare homogeneous membranes with uniform thickness. The final thickness of the membrane depends on many factors such as the viscosity of the freely spread casting solution, and the uniformity and flatness of the surface on which the solution is cast. The viscosity of the casting solution depends on the extent of solvent evaporation, which is difficult to control precisely. However, it was observed that the particle size should be less than 0.5 μm to ensure good particle dispersion in the polymer solution. This is due to the fact that ultrafine particles can be homogeneously dispersed in the polymer, thus all of the particles are surrounded by

polymer matrix. This was observed in our work, when particles were not well ground the dispersion was not good, while for smaller particles the dispersion was better.

In this work the solid inorganic conducting powder was first well ground in order to get good dispersion in the polymer solution. It was then dried at around 140 °C to remove any adsorbed moisture and avoid precipitation in the polymer solution. The pure polymer and inorganic solid powder suspensions were prepared separately by dissolving and heating them in dimethylacetamide (DMAc). The initial composition of the polymer and the inorganic solid powder was 2-5 weight percent in DMAc. The two solutions were then mixed and stirred vigorously to avoid any agglomeration of the inorganic solid particles. The resulting suspension was heated gradually upto 120 – 140 °C under stirring for 8-12 hours. When the mixture became homogeneous the solvent was evaporated. Care was taken not to evaporate the solvent too fast as sometimes under high heating rates the inorganic solid particles were found to stick to the bottom of the glass beaker. The suspension was then cooled to around 30-40 °C and poured onto the glass plate and spread by using casting knife. The glass surface was leveled using a leveler in order to make the surface as flat as possible, because the evenness and uniform thickness of the membranes depends on the flatness of the surface. The cast membranes were first dried at room temperature overnight, then at 60 °C for 4 hours and then at 120-150 °C for 12 hours. It was observed that the slow and gradual drying procedure resulted in membranes free from defects and irregularities. In our work, maximum effort was made to get reproducible membranes by controlling the above-mentioned factors precisely.

3.4. Proton conductivity measurements by impedance spectroscopy

The bulk ionic conductivity of solids cannot be measured straightforwardly by a D. C. bridge which is customary practice for electron conductors. The reason is that in case of ionic conductors the measurements are hindered by polarization effects mainly on the electrodes. To avoid this, previously proton conductivity was measured by D. C. techniques in hydrogen atmosphere using special reversible electrodes, such as hydrogen bronzes, hydrides, Pt-black and some others. This direct method however was time consuming and tedious in use and still was not free from polarization drawbacks. It should be mentioned that passage of current in only one direction always results in a concentration gradient, which opposes the effect of applied field, producing the concentration polarization.

Measurements employing AC bridges may circumvent polarization problems; however the most powerful and efficient way to measure ionic conductivity in general is AC impedance spectroscopy (IS). This technique has gained broad acceptance recently with most of the researchers reporting conductivities results by using this technique. For conductivity measurements by impedance spectroscopy, membrane samples were cut into square shape of 1cm×1cm in dimensions and were placed between two blocking electrodes as shown in [Figure 3-3](#).

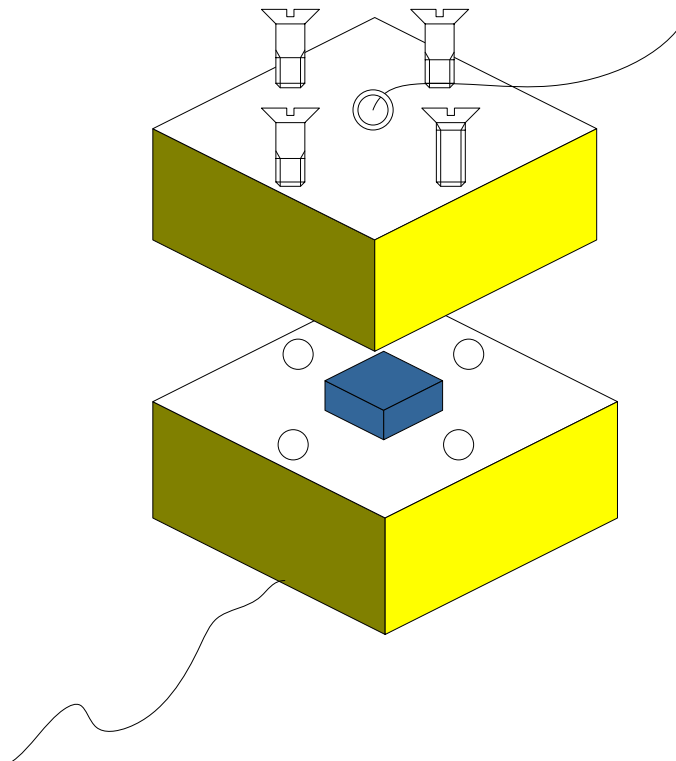


Figure 3-3 Conductivity measurement cell

The impedance spectroscopy (IS) measurements were performed over the frequency range $0.1-1.2 \times 10^6$ Hz with oscillating voltage 10 mV, using a PC controlled SI 5210 impedance/gain-phase analyzer. The impedance data were corrected for contribution from the empty and short-circuited cell. Acquisition and analysis of the impedance spectra were performed employing the Zsimpwin software, provided by Solartron. The cell for measurements of proton conductivity of polymer membranes for ambient temperature was manufactured with simple two stainless steel electrodes supported on perplex sheets, while for high temperature proton conductivity measurements Teflon sheets were used as cell supports. Both the electrodes were clamped tightly during the experiments. Care was taken to maintain the pressure uniform in order to avoid any

change of conditions during the experiments. The main shortcoming of an open cell, the specimen dehydration during the measurement, is compensated by such advantages as the possibility to provide good electrode-specimen contact and access to a larger temperature range (typically upto 150 °C). The impedance measurements were repeated and the reproducibility was within the tolerance limit.

3.5. Methods of characterization

3.5.1 Atomic absorption spectrophotometry

The analysis of the prepared solid conducting powders for the elements Mo (molybdenum) were performed by atomic absorption spectrophotometry (Perkin-Elmer, model no. 100B) using air-acetylene and acetylene-nitrous oxide flames, while for Tungsten metal leaching study, Inductively Coupled Plasma (ICP) analysis technique was used.

3.5.2. Proton conductivity measurement by impedance spectrometry

The impedance spectroscopy technique was used to carry out the proton conductivity measurements of the synthesized solids. The impedance spectroscopy (IS) measurements were performed over the frequency range $0.1-1.2 \times 10^6$ Hz with oscillating voltage 10 mV, using a PC controlled SI 5210 impedance/gain-phase analyzer. The impedance data were corrected for contribution from the empty and short-circuited cell. Proton conductivity mechanism in solids is strongly a water assisted phenomenon which is extremely

dependent on the water present. The detailed procedure of conductivity measurements used in this work is described elsewhere [19].

Measured amounts of dry solids at ambient conditions were mixed with distilled water and the wet powders were immediately placed into a 2 mm inner diameter Teflon spacer which was then placed in between the two stainless steel electrodes of the conductivity cell and clamped therein. Since the design of conductivity cell is such that four clampers are equidistant which ensure homogeneous and equal pressure in all of the cases, moreover equal amounts of each samples were used to ensure the homogeneity in performing the experiments.. Also, the use of Teflon spacer ensured almost zero conductivity because of the insulation properties of Teflon material between the electrodes. The sample weight was measured before and after the impedance test in order to detect any decrease in water content. Since the duration of acquisition of a complex impedance spectrum did not exceed more then 10 minutes, the hydration degree did not change by more than 10- 20%.

The advantage of above-mentioned measurement method apart from its rapidity is that it allows the study of solid behavior at water content higher than 100 % RH. This sounds important, because some applications of solid electrolytes involve the direct exposure of materials with liquid water such as in the case of direct methanol fuel cell applications.

3.5.3. Water uptake of membranes

The water absorption of SPEEK membranes was determined from the difference in weight (W) between the dry membranes at ambient conditions and the swollen

membranes. At ambient conditions, it is meant that the membranes, cast from DMAc solution after drying, was used as such and soaked in distilled water. It was then taken out, wiped with blotting paper (soaking paper) and weighed again. The percentage of water absorbed was calculated with reference to the weight of the dry specimen from the following equation:

$$\text{Water uptake} = [(W_{\text{wet,ambient}} - W_{\text{dry,ambient}}) / W_{\text{dry,ambient}}] \times 100 \quad (3.5.3)$$

3.5.4. Fourier transform infra red (FTIR)

FTIR spectra were measured in transmittance mode on a Perkin-Elmer FC-16 FTIR spectrometer. Spectra were taken by making pellet of different powder samples with potassium bromide (KBr). Around 4-5 mg of sample was mixed with approximately 200 mg of KBr to prepare the pellets. In the case of membranes samples, the samples were first dried at 100 °C to remove any moisture/solvent for 30 minutes. Small pieces were then cut for each run. The spectrum for each pellet was taken with the above-mentioned spectrometer in the range 400 to 2000 cm^{-1} .

3.5.5. X-ray diffraction

X-ray powder diffraction measurements were carried out on a JEOL JDX-3530 X-ray diffractometer instrument. Each sample was gently ground in an agar pestle and mortar. In finely powdered form many grains come into orientation and greatly improve the quality of diffraction pattern. The fine powder was packed into a sample holder having a

diameter of ~ 25 mm and depth of ~ 3 mm. The surface of the packed sample was smoothed with a piece of flat glass. In case of membranes, all the membranes characterized by this technique were first dried at 100 °C for 30 minutes in order to remove any moisture or solvent. The samples were then cut neatly and packed in sample holder mentioned above. Cu broad focus tube at 40 kV and 40 mA was used with a divergence slit of 1 degree and scatter slit of 1 degree. A curved graphic monochromator was used with a receiving slit of 0.2 mm. Scanning speed and interval of data collection was 0.01 degree and 2 θ /sec respectively. The diffraction patterns were recorded for 2 θ between 4 to 80°.

3.5.6. Scanning electron microscopy (SEM)

SEM images of pure heteropolyacids as well as that of synthesized solids were taken. Small amounts of the samples were spread on adhesive conductive copper tapes attached to a sample holder and examined with the JEOL (Model 5800LV SEM) scanning electron microscope with low vacuum capability. In case of membranes, the samples were first frozen into liquid nitrogen. Small pieces of swollen samples were then broken and attached to a sample holder and examined with the microscope equipped with an energy dispersive spectrometer (EDS) with low vacuum capability. Fresh broken surfaces of the samples were spray coated with a thin layer of Au/Pd prior to viewing in SEM. All of the images were taken in backscattered electron (BEI) mode.

Results and discussion: Solid proton conductors

4.1. Development of solid proton conductors

Experimental results of solid proton conductors are presented and discussed here. Results are discussed for powders samples with different weight percentages of heteropolyacids loaded into Y-zeolite and MCM41 as well as prepared composite polymeric membranes. First, the results for powder sample have been presented followed by the results for composite membranes. The results for synthesized powders samples are presented in the following sequence:

- 4.1.1. Flow study
- 4.1.2. Proton conductivity measurement through Impedance Spectroscopy
- 4.1.3. FTIR analysis
- 4.1.4. XRD analysis
- 4.1.5. SEM technique

4.1.1. Flow Study

The flow studies were carried out only on the samples containing 40 and 50% heteropolyacids respectively since impedance spectroscopy technique confirmed their

highest proton conductivities for the samples containing 40 and 50 weight percentages of heteropolyacids loaded on Y-zeolite as well as MCM41. Results of leaching study showed strong interaction of heteropolyacids and Y-zeolite. Table 4-1 shows the amounts of tungsten and molybdenum detected through inductively coupled plasma (ICP) analysis and atomic absorption spectrophotometer (AAS) techniques. The results show that TPA is relatively strongly bound to the zeolite as compared with that of MPA. However, overall leaching of the metals in both the cases is very small comparing the amount of HPAs loaded, i.e., 40 and 50 wt. %. The amounts of tungsten and molybdenum were found to be decreasing with increasing time intervals. The leaching studies were carried out on high HPA loaded samples containing 40 and 50% heteropolyacids respectively since with these percentages samples were found to be more proton conductive. The initial concentrations of tungsten and molybdenum at various time intervals are given in [Table 4-1](#). It is clear from [Table 4-1](#) that the amount leached out through the leaching studies is quite negligible as compared to loaded amounts of heteropolyacids onto Y-zeolites. In case of TPA loaded Y-zeolite, it was found out that 9 % of the initial amount of TPA was leached out in case of solid powder containing 40 wt. % TPA, while 10 % of the initial amount of TPA was leached out of solid powder containing 50 wt. % TPA. In case of MPA loaded Y-zeolite, It was found out that 20 % of the initial amount of MPA was leached out in case of solid powder containing 40 wt. % MPA, while 19 % of the initial amount of MPA was leached out of solid powder containing 50 wt. % MPA. Therefore, leaching study confirmed that the material leached out through the experiment was still acceptably low and hence significant loading of HPAs onto the Y-zeolite structures was ensured. It is also clear from [Table 4-1](#) that the leached amounts become

few ppm after 4 hours of continuous flow through the prepared solid powders. Actually the total run time for each leaching experiment was 24 hours but since after 4 hours there was no significant leaching observed at other time intervals above 4 hours, so results only upto 4 hours have been reported here. Leaching results have been depicted graphically in [Figure 1](#). This appears interesting, because some applications of solid electrolytes involve the direct exposure of materials to liquid water for long periods of time such as in the case of direct methanol fuel cell applications.

Similar trends were also observed with solids prepared from the loading of heteropolyacids onto MCM41. [Table 4-2](#) shows the initial amounts of tungsten and molybdenum detected at various time intervals through inductively coupled plasma (ICP) analysis and atomic absorption spectrophotometer (AAS) techniques. The amounts of tungsten and molybdenum were found to be decreasing with increasing time intervals. In case of TPA loaded MCM41, it was found out that 8 % of the initial amount of TPA was leached out in case of solid powder containing 40 wt. % TPA, while 7 % of the initial amount of TPA was leached out of solid powder containing 50 wt. % TPA. That means 36.8 and 46.5 wt. % of TPA was still present on MCM41 in case of 40 and 50 wt. % initial loading of TPA on MCM41 respectively. In case of MPA loaded MCM41, It was found out that 18 % of the initial amount of MPA was leached out in case of solid powder containing 40 wt. % MPA, while 14 % of the initial amount of MPA was leached out of solid powder containing 50 wt. % MPA. That means 32.8 and 43 wt. % of MPA was still present on MCM41 in case of 40 and 50 wt. % initial loading of MPA on MCM41 respectively.

Table 4-1 Amount of tungsten and molybdenum leached out through flow experiments

No. of hours	Y-T1			Y-T2			Y-M1			Y-M2		
	C, mg/lit	F, lit/hr	CF, mg/hr									
0	97.7	0.3	29.31	107.3	0.3	32.19	435	0.3	130.5	467	0.3	140.1
1	36	0.3	10.8	56	0.3	16.8	87	0.3	26.1	103	0.3	30.9
2	23.8	0.3	7.14	33.8	0.3	10.14	22	0.3	6.6	29	0.3	8.7
3	16.8	0.3	5.04	26.3	0.3	7.89	7.4	0.3	2.22	9.8	0.3	2.94
4	16.1	0.3	4.83	24.2	0.3	7.26	6.9	0.3	2.07	9.4	0.3	2.82

* where Y-T1 = Y-zeolite + 40% TPA, Y-T2 = Y-zeolite + 50% TPA, Y-M1 = Y-zeolite + 40% MPA and Y-M2 = Y-zeolite + 50% MPA and C is the concentration of heteropolyacids leached in mg/lit, F is the flow rate of water through the U-tube and CF is the mass flow rate of the HPA at different time intervals.

Table 4-2 Flow study data for the amounts of tungsten and molybdenum leached out from TPA and MPA loaded MCM41

No. of hours	M41-T1			M41-T2			M41-M1			M41-M2		
	C, mg/lit	F, lit/hr	CF, mg/hr									
0	81.5	0.3	24.45	92.9	0.3	27.87	366	0.3	109.8	500	0.3	150
1	32.7	0.3	9.81	34.6	0.3	10.38	72	0.3	21.6	28	0.3	8.4
2	19.4	0.3	5.82	22.1	0.3	6.63	18	0.3	5.4	11	0.3	3.3
3	12.8	0.3	3.84	15.2	0.3	4.56	4.5	0.3	1.35	4.7	0.3	1.41
4	11.1	0.3	3.33	14.5	0.3	4.35	4.1	0.3	1.23	4.5	0.3	1.35

* Where M41-T1 = MCM-41 + 40% TPA, M41-T2 = MCM-41 + 50% TPA, M41-M1 = MCM-41 + 40% MPA and M41-M2 = MCM-41 + 50% MPA

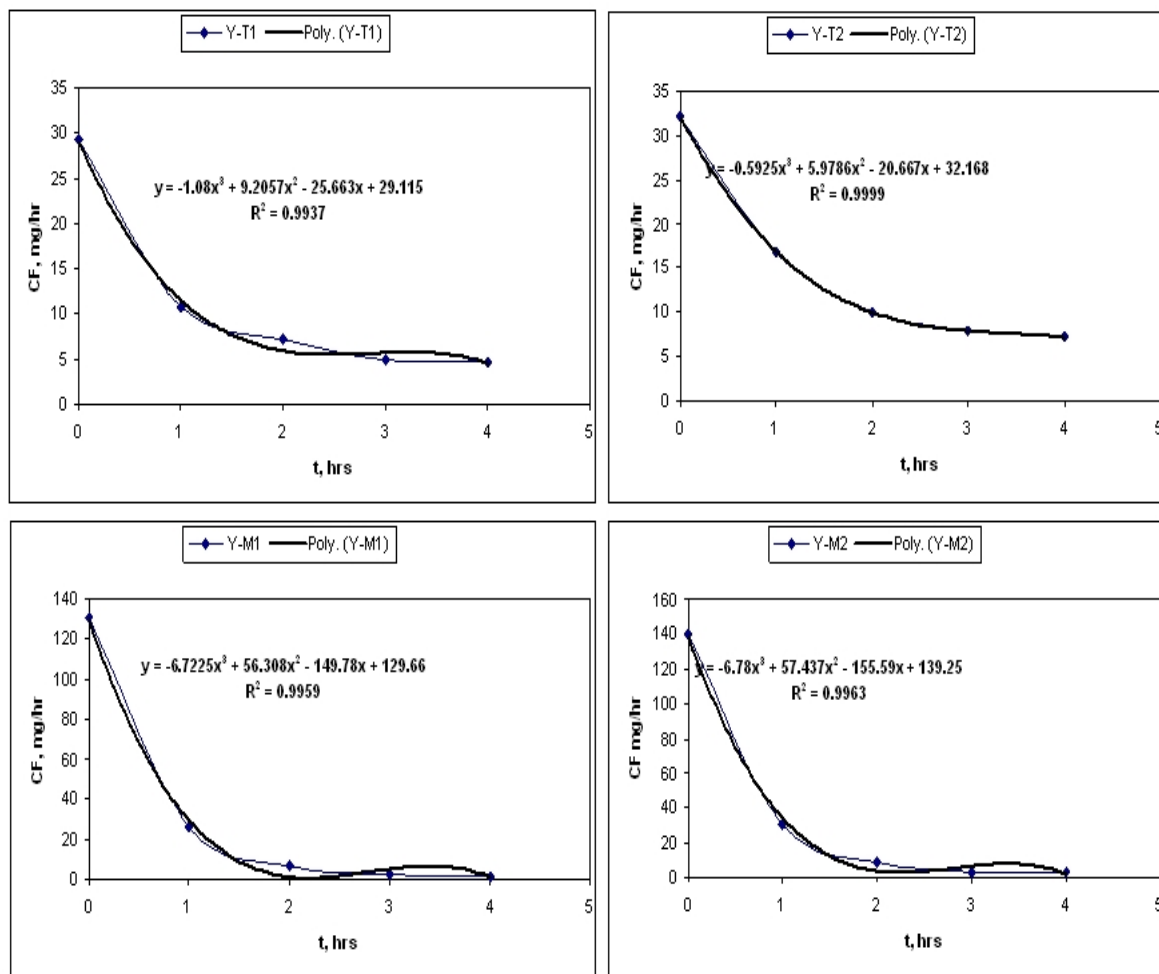


Figure 4-1 Leaching plots for heteropolyacids loaded Y-zeolite with respect to time

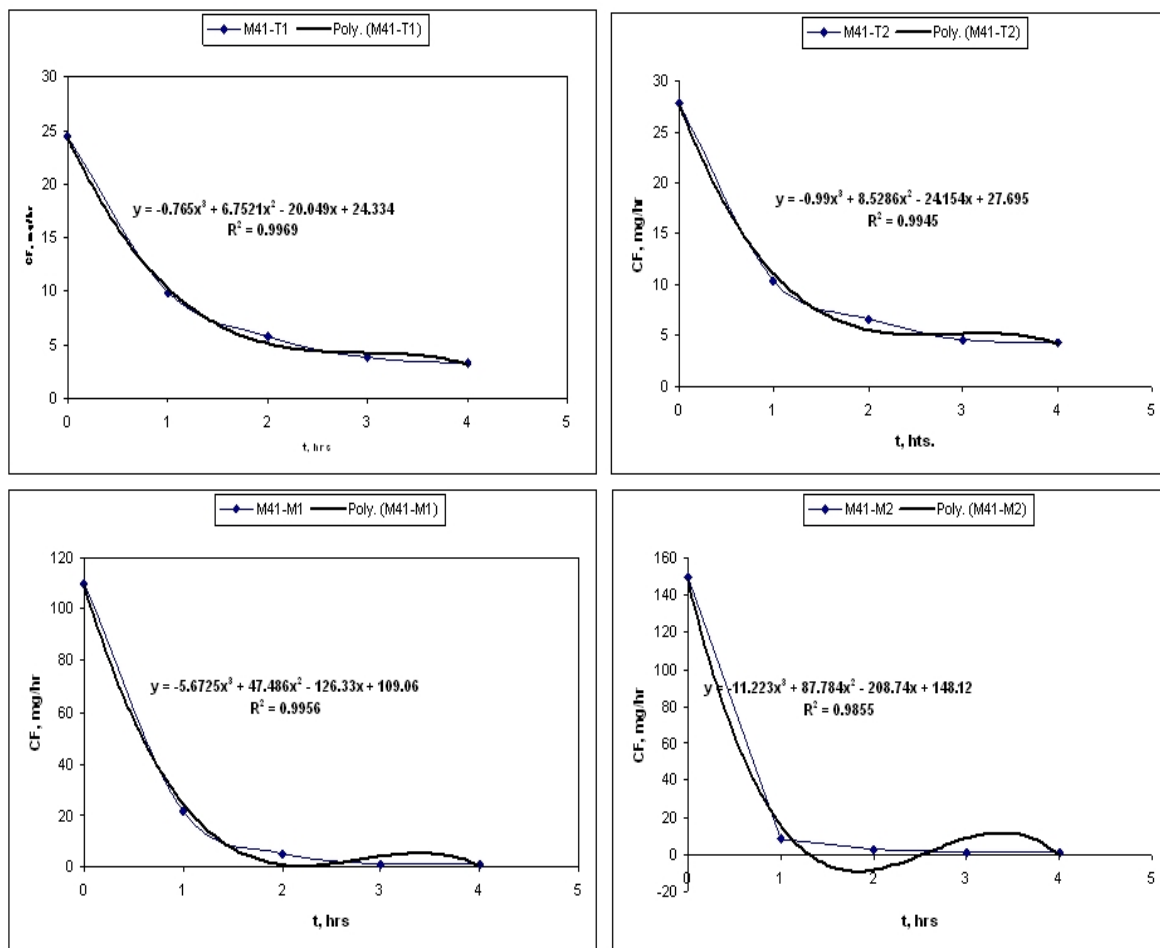


Figure 4-2 Leaching plots for heteropolyacids loaded MCM41 with respect to time

4.1.2. Proton conductivity through Impedance Spectrometry

Proton conductivity through impedance spectroscopy (IS) measurements were determined at ambient temperature over the frequency range $0.1-1.2 \times 10^6$ Hz with an oscillating voltage of 10 mV, using a PC controlled SI 5210 impedance/gain-phase analyzer. The impedance data were corrected for contribution from the empty and short circuited cell. Proton conductivities for pure zeolite, pure tungstophosphoric acid (TPA), pure molybdophosphoric acid (MPA) and synthesized powders from Y-zeolite with different weight percentages of TPA and MPA were measured. Proton conductivities as well as resistances observed by the solids at room temperature (under dry conditions) for all of the above-described materials are given in [Table 4-3](#). It is evident from [Table 4-3](#) that as the wt. percentages of TPA and MPA increase in Y-zeolite, the conductivity also increases which accords with initial conjecture. Pure Y-zeolite with 20, 30, 40 and 50 wt. % TPA exhibit conductivities at 20 °C of 0.016, 0.021, 0.025, 0.0301 and 0.043 mS/cm, respectively, while, pure zeolite with 20, 30, 40 and 50 wt. percent MPA exhibit conductivities at 20 °C of 0.016, 0.0179, 0.0181, 0.0301 and 0.0312 mS/cm, respectively. Proton conductivity data for Y-zeolite with different weight percentages of TPA and MPA is plotted in [Figure 4-3](#) and [Figure 4-4](#) to depict the proton conductivities of Y-zeolite with increasing wt. percentage of heteropolyacids. Proton conductivity in case of TPA loading is higher as compared to MPA loading. This is because TPA is highly proton conductive as compared to MPA. Proton conductivity with 50 wt. % loading of heteropolyacids was found to be highest in both the cases, however loading of more than 50 wt. % TPA and MPA into Y-zeolite gave anomalous results, while there was no significant difference in conductivity for 40 and 50 wt. % loading of MPA into Y-zeolite.

Table 4-3 Resistances and conductivity values of composite powder samples done and analyzed at ambient conditions

Powder sample specification	Resistances in $\Omega\text{-cm}^2$	Conductivity in mS/cm
Y	6507	0.016
TPA	29.68	3.37
MPA	1186	0.084
YT1	4843	0.021
YT2	3946	0.025
Y-T1	3315	0.0301
Y-T2	2337	0.043
YM1	5557	0.0179
YM2	5520	0.0181
Y-M1	4315	0.0301
Y-M2	4205	0.0312

* Where Y = Y-zeolite, TPA = tungstophosphoric acid, MPA = molybdophosphoric acid, YT1 = Y-zeolite + 20% TPA, YT2 = Y-zeolite + 30% TPA, Y-T1 = Y-zeolite + 40% TPA, Y-T2, YM1 = Y-zeolite + 20% MPA, YM2 = Y-zeolite + 30% MPA, Y-M1 = Y-zeolite + 40% MPA and Y-M2 = Y-zeolite + 50% MPA

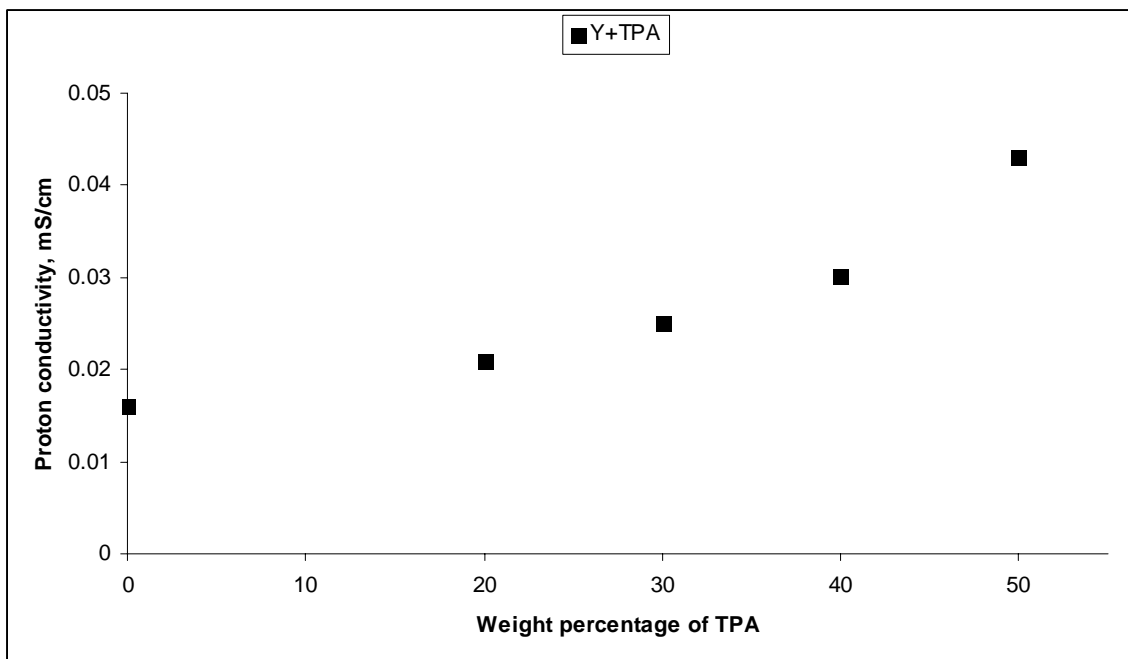


Figure 4-3 Variation of proton conductivity of Y-zeolite with increasing percentage of TPA

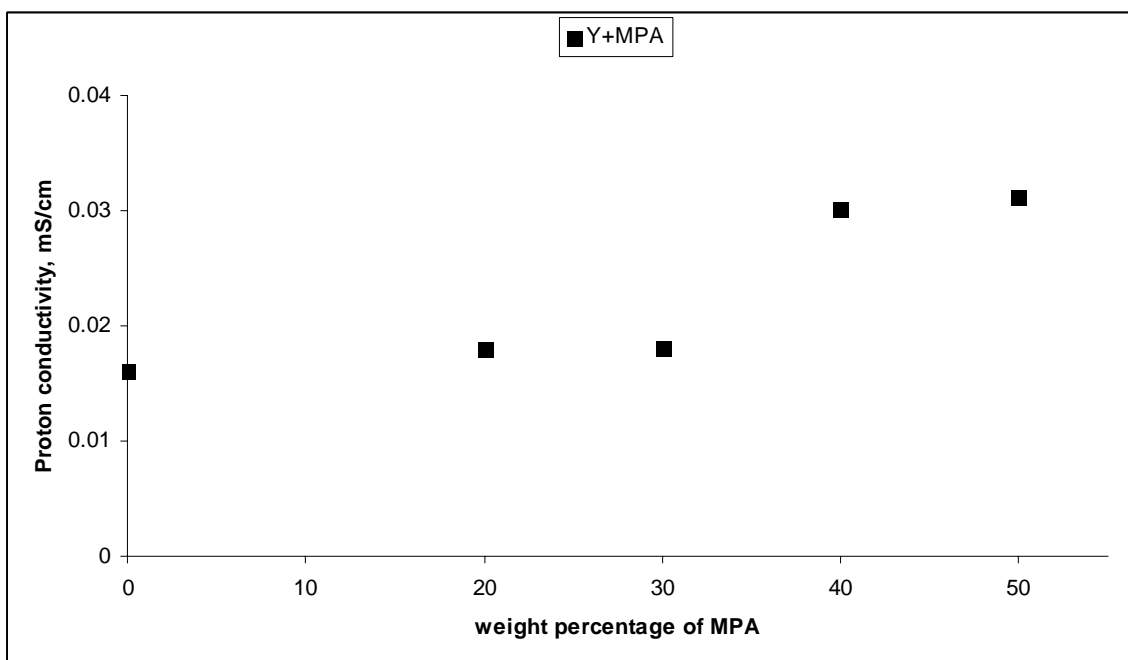


Figure 4-4 Variation of proton conductivity of Y-zeolite with increasing percentage of MPA

It is well known that proton conductivity is strongly a water promoted phenomena and a considerable increase in protonic conductivities was observed for all the prepared solids with increasing water contents. Since samples of Y-zeolite with 40 and 50 % TPA and MPA showed highest proton conductivity, proton conductivity measurements with varying percentages of added water were carried out for these samples. [Table 4-4](#) shows the conductivity variation with water content in Y-zeolite with 40 and 50 wt. % of TPA and MPA. From [Table 4-4](#), it is evident that proton conductivity shoots to very high values at 30 and 40 wt. % water amounts. Water percentages above 40 wt. % were also tried but the problem arose in case of water amounts larger than 40 wt. % as all of the prepared solid composite powders started to flow. This made the handling of solids very difficult and also made the measurements questionable. Nevertheless, with 40 wt. % water contents, samples tested still showed encouraging results for both of the cases i.e. TPA and MPA loaded Y-zeolites.

Table 4-4 Resistances and conductivities values of powder samples with varying percentages of water (weight percent).

Sample specification	Resistances, $\Omega\text{-cm}^2$				Proton conductivity, mS/cm			
	% of added water				% o added water			
	10%	20%	30%	40%	10%	20%	30%	40%
Y-T1	1904	216.3	50.09	14.31	0.053	0.4653	1.996	6.988
Y-T2	1973	250.6	40.08	9.169	0.051	0.399	2.495	10.91
Y-M1	2483	1763	86.09	12.49	0.040	0.057	1.162	8.01
Y-M2	926	650.8	34.81	11.33	0.11	0.154	2.873	8.83

Figure 4-5 and Figure 4-6 show the conductivity variations with added wt. % of water for Y-zeolite loaded with 40 and 50 weight percent of TPA and MPA respectively. It is evident from the graphs that as the wt. % water goes on increasing in the solid powder, conductivities also start increasing. There is significant change in the conductivities at about 20 % addition of water, however it jumps to still high values at 30 wt. % water and exceptionally high at 40 wt. % water for both the cases. It can be seen from Figures 4-5 and 4-6 that conductivity of these solid powders is very sensitive to water absorption and increases with the variation of water contents appreciably. It changes for instance from 0.051 mS/cm for MPA loaded Y zeolite at 10 % water content to 11.0 mS/cm for 40 wt. % water content. As is known the proton conduction is a water assisted phenomenon, and water has a profound effect on proton conductivity. Higher water generates a more solvated species, which is needed for high proton conductivity. In all cases proton transfer is obviously associated with acid sites which take water molecule from one site and transfer it to another site. Hydration allows bridging acidic sites assisting ion hopping and providing additional charge carriers [4]. Hence, protonic conductivity increases with increasing water content for all solid proton conducting hydrates. Therefore, protonic conductivity increases with increasing water content for all solid proton conducting hydrates [14].

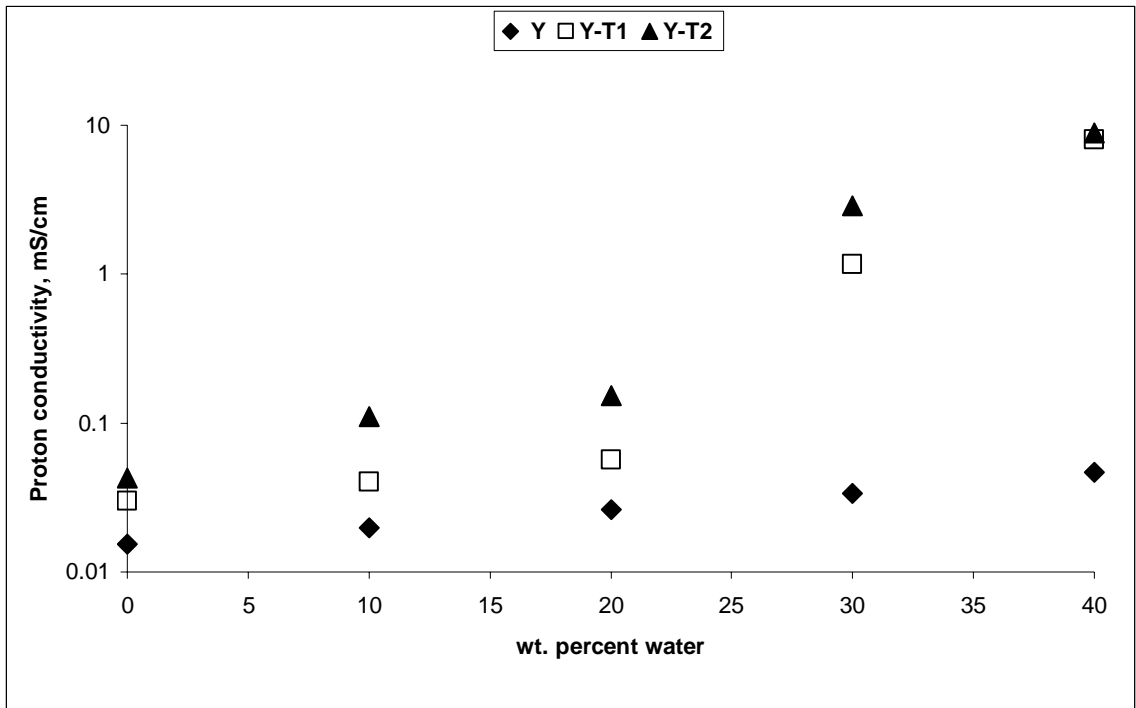


Figure 4-5 Proton conductivity variation with increasing water content for (a) pure Y-zeolite; (b) Y-zeolite+40% TPA and (c) Y-zeolite+50% TPA.

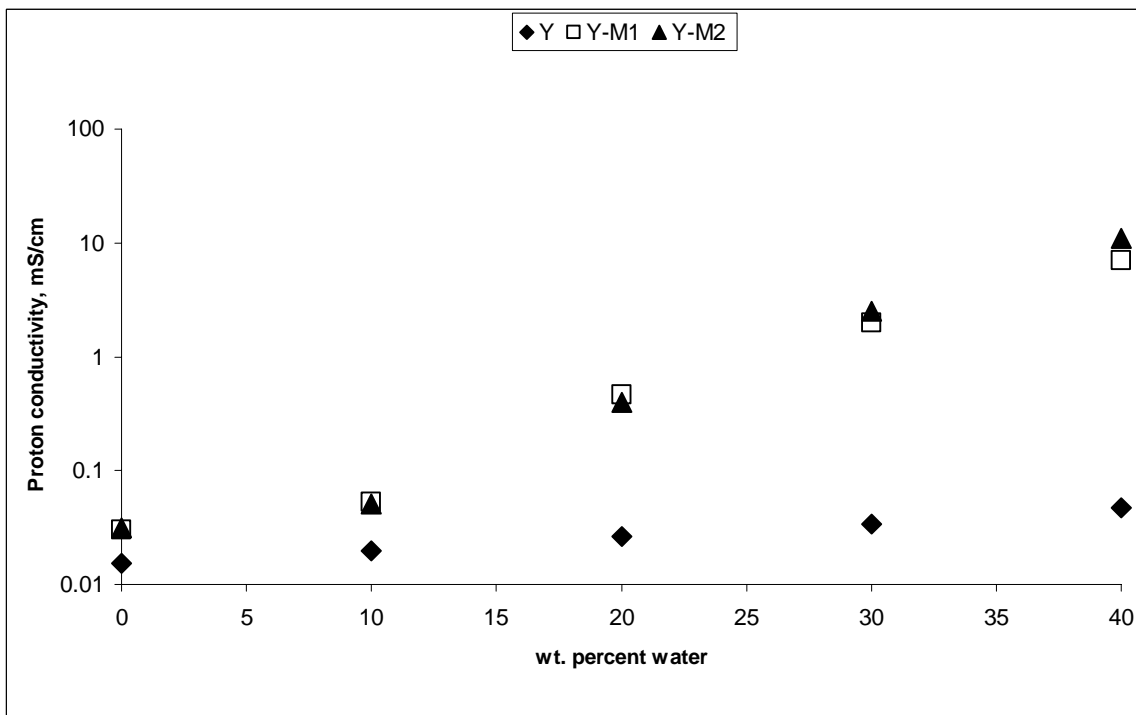


Figure 4-6 Proton conductivity variation with increasing water content for (a) pure Y-zeolite; (b) Y-zeolite+40% MPA and (c) Y-zeolite+50% MPA.

Proton conductivities for pure MCM41, pure tungstophosphoric acid (TPA), pure molybdophosphoric acid (MPA) and synthesized powders from MCM41 with different weight percentages of TPA and MPA were calculated using equation A (Appendix A). Proton conductivities as well as resistances observed by the solids at room temperature for all of the above-described materials are given in [Table 4-5](#), which indicates that as weight percentages of heteropolyacids increases in MCM41, proton conductivity also increases. For example, pure MCM41 with 40 and 50 wt. % of TPA exhibit conductivities at 20 °C of 0.023 and 0.033 mS/cm respectively, while pure MCM41 with 40 and 50 wt. % MPA exhibit conductivities at 20 °C of 0.019 and 0.031 mS/cm respectively. For pure MCM41 the proton conductivity at room temperature (20 °C) was found to be 0.011 mS/cm which is modified to considerably high values by loading heteropolyacids into the MCM41 material structure. [Table 4-6](#) shows the conductivity values of heteropolyacids loaded MCM41 with varying percentages of water. It is clearly evident from the table that as the amount of water increases, proton conductivity of the solid powder increases and it is more prominent at higher amounts of water.

Table 4-5 Resistances and conductivity values of composite powder samples analyzed at ambient conditions.

Powder sample specification	Resistances in ohm-cm ²	Conductivity in mS/cm
M41	9067	0.011
TPA	29.68	3.37
MPA	1186	0.084
M41-T1	5336	0.0186
M41-T2	5026	0.0197
M41-M1	6366	0.0157
M41-M2	5277	0.0189

*where M41 = MCM-41; TPA = tungstophosphoric acid; MPA = molybdophosphoric acid; M41-T1=MCM41+40 % TPA; M41-T2=MCM41+50 % TPA; M41-M1=MCM41+40 % MPA and M41-M2=MCM41+50 % MPA.

Table 4-6 Proton conductivity values of solid powders synthesized from MCM41 with MPA and TPA for different wt. percentages of water

Sample Specification	Resistances, Ω -cm ²						Proton conductivity, mS/cm					
	Weight percentages of added water						Weight percentages of added water					
	0%	10%	20%	30%	40%	50%	0%	10%	20%	30%	40%	50%
M41-T1	5336	2629	984.7	598.3	117.3	17.1	0.019	0.038	0.101	0.167	0.853	5.85
M41-T2	5026	3061	2749	107.4	28.31	9.472	0.02	0.033	0.036	0.931	3.532	10.56
M41-M1	6366	4941	3769	1681	747.4	153.3	0.016	0.020	0.027	0.059	0.134	0.652
M41-M2	5277	4271	2229	940.3	358.1	98.99	0.019	0.023	0.045	0.106	0.279	1.01

Figures 4-7 and 4-8 show the conductivity variations with wt. % of added water for MCM41 loaded with 40 and 50 weight percent of TPA and MPA respectively. It is evident from the graphs that almost similar trends were found for the conductivities in these cases, however the magnitude of conductivities was found to be lower than that of solids containing Y-zeolite, since MCM41 is virtually non-conductive in its native state while Y-zeolite possesses some conductivity. It can be seen from these figures that conductivity of these composite powders is very responsive to water absorption and increases appreciably with varying percentages of water. It changes for instance from 1.98×10^{-2} mS/cm for dry MCM-41/TPA to 10.6 mS/cm for 50 wt. % water content. Also, it was observed for all the solid powders that conductivity increase is marginal at low water content upto 20 % but above 30 % it jumps to very high values to more than ten to fifteen times than at 30 wt. % water content.

The samples of TPA/MCM-41 display higher conductivity than MPA/MCM-41 samples as TPA is the strongest HPA in the Keggin series and possessed highest conductivity. In pure MCM-41 sample, there are no acid functions as those of HPAs so its conductivity did not change appreciably with increase in water content. However, a large number of silanol groups present in the MCM-41 structure may be desirable for designing excellent proton conductor [55]. There could be a slight compromise as far as proton conductivity is concerned in case of solid proton conductors from MCM41 but other major factors e.g. uniform pore size, high thermal and structural stability (except in FCC catalysts) and superlative mechanical properties promise MCM41 material to be one of the potential candidate in the development of solid proton conductors.

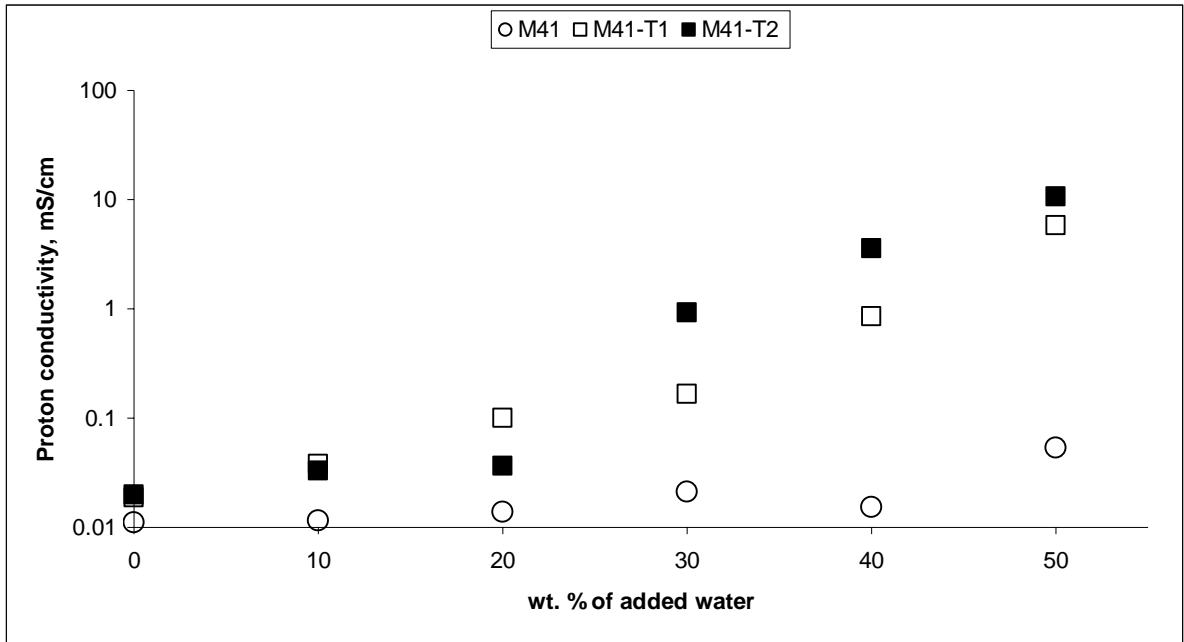


Figure 4-7 Proton conductivity vs. wt. percentage of water plot for (a) Pure MCM41; (b) MCM41+40 % TPA and (c) MCM41+50 % TPA.

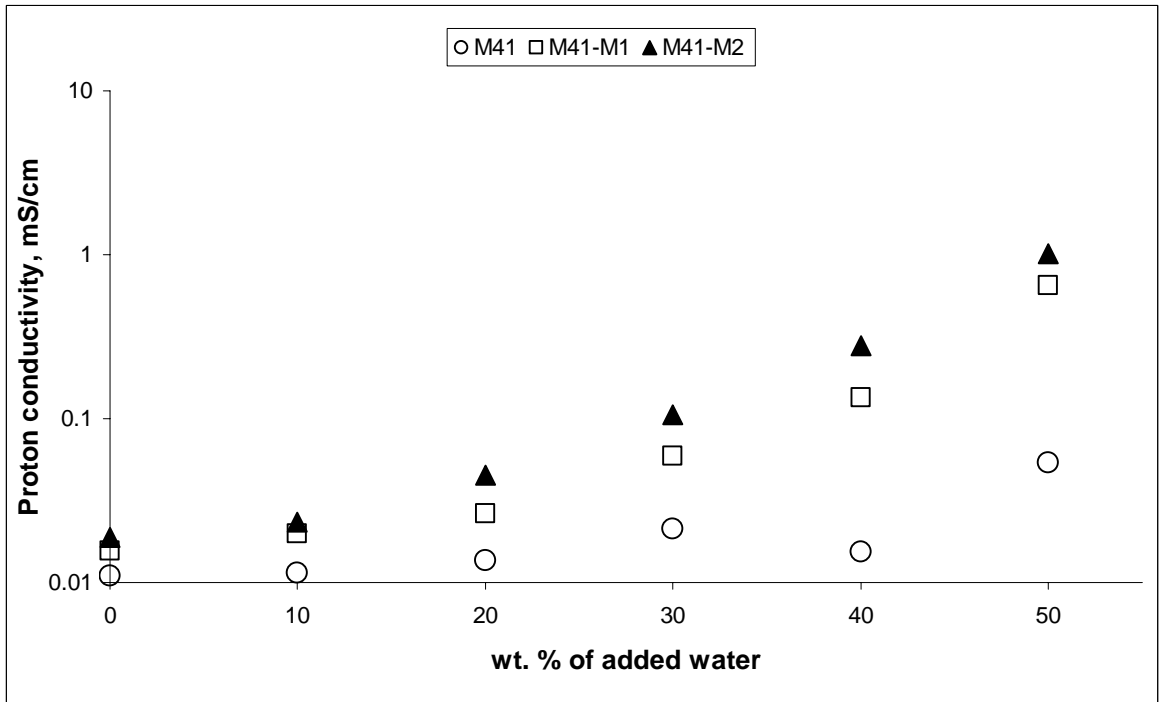


Figure 4-8 Proton conductivity vs. wt. percentage of water plot for (a) Pure MCM41; (b) MCM41+40 % MPA and (c) MCM41+50 % MPA.

4.1.3. FTIR Analysis

FTIR spectroscopy is an experimental tool used for detecting changes in the coordination and configuration of molecular species in a system. The underlying reason is that electromagnetic radiation in the infrared region has the same frequency as molecular vibrations. FTIR spectra confirm the existence of TPA and MPA on the solid composite material. [Figure 4-9](#) shows the infrared spectra of the pure tungstophosphoric acid (TPA) powders and TPA/Y-zeolite composite powders while [Figure 4-10](#) shows the IR spectra of the pure molybdophosphoric acid (MPA) powders and MPA/Y-zeolite composite powders. For pure TPA, characteristic peaks of its keggin structure were observed at 980 and 888 cm^{-1} , respectively [76]. In the IR spectrum of the solid composite solids, the characteristic peaks of the keggin anion were also observed. In addition, we have observed a small shift of (W-O_b-W) band from 888 cm^{-1} in pure TPA to 896 cm^{-1} in the composite powder with 40 wt. % TPA, which may be due to various functional group interactions [76,77].

In case of molybdophosphoric acid loading into Y-zeolite, six characteristic peaks of its keggin structure were observed at 1062, 956 and 806 cm^{-1} , respectively. In the IR spectrum of the solid composite solids with MPA, a small shift of (Mo-O_b-Mo) band from 956 cm^{-1} in pure MPA to 960 cm^{-1} in the composite solid powder containing 50 wt. % MPA was observed. The frequency shift of about 8 and 10 cm^{-1} in case of TPA loading, while frequency shift of about 4 cm^{-1} in case of MPA loading reveals that the keggin structure of TPA and MPA interacts with Y-zeolite mostly through corner-shared oxygen (O_b). So from the IR spectra of the solid composite powders, it is found that the

keggin structure characteristic of the heteropoly anions ($PX_{12}O_{40}^{-3}$) is present in these solid powders which is strongly responsible for the high proton conductivity of heteropolyacids.

Figure 4-11 shows the infrared spectra of the pure tungstophosphoric acid (TPA) powders and TPA/MCM41 composite powders while Figure 4-12 shows the IR spectra of the pure molybdophosphoric acid (MPA) powders and MPA/MCM41 composite powders. For pure TPA, characteristic peaks of its Keggin structure were observed at 980 and 888, cm^{-1} , respectively [78], while MCM41 shows strong IR bands in the range 750-1250 cm^{-1} . To confirm the presence of heteropolyacids onto MCM41 framework, IR spectra of composite powders with 40 wt. % HPAs are also shown in Figure 4-11 and 4-12. It can be observed that the characteristics peaks of tungstophosphoric acid as well as the peaks of MCM41 were also observed in the synthesized solid powders [78]. Pure tungstophosphoric acid shows distinctive, strong IR bands in the range of 500-1200 cm^{-1} while pure MCM41 shows a weak shoulder at about 960 cm^{-1} which broadens to 964 cm^{-1} in case of 40 wt. % loading of TPA loading. This band-broadening can be attributed to heteropoly anion which dominates over the characteristic peaks of MCM41 [51,79]. Characteristics peaks of its keggin structure are also observed in case of MPA loaded MCM41. These peaks are also found in the solid composite powder containing 40 wt. % MPA which confirms the presence of MPA onto MCM41.

The explanation of the FTIR spectra also justifies the impedance spectroscopy measurements. Since MCM41 is barely proton conductive but as we increase the loading

of heteropolyacids into MCM41, the proton conductivity becomes very high in case of 40 and 50 wt. % loading. Almost same behavior is observed for solid composite powders of molybdophosphoric acid loaded into MCM41.

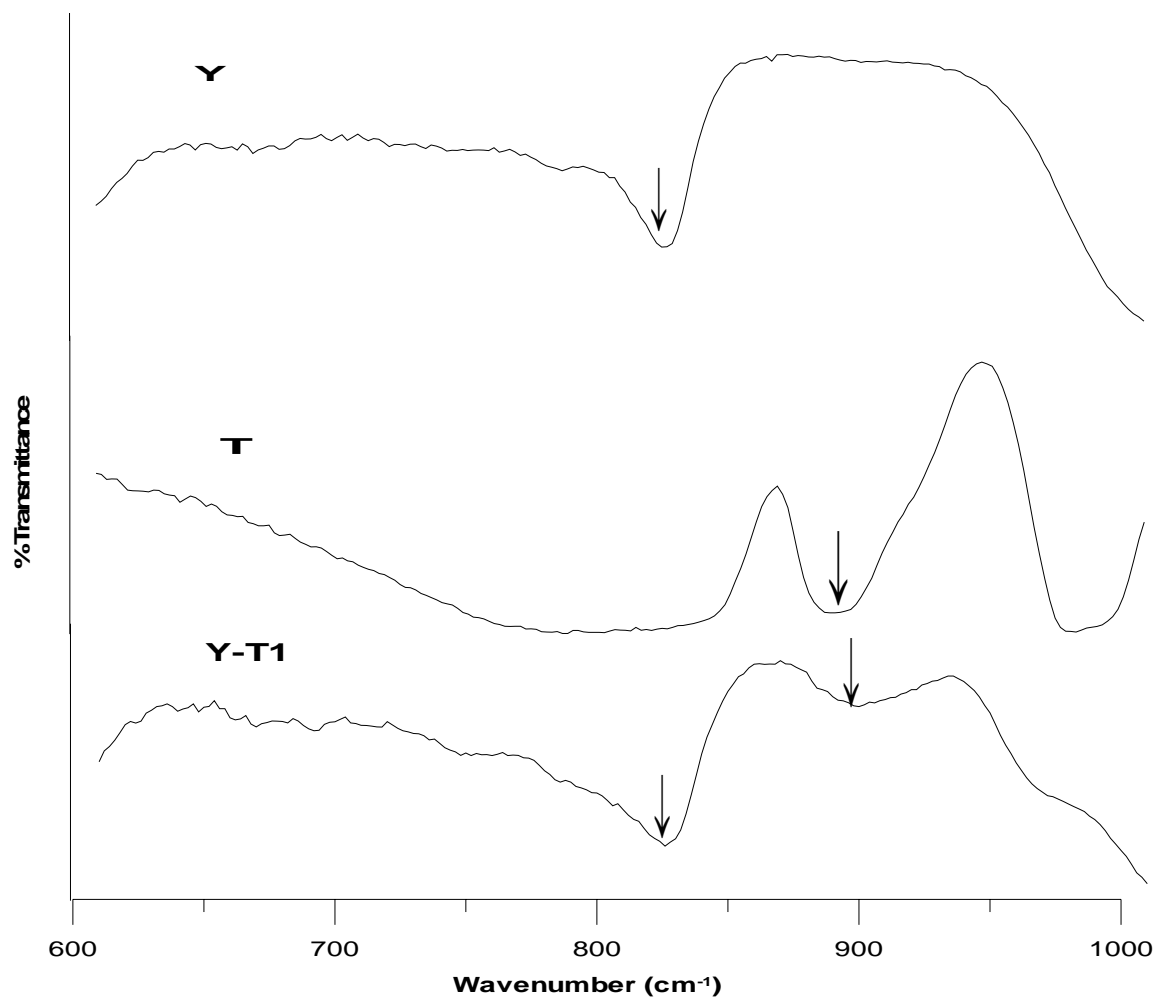


Figure 4-9 FT-IR data comparison for pure Y-zeolite; pure TPA and Y-zeolite+40% TPA.

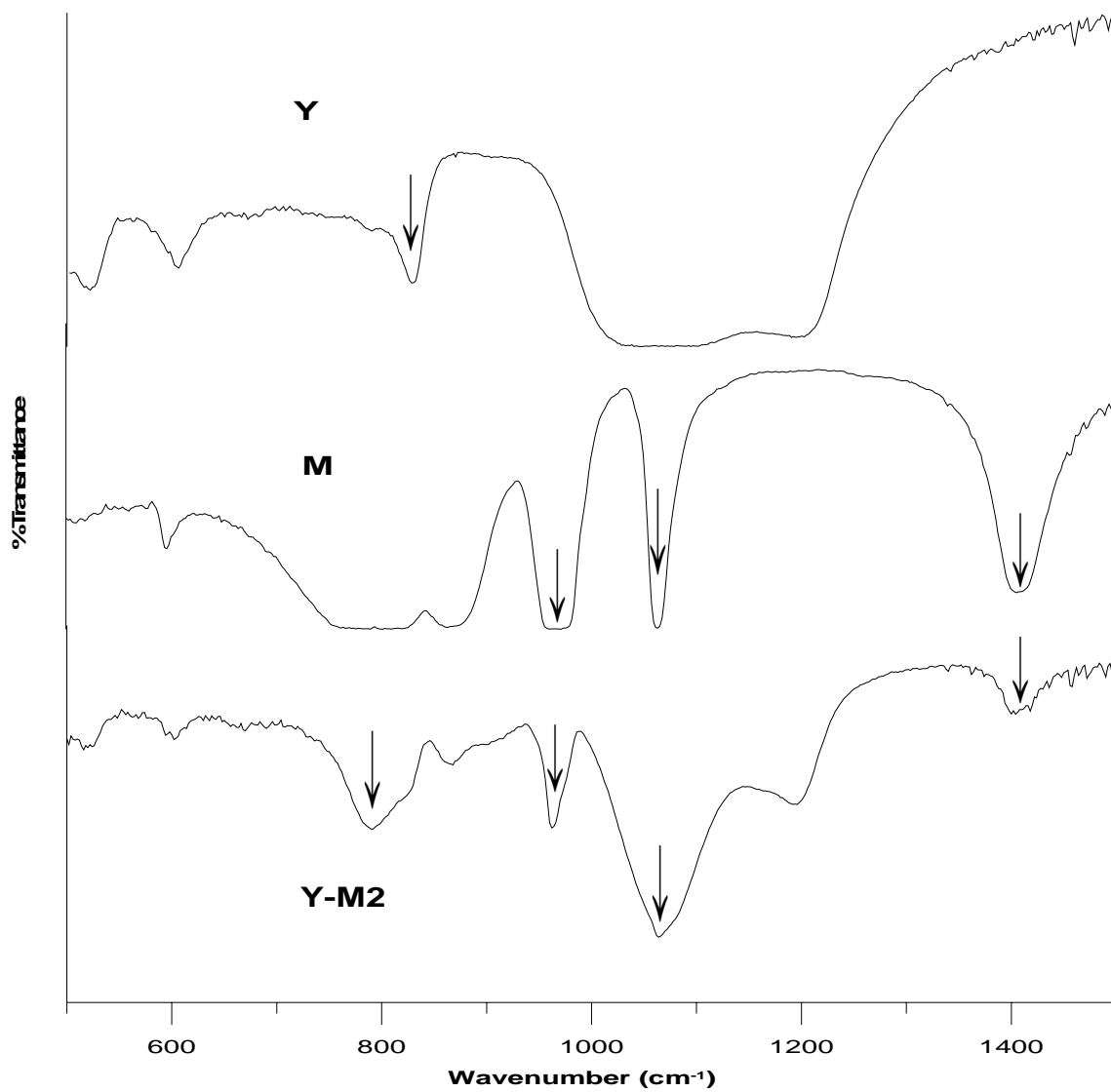


Figure 4-10 FT-IR data comparison for pure Y-zeolite; pure MPA and Y-zeolite+50%MPA.

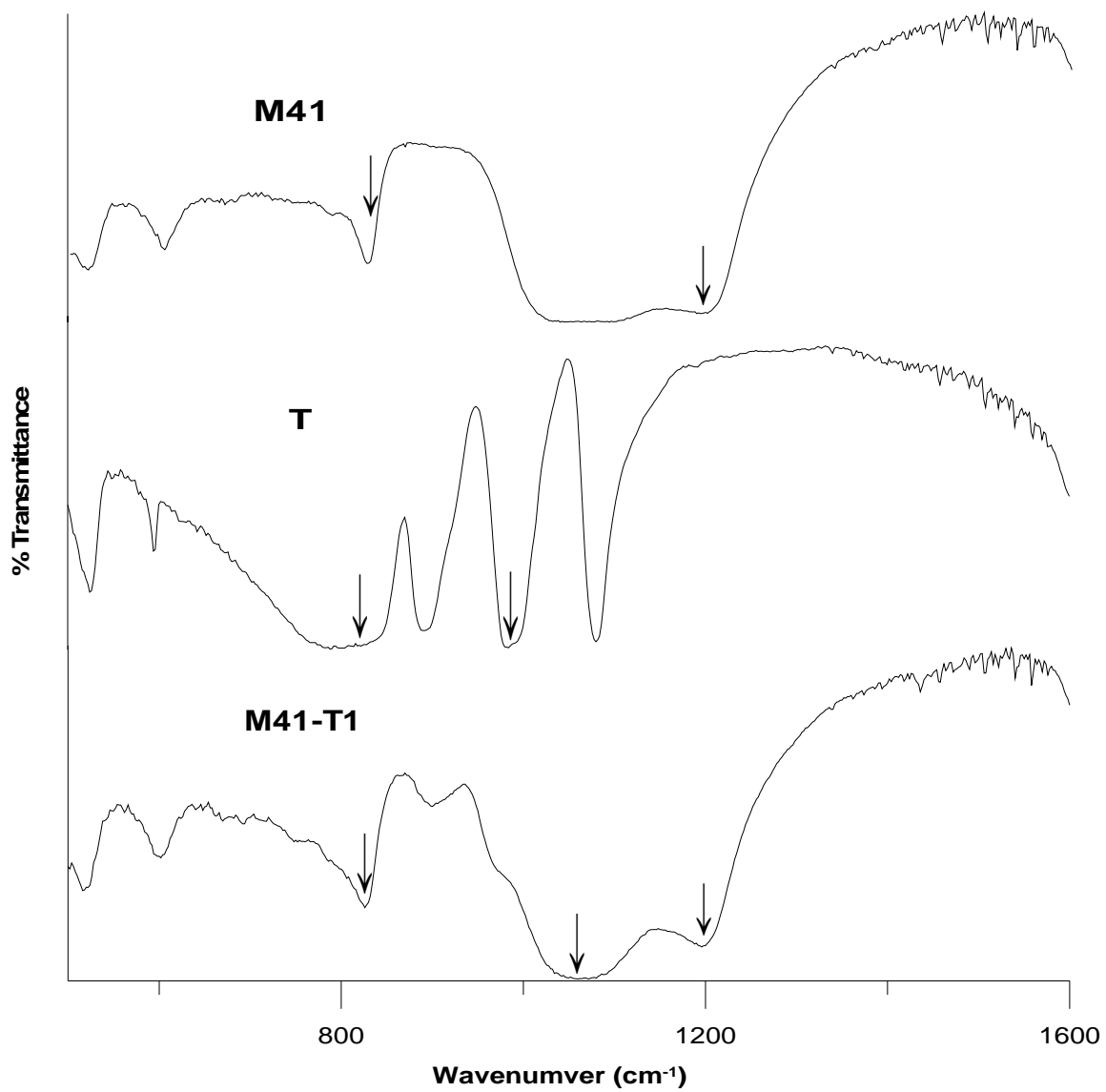


Figure 4-11 FT-IR data comparison for pure MCM41; pure TPA and MCM41+40%TPA.

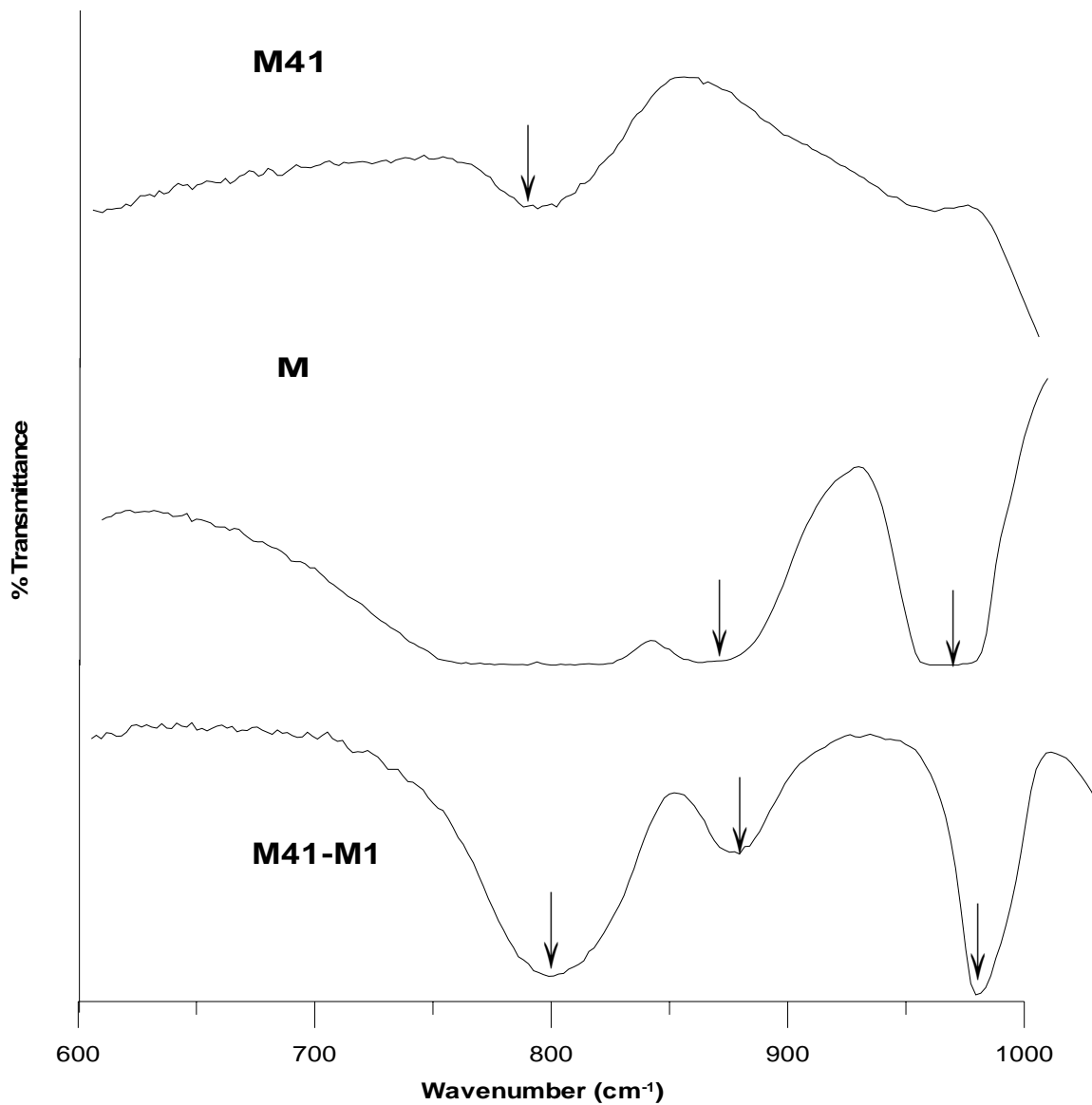


Figure 4-12 FT-IR data comparison for pure MCM41 (top); pure MPA (middle) and MCM41+40%MPA (bottom).

4.1.4. XRD Analysis

Most of the materials are crystalline and hence show symmetry and regularity. This can be made visible by X-ray diffraction producing patterns characteristic of each material. The ground sample is actually made up of thousands of small crystal (crystallites). The random orientation of these crystallites in the specimen ensures that every possible reflecting plane is presented parallel to the specimen surface by at least some crystallites. X-ray powder diffraction (XRD) patterns of pure Y-zeolite, pure TPA and MPA and that of solid composite powders are shown in [Figures 4-13](#) and [4-14](#). Although the intensities are changed due to the influence of Y-zeolite, the characteristic diffraction peaks of pure TPA and pure MPA were still observed in the patterns of solid composite powders containing 50 wt. % of TPA and MPA respectively. This finding proves the existence of the keggin anions in the Y-zeolite matrix again, and is in accordance with the infrared spectra findings.

The XRD patterns of Y-zeolite containing 50 % tungstophosphoric acid (TPA) and molybdophosphoric acid (MPA) show the amorphous states, but they are different from that of pure Y-zeolite whose most intense peak exists at about 15.8° , while in case of TPA the most intense peak exists at about 7.6° [[18,78](#)]. Diffraction patterns of solid composite powder with 50 wt. % TPA shows its most intense peak at about 8.4° which shows the dominance of TPA on Y-zeolite. This above observation is also strengthened by the impedance spectroscopy of the solid composite powders in which solid composite powders are found to be highly proton conductive. Again, in case of MPA loading on Y-zeolite, the most intense peak for MPA exists at about 10.5° , while with 50 wt. % MPA

loaded in Y-zeolite, the most intense peak occurs at about 10.6° . Again for the case of MPA loading into Y-zeolite the particular characteristic of heteropolyacids dominate over Y-zeolite and hence confirms the findings of infrared spectra and impedance spectroscopy.

X-ray diffraction patterns of pure MCM41 and with 40 and 50 wt. % tungstophosphoric acid (TPA) are shown in [Figure 4-15](#). From the figure, it is evident that pure MCM41 is almost amorphous [76], while pure TPA is highly crystalline. However, the diffraction pattern of MCM41 with 50 wt. % TPA is not amorphous and shows crystallinity with less intense peaks as compared to pure TPA. Since MCM41 powder is not crystalline at the atomic level so no reflections at higher angles are observed. Actually the patterns obtained for MCM41 represents poor crystallinity of the material and indicates a distortion of the long range ordering of the mesoporous structure and/or badly built hexagonal arrays. This is perhaps the result of the incorporation of aluminum into the silicate walls, causing structural irregularity.

On the other hand, XRD patterns of MCM41 with 50 wt. % of TPA shows strong and regular peaks in the range of $4-40^\circ$. The strongest peaks for TPA occur at about 6.8° with other significant peaks at $8.4, 10.8, 13.5, 15.96, 17, 18.2, 20.2, 22, 25, 26.4, 27.9, 29$ and 35.64° respectively. However, the XRD pattern of MCM41 with 50 wt. % TPA shows its strongest peak at about 7.8° which is shifted from 6.8° in case of pure TPA. This shift could be due to the specific interactions of MCM41 with TPA and perhaps also due to the heteropoly anion dominance over the characteristics peaks of MCM41. These specific

interactions may be due to the corner-shared oxygen (O_c) present in the heteropoly anion, nevertheless, interaction due to edge-shared (O_e) oxygen atoms can not be ruled out completely.

Similarly from [Figure 4-16](#), it is clear that the XRD pattern of pure molybdophosphoric acid (MPA) shows excellent crystallinity and regularity with a large band of intense peaks among $4-60^\circ$. The strongest peaks occur at about 26.2° with other significant peaks occurring at 10.6 , 15 , 21.4 , 30.5 , 36 , 39.2 , 43.8 , 47.96 and 55.6° respectively. The little shift in the most intense peak from 26.2 to 26.4° was observed in MPA which could be considered negligible. This observation shows that the characteristics peaks of MCM41 do not affect the characteristics keggin structure of MPA and thus confirming the conclusions drawn from impedance spectroscopy measurement which showed considerable high protonic conductivities for MPA loaded MCM41, especially for 40 and 50 wt. % of MPA loaded into MCM41. apart from the most intense peak, other significant peaks of MPA also do not get affected due to MCM41 and hence confirm the hypotheses that the solid composite material with 40 and 50 wt. % of molybdophosphoric acid (MPA) is highly proton conductive with no significant change in crystal structure.

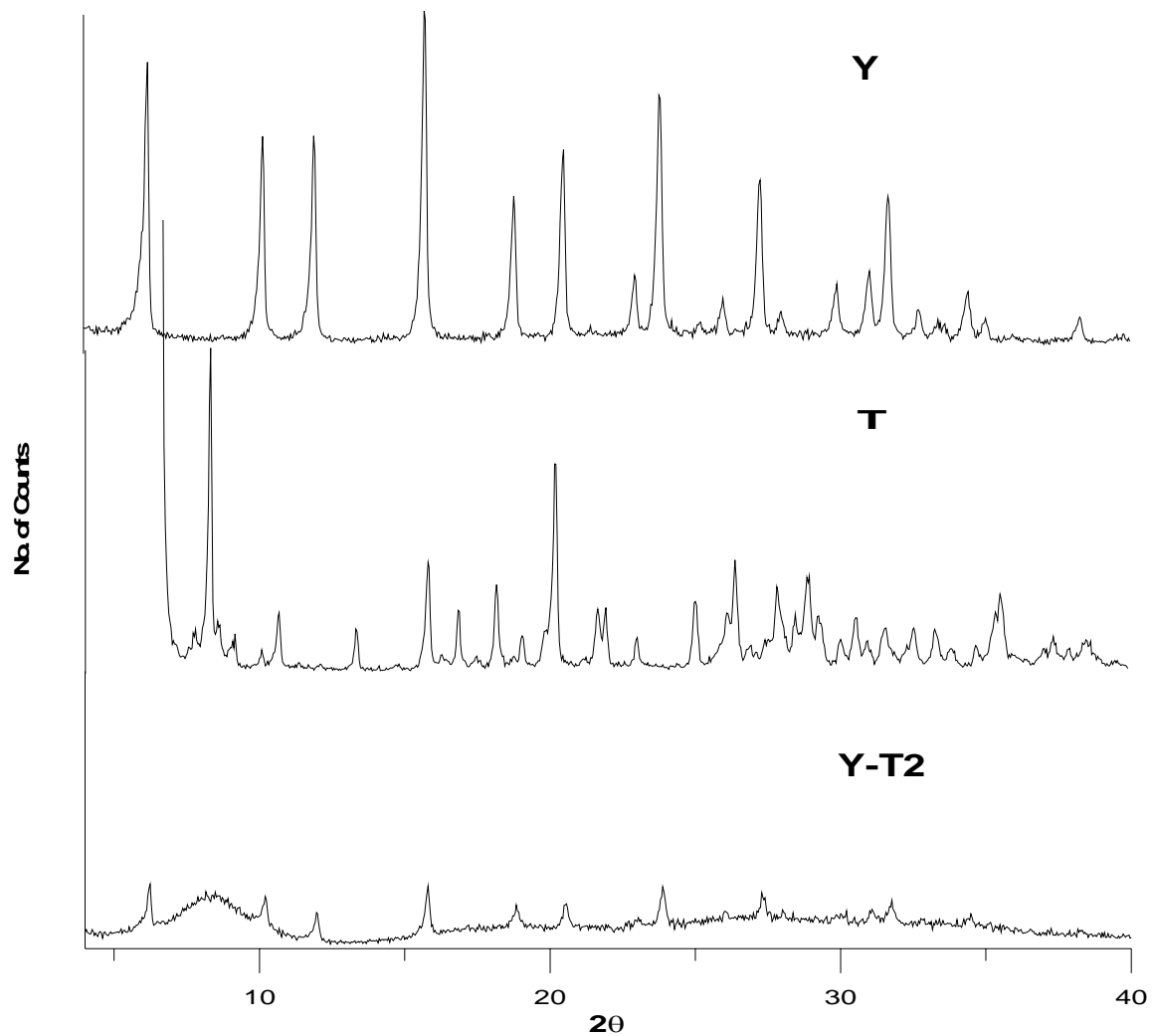


Figure 4-13 XRD data comparison for pure Y-zeolite (top); pure TPA (middle) and Y-zeolite+50%TPA (bottom).

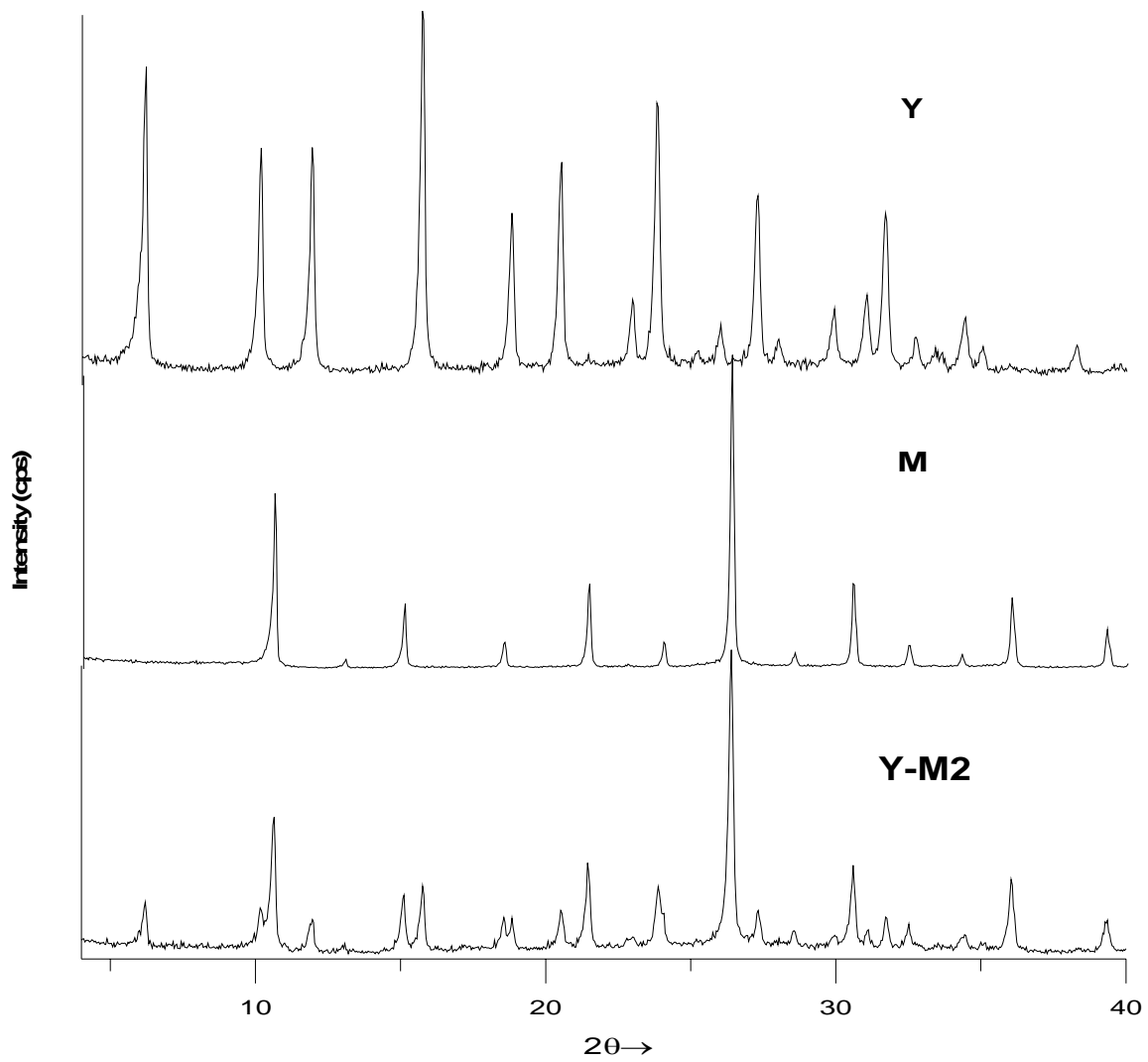


Figure 4-14 XRD data comparison for pure Y-zeolite (top); pure MPA (middle) and Y-zeolite+50 % MPA (bottom).

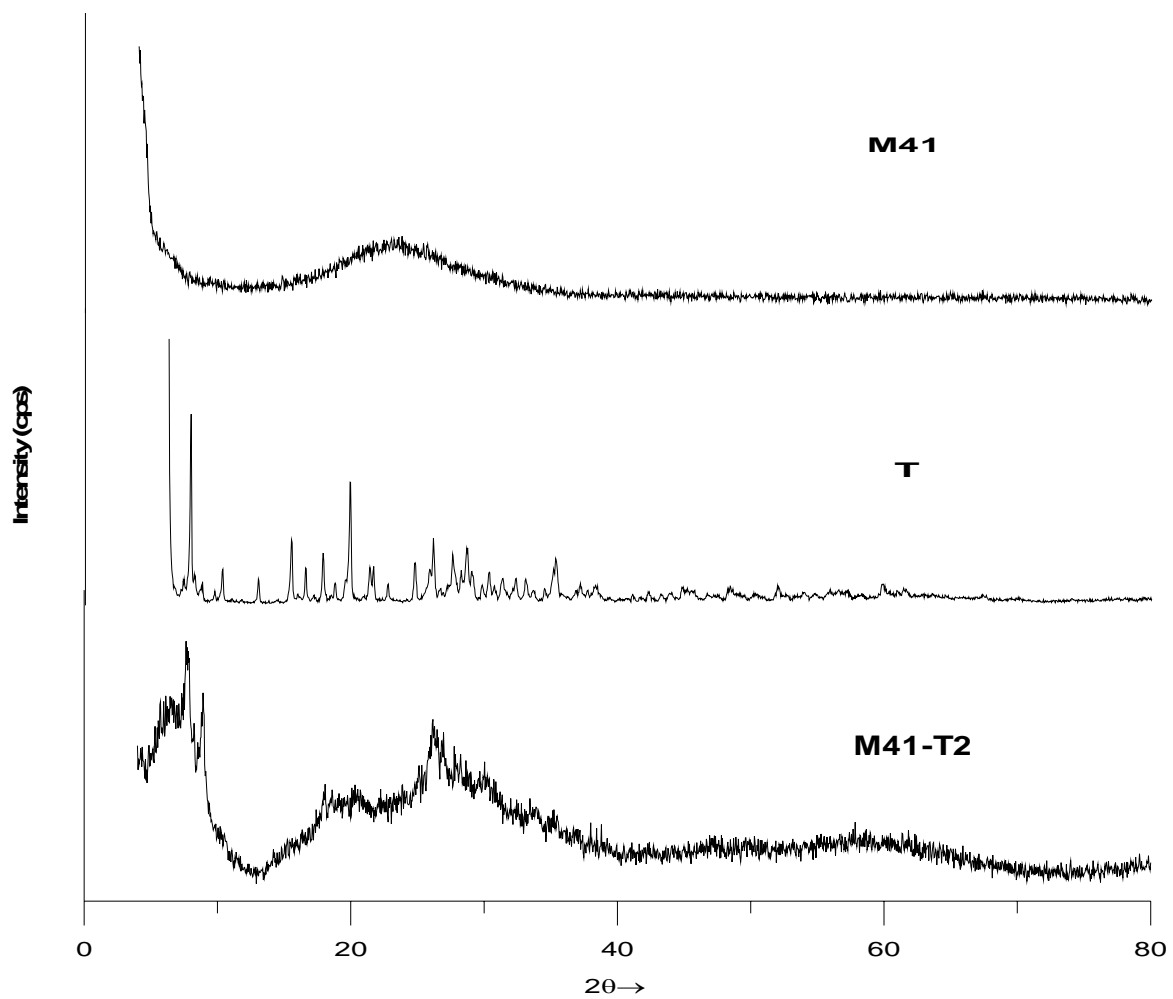


Figure 4-15 XRD plots for pure MCM41 (top); pure TPA (middle) and MCM41+50 % TPA.

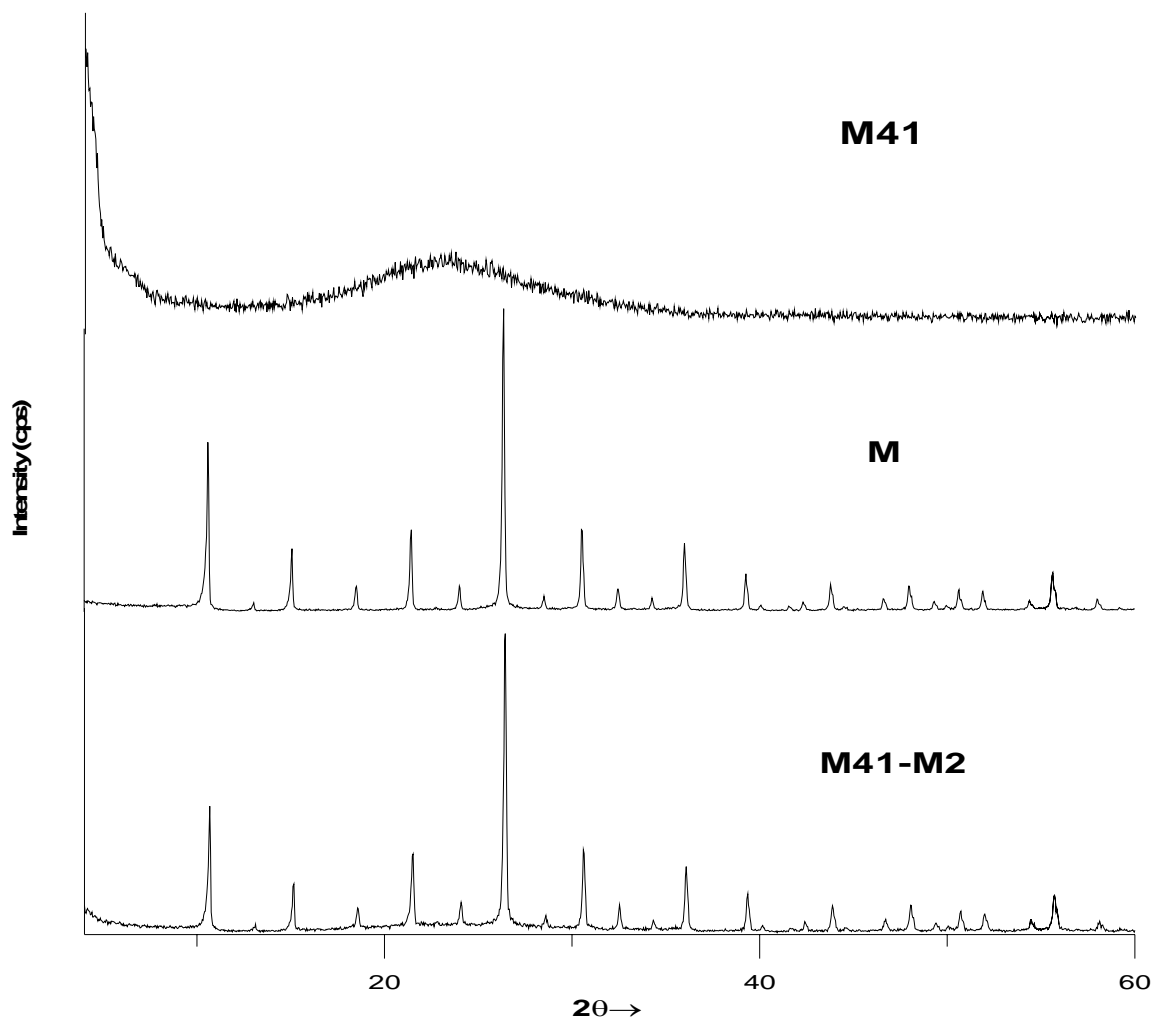


Figure 4-16 XRD data comparison for (a) pure MCM41; (b) pure MPA; (c) MCM41+50 % MPA.

4.1.5. SEM Technique

Electron microscopes use electrons produced by a heated tungsten filament to illuminate an object. In addition, lenses & magnetic coils are also used to speed up these electrons and focus them into a narrower beam that moves across the specimen kept in vacuum. Small amounts of the samples were spread on adhesive conductive copper tapes attached to a sample holder and then scanned with the microscope. [Figure 4-17](#) shows the electron micrograph of pure Y-zeolite, pure TPA, pure MPA and pure MCM41. [Figure 4-17 \(a\)](#) shows the SEM micrographs of the pure Y-zeolite which suggests almost uniform crystal sizes with few large crystals [\[51,78\]](#). The large particles could actually be aggregates of independent crystals of considerably smaller size. SEM micrograph of pure TPA in [Figure 4-17 \(b\)](#) suggests a mixture of small crystals with few big crystals [\[79\]](#). The micrograph suggests that the large particles are observed possibly due to the polyoxometalate present in the heteropolyacids, which is responsible mainly for the keggin structure. [Figure 4-17 \(c\)](#) represents the SEM micrograph of the pure molybdophosphoric acid (MPA) in which an array of uniform small crystals is observed with few sparse areas. SEM micrograph of pure MPA suggests more uniformity as compared to pure TPA micrograph. The presence of Keggin structure is not so prominent in MPA as compared to TPA because molybdenum (Mo) atom is far smaller in size as compared to tungsten (W). SEM image of pure MCM41 ([Figure 4-17 d](#)) shows almost regular dispersion of silica and alumina channels which consequently evidences the large pore sizes in the crystal structure

Figure 4-18 show the SEM micrographs of Y-zeolite and MCM41 loaded with heteropolyacids. SEM micrograph of Y-zeolite with 50 wt. % tungstophosphoric acid (TPA) (Figure 4-18a) suggests almost uniform dispersion of HPA onto the zeolite structure except very few cluster-like areas. These clusters could actually be aggregates of independent crystals of Y-zeolite and TPA. Nevertheless, these clusters do not at all affect the protonic conductivity of the solid composite powder which increases as the amount of TPA increases. Definite evidence that the TPA is evenly dispersed throughout the thickness comes from the EDAX analysis. We monitored the concentrations of tungsten, silicon and aluminum along the layer thickness of the solid powder. Tungsten is indicative of TPA whilst silicon and aluminum are indicative of Y-zeolite. With different wt. percentages of heteropolyacids into Y-zeolites, the amount of major constituents like tungsten (W), molybdenum (Mo), silicon (Si) and aluminum (Al) varied accordingly which complement the FTIR, XRD and SEM studies. Although, SEM image of Y-zeolite with 50 wt. % molybdophosphoric acid (MPA) (Figure 4-18b) suggests a poor dispersion of MPA into Y-zeolite, still the impedance spectroscopy experiments suggest highest conductivity for 50 wt. % loaded Y-zeolite. This can be justified because the proton conductivity in solid powders is mainly due to surface movement of the protons and the considerable presence of MPA on Y-zeolite is mainly responsible for the high proton conductivity of this solid composite powder. EDAX study for this sample also confirmed poor dispersion of MPA into Y-zeolite.

SEM images of MCM41 with 50 wt. % of each TPA and MPA are shown in Figure 4-18 (c and d). Observation of SEM images of solid powder of MCM41 with 50 wt. % TPA

accords with the SEM image of pure MCM41 which demonstrates the uniform dispersion of TPA into MCM41 (Figure 4-18c). Although some big cluster-like areas are also seen, this may be due to heteropoly anions present in TPA. As described earlier, the protonic conductivities of solid powders with 50 wt. % TPA was found to be considerably high, which could be due to these heteropoly anions present inside the pores (probably) as well as on the surface of the MCM41. On the other hand, the SEM image of MCM41 with 50 wt. % of molybdophosphoric acid (MPA) (Figure 4-18d) shows absolute uniformity with regular crystal structure arrays as that of pure MPA. This could again be due to the compatibility of MPA and MCM41 material as compared to TPA and MCM41; however high proton conductivity factor in case of TPA dominates over MPA and that is why we got higher conductivities in case of TPA loading rather than MPA loading. So, it can be concluded from these loaded heteropolyacids in MCM41 that from structural point of view MPA loaded MCM41 are more uniformly dispersed as compared to TPA loaded MCM41 while from proton conductivity point of view TPA loaded solid powders show promising performance as compared to MPA loaded in MCM41. EDAX microanalysis reveals the presence of silicon and aluminum in pure MCM41 as well as in heteropolyacids loaded MCM41. Tungsten and molybdenum findings in pure TPA and MPA also support the presence of heteropolyacids in solid composite powders.

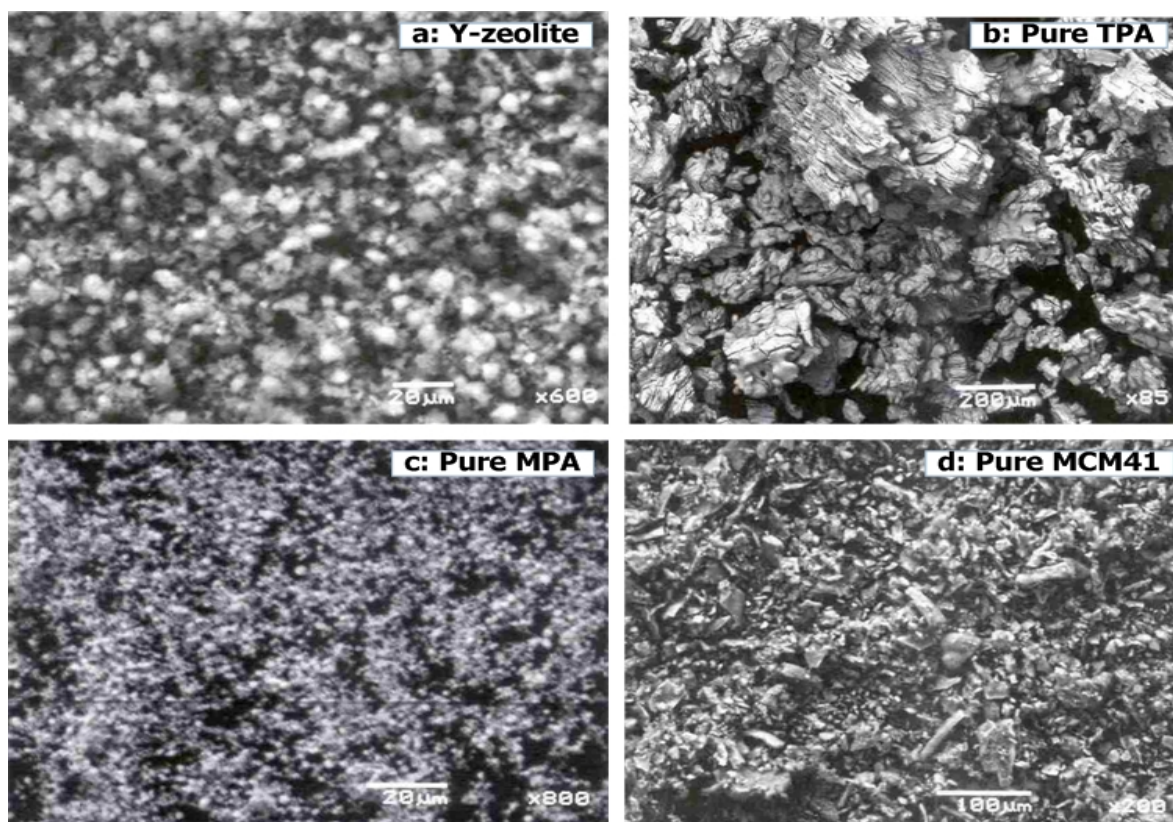


Figure 4-17 SEM images of pure Y-zeolite (a), pure TPA (b), pure MPA (c) and pure MCM41 (d).

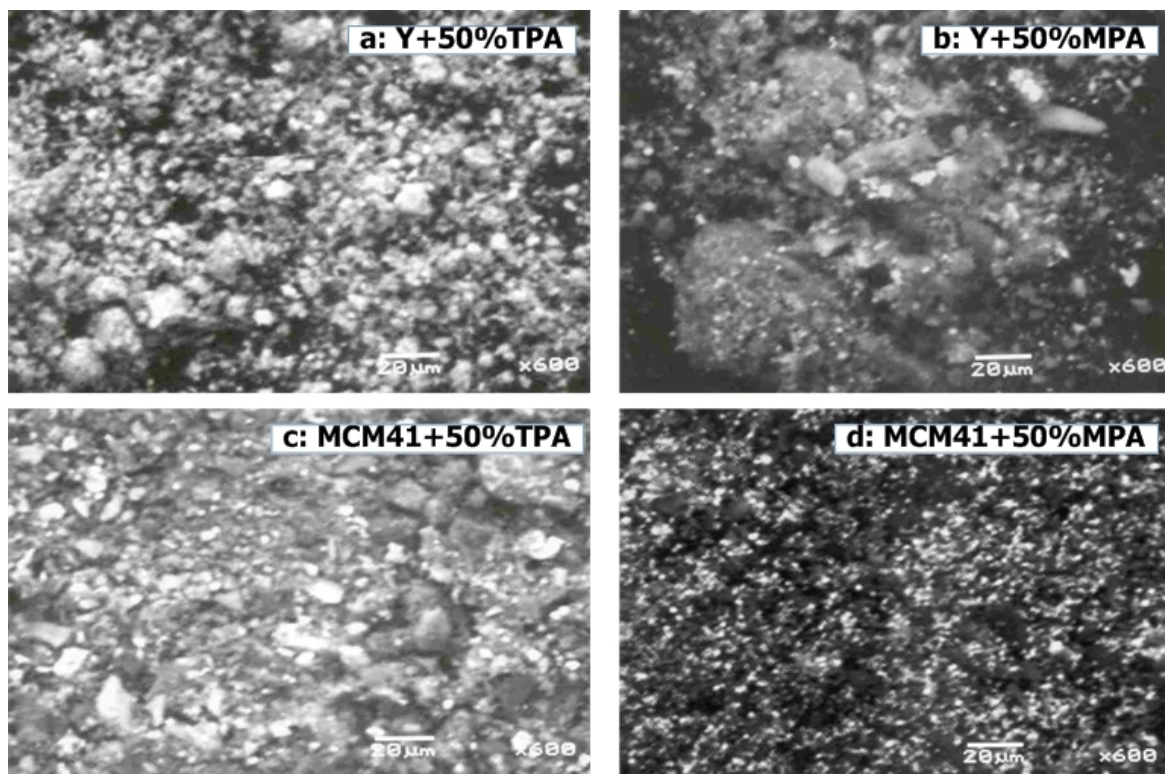


Figure 4-18 SEM images of Y-zeolite+50 % TPA (a), Y-zeolite+50 % MPA (b), MCM41+50 % TPA (c) and MCM41+50 % MPA (d).

Results and discussion: Composite polymeric membranes

5.1. Composite membranes development

With the help of synthesized solid proton conductors in the previous chapter and based on the results of characterization techniques, samples with highest protonic conductivities were selected for the preparation of composite membranes. From the results of solid proton conductors, it was found that solids with 40 and 50 wt. % heteropolyacids possessed highest conductivities; therefore they were loaded into SPEEK polymer from 10-40 percent by weight. The results for synthesized composite membranes are presented in the following sequence:

- 5.1.1. Proton conductivity through Impedance spectroscopy
- 5.1.2. Water uptake of membranes
- 5.1.3. FTIR Analysis
- 5.1.4. XRD Analysis
- 5.1.5. SEM analysis

5.1.1. Proton conductivity studies

All of the membranes measured for their conductivities were soaked overnight in distilled water prior to make impedance measurements. Conductivity measurements were carried

out for wet membranes since dry membranes show negligible conductivities, as it is a well known fact that proton conductivity of membranes is a water assisted phenomena. Since the time required for the completion of conductivity measurement was short (~ of the range of 2-5 minutes), so the dehydration of membrane during experiment may be termed as negligible. The experiments on all of the samples were repeated thrice and the values obtained were in tolerance limit i.e. $\sim \pm 2\%$, so reproducibility was taken care of automatically.

Effect of casting solvent on membrane characteristics has also been studied by the researchers to choose appropriate solvent for casting of composite membrane containing SPEEK polymer [80]. The sulfonic acid groups of SPEEK, responsible for charge transfer in PEMs, are able to form strong hydrogen-bonding with some solvents such as dimethyl formamide (DMF) or dimethyl acetamide (DMAc). That may significantly affect the conductivity of the membranes as this actually reduces the charge carrier number and/or mobility. In our work, we have used DMAc solvent to cast composite membranes, but prior to choosing DMAc, one sample membrane were prepared using DMF and DMAc as solvent. Conductivities of these samples were measured immediately after preparation, using vacuum treatment at 60 and 130 °C. All samples were fully hydrated by soaking in water overnight immediately prior to the measurements. Membranes prepared with DMAc were found to be more conductive as compared to those prepared with DMF. As DMF is the lower boiling point solvent, this anomalously low proton conductivity may be explained by strong hydrogen-bonding of solvent or decomposition product that reduces the number of protons available for proton transport.

Therefore, the lower conductivity of the hydrated film cast from DMF compared with DMAc may be due to its lesser number of available acid groups. Hence, DMAc was selected as solvent to prepare the composite membranes. It is reported that the proton conductivity mechanism of hydrated materials is due to the transportation of H_3O^+ or H_5O_2^+ .

Proton conductivities for pure SPEEK polymeric membranes and composite membranes with Y-zeolite loaded with tungstophosphoric acids (TPA) and molybdophosphoric acid (MPA) into SPEEK polymer with various weight percentages from 10 to 40 wt. % have been measured and are given in [Table 5-1](#). Similarly, the proton conductivity and resistances values for composite membranes with MCM41 loaded with TPA and MPA into SPEEK polymer with various weight percentages are given in [Table 5-2](#). It is evident from [Tables 5-1 and 5-2](#) that as the weight percentages of TPA and MPA increase in Y-zeolite as well as in MCM41, the conductivity also increases. For example, pure SPEEK has conductivity at 20 °C of 0.73 S/cm while with 40 wt. % solid proton conductors SPEEK exhibit conductivities at 20 °C of 3.24, 4.28, 2.36 and 3.23 mS/cm respectively. It is obvious from the results that composite membranes with Y-zeolite loaded with TPA showed higher protonic conductivities as compared to Y-zeolite loaded with MPA, which is quite expected as the proton conductivity of TPA is higher as compared to MPA. On the other hand, from [Table 5-2](#), it is also very clear that composite membrane with 40 wt. % solid inorganic powders containing MCM41 exhibit conductivities at 20 °C of 3.09, 3.26, 2.55 and 2.87 mS/cm respectively. This value is lower for a similar loading of

TPA/Y-zeolite. This may be because of small amount of conductivity possessed by MCM41 as compared to Y-zeolite.

Table 5-1 Proton conductivities of the prepared composite membranes at room temperature with the help of Y-zeolite loaded with TPA and MPA into SPEEK

Sample Name	Thickness of the sample, cm				Proton conductivity, mS/cm			
	Wt. % of SPC in composite membrane				Wt. % of SPC in composite membrane			
	10%	20%	30%	40%	10%	20%	30%	40%
S	0.014				0.73			
SY-T1	0.020	0.018	0.017	0.012	1.27	1.67	2.91	3.24
SY-T2	0.019	0.019	0.016	0.022	1.75	2.30	3.44	4.28
SY-M1	0.016	0.012	0.017	0.018	0.924	1.14	1.67	2.36
SY-M2	0.014	0.010	0.010	0.010	0.971	1.31	1.91	3.23

* where SPC=solid proton conductor; S = SPEEK1.6 polymer; TPA = tungstophosphoric acid; MPA = molybdophosphoric acid; Y-T1 = [Y-zeolite+40 % TPA]; Y-T2 = [Y-zeolite+50 % TPA]; Y-M1 = [Y-zeolite+ 40 % MPA]; Y-M2 = [Y-zeolite+50 % MPA]; SY-T1 = SPEEK with [Y-zeolite+40 % TPA] and SY-T2 = SPEEK with [Y-zeolite+50 % TPA].

Table 5-2 Proton conductivities of the prepared composite membranes at room temperature with the help of MCM41 loaded with TPA and MPA into SPEEK

Sample Name	Thickness of the sample, cm				Proton conductivity, mS/cm			
	Wt. % of SPC in composite membrane				Wt. % of SPC in composite membrane			
	10%	20%	30%	40%	10%	20%	30%	40%
S	0.014				0.73			
SM41-T1	0.020	0.017	0.010	0.016	1.19	1.71	2.45	3.09
SM41-T2	0.014	0.012	0.020	0.012	1.49	1.85	2.75	3.26
SM41-M1	0.012	0.014	0.014	0.011	0.89	1.06	1.55	2.55
SM41-M2	0.010	0.010	0.010	0.010	0.98	1.16	1.79	2.87

* where SY-M1 = SPEEK with [Y-zeolite+40 % MPA]; SY-M2 = SPEEK with [Y-zeolite+50 % MPA]; SM41-T1 = SPEEK with [MCM41+40 % TPA]; SM41-T2 = SPEEK with [MCM41+50 % TPA]; SM41-M1 = SPEEK with [MCM41+40 % MPA] and SM41-M2 = SPEEK with [MCM41+50 % MPA]

Researchers in recent past have tried to modify SPEEK by incorporation of heteropolyacids into polymer matrix [27], but the problem with these membranes was that most of the heteropolyacid was leached out of the membrane due to high solubility of heteropolyacids in water. The advantage of using Y-zeolite and MCM41 becomes very important in the above-mentioned situation, since heteropolyacids do not directly interact with water but are supported by the frameworks of Y-zeolite and/or MCM41. Since water retention properties of Y-zeolite and MCM41 are well known, these only augment the good water retention properties of composite membranes.

Conventional Nafion[®] membranes have also been reported with slight modification with various solid inorganic materials such as zirconium phosphate (ZrPO₄), silica (SiO₂) and heteropolyacids [33,34,39,59,65]. Although proton conductivity was enhanced by the incorporation of inorganic materials but it was not so significant because Nafion[®] consists of both hydrophilic and hydrophobic domains. Hydrophilic domain welcomes the water thus resulting in increased conductivity; while hydrophobic domain resists water resulting in decreased conductivity. Hence, addition of inorganic material does not significantly augment the water retention properties of modified Nafion[®] membranes.

In general, the improved conductivity reflects mainly a better proton transport across the composite membranes. The observed differences in the conductivity introduced by the solid proton conductors have to be interpreted regarding their structural modification. A structure modification of the membrane due to the addition of inorganic components and proton conduction due to new interfacial polymer–particle properties can be assumed.

However, at present we do not have enough structural information to speculate on the nature of the additional conductivity channel in the composite membranes.

Figures 5-1 to 5-4 depict the variation in proton conductivities for different composite membranes containing 40 and 50 weight percentages of TPA and MPA into Y-zeolite and MCM41 respectively.. The amounts of solid inorganic powders in composite membranes varied from 10 to 40 wt. % in pure SPEEK polymer. It can be seen from Figure 5-1 to Figure 5-4 that the results for conductivity up to 20 wt. % loading of solid proton conductor showed a marginal increase while at higher loadings the improvement in conductivity is significant. Although, membranes with higher than 40 weight percentages of solid loading were also prepared, they suffered from poor mechanical strength and uneven solid dispersion, so the conductivity results for them are not reported here. Researchers in the past have reported composite membranes of SPEEK with various solid inorganic materials. One such composite membrane of SPEEK with BPO_4 was reported by Zaidi et al. [48]. Composite membranes upto 40 wt. % loading of BPO_4 showed marginal increase in conductivity while loading of 60 wt. % BPO_4 indicated an appreciable increase in proton conductivity. Although these membranes showed conductivities a little higher as compared to our membranes, but they suffered with high amount of BPO_4 leaching out of composite membranes. The trends of proton conductivity obtained in this study are shown in Figure 5-5.

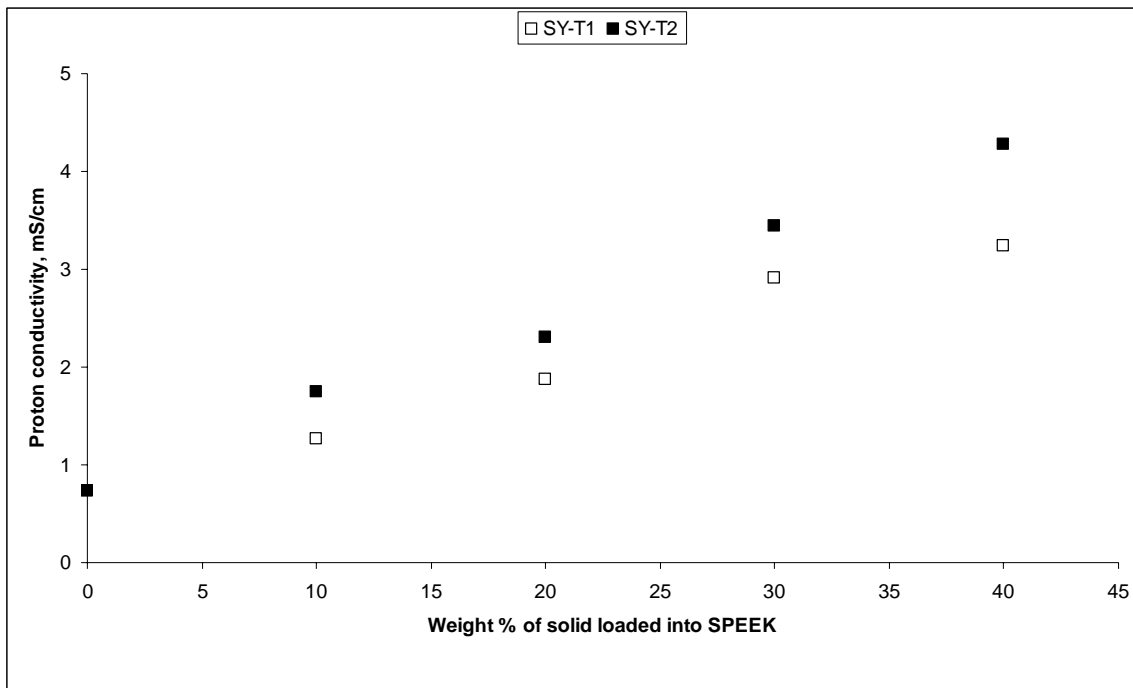


Figure 5-1 Proton conductivity comparison of SPEEK+[Y-zeolite+40 % TPA] and SPEEK+[Y-zeolite+50 % TPA] at ambient temperature.

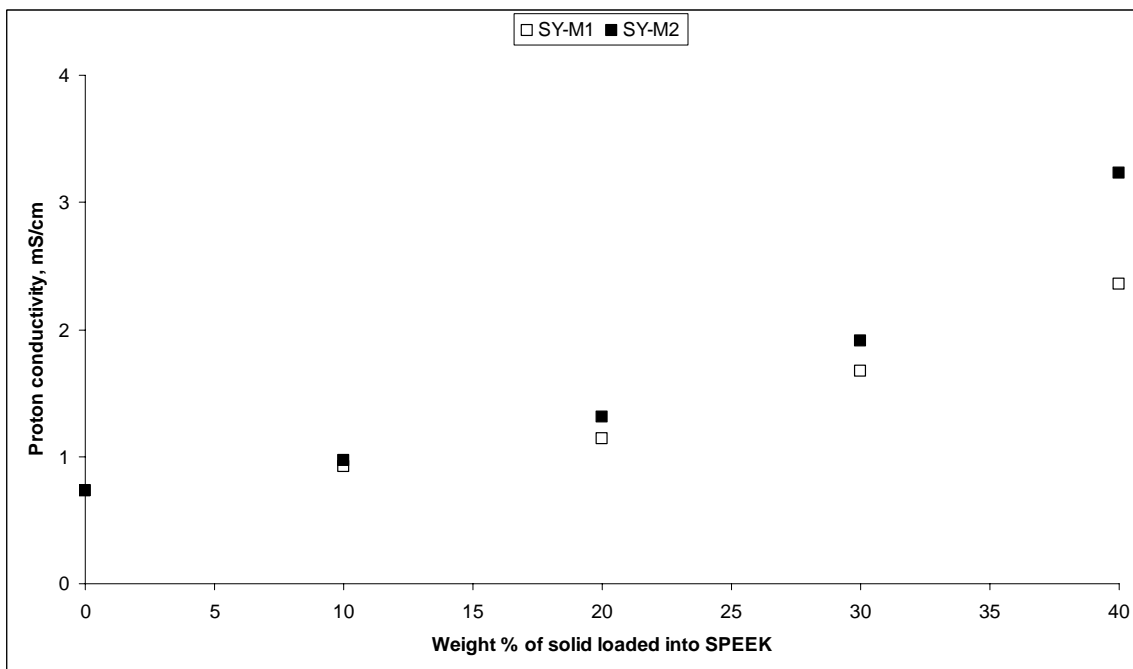


Figure 5-2 Proton conductivity comparison of SPEEK+[Y-zeolite+40 % MPA] and SPEEK+[Y-zeolite+50 % MPA] at ambient temperature.

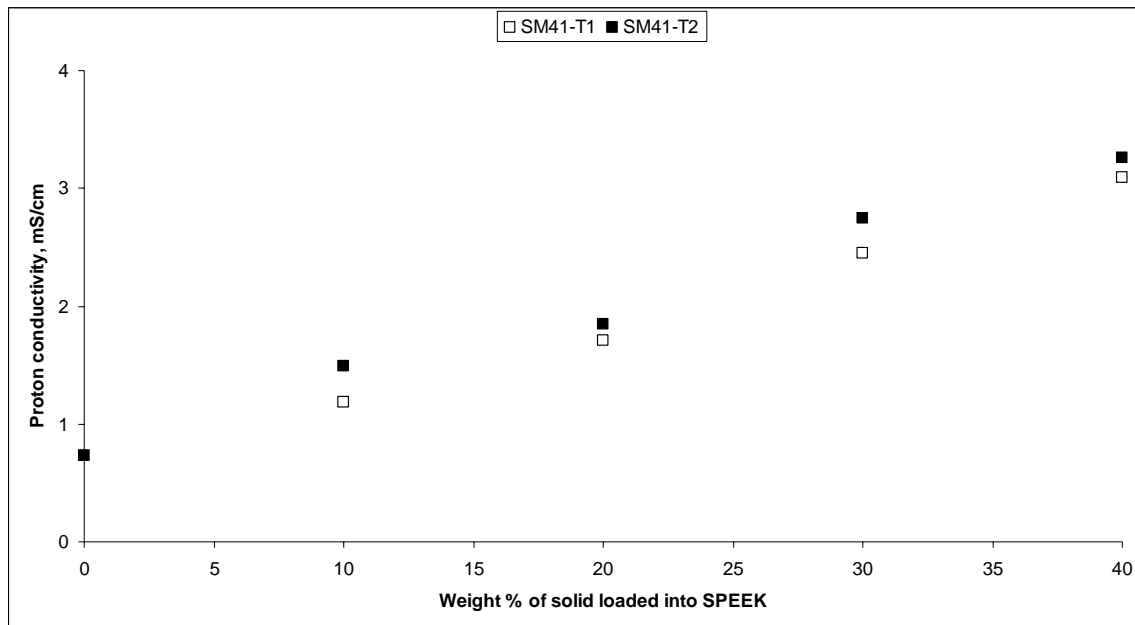


Figure 5-3 Proton conductivity comparison of SPEEK+[MCM41+40 % TPA] and SPEEK+[MCM41+50 % TPA] at ambient temperature.

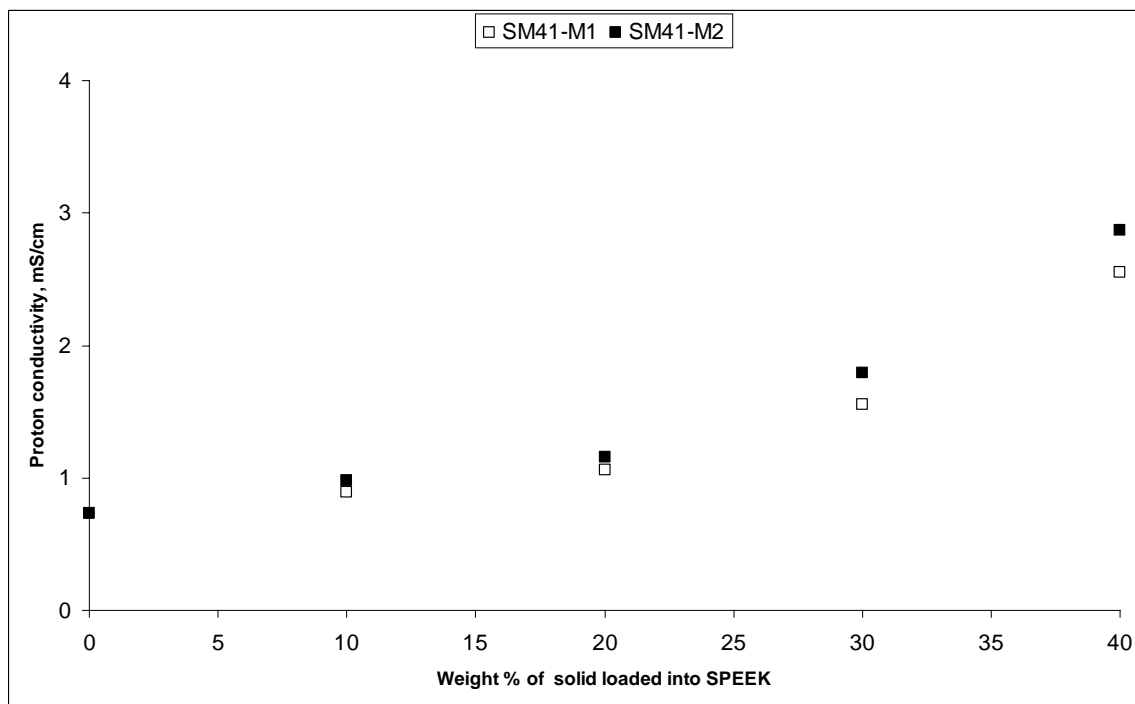


Figure 5-4 Proton conductivity comparison of SPEEK+[MCM41+40 % MPA] and SPEEK+[MCM41+50 % MPA] at ambient temperature.

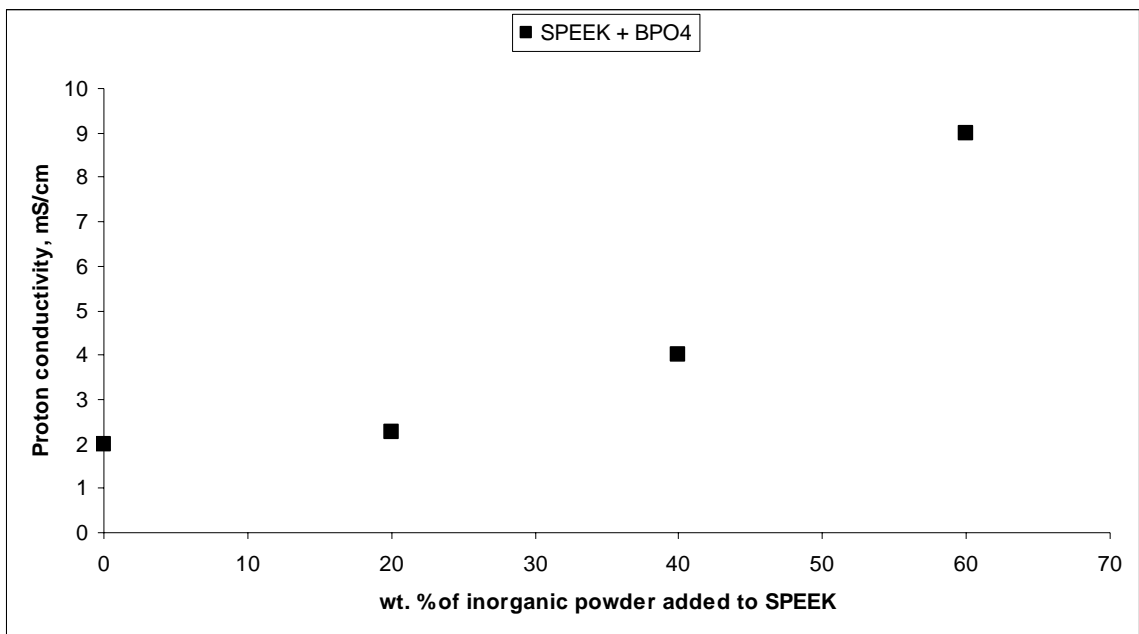


Figure 5-5 Proton conductivity trends of SPEEK with various wt. percentages of BPO₄ at ambient temperature [48].

From these results, it can be observed that almost all of the composite membranes showed significant enhancement in proton conductivities at room temperature. Due to these encouraging results, composite membranes were also measured for their protonic conductivities at high temperatures for their use in medium temperature fuel cell applications. Composite membranes with highest proton conductivities at ambient temperatures were selected for high temperature experiments. All composite membranes contained 40 wt. % of solid proton conductors (SPC) and 60 wt. % of SPEEK polymer. [Tables 5-3 and 5-4](#) show the variations in proton conductivities of various composite membranes with varying temperatures. All of the measurements were taken between the temperature ranges of 20 to 140 °C as this is the range for the membranes to be used in medium temperature fuel cell applications. Prior to high temperature experiments, composite membranes were put in distilled water overnight. Wet membranes after cleaning extra surface water were put between two stainless steel electrodes of the conductivity cell which was maintained at a particular temperature. Conductivity cell was maintained at that particular temperature during the experiment.

In all cases, the introduction of the HPAs loaded Y-zeolite and/or MCM41 improves the proton conductivity of the composite membranes with increasing temperatures. The conductivity of all the composite membranes behaved in a similar fashion: the TPA based membranes showed a higher conductivity than MPA based composite membranes. It appears that TPA, being a stronger acid, systematically yields a higher proton conductivity increase as well as a better water retention at high temperature. These results

evidence that the proton conductivity of SPEEK matrices by incorporation of solid HPAs loaded Y-zeolite/MCM41 can be increased significantly.

From the results presented in [Tables 5-3 and 5-4](#), it can be seen that proton conductivity increases up to 120 °C, and becomes constant above 120 °C with no further appreciable increase in conductivity at 140 °C. This may be due to partial dehydration of the wet membrane during the experiment. Apparently, the dehydration of membranes seems to be the reason for the fall in conductivity but it also may be due to complex structural interactions of polymer matrix and solid conducting material. Since at high temperature orientation and re-orientation of polymer backbone takes place which in turn creates numerous possibilities for polymer matrix to interact with polymer chain as well as other materials blended with polymer matrix. It is also very clear that proton conductivity for the composite membranes containing solid proton conductors (SPC) of Y-zeolite loaded with heteropolyacids shows exceptional increase in conductivity as compared to MCM41 loaded heteropolyacids SPC. This particular characteristic may be attributed to the high water retention properties of the Y-zeolite as compared to MCM41. Since at high temperatures there are chances that membranes get dehydrated so the membranes containing Y-zeolite endures for a longer time and retain more water at high temperature conditions as compared to membranes which contain MCM41.

Table 5-3 Proton conductivity values for various composite membranes prepared from Y-zeolite and heteropolyacids at varying temperatures from 20 to 140 °C.

Membrane sample specification	Proton conductivity in mS/cm					
	Temperature (°C)					
	20	50	70	100	120	140
SY-T1	3.17	3.87	5.34	6.76	7.87	7.57
SY-T2	4.31	4.84	6.88	8.54	9.62	9.56
SY-M1	2.36	3.84	5.56	6.22	7.08	7.18
SY-M2	3.35	4.74	5.64	6.48	7.79	7.82

Table 5-4 Proton conductivity values for various composite membranes prepared from MCM41 and heteropolyacids at varying temperatures from 20 to 140 °C.

Membrane sample specification	Proton conductivity in mS/cm					
	Temperature (°C)					
	20	50	70	100	120	140
SM41-T1	2.92	3.57	4.67	5.82	6.93	6.87
SM41-T2	3.37	4.51	5.83	7.18	8.28	8.15
SM41-M1	2.55	3.16	3.96	5.20	6.64	6.70
SM41-M2	2.76	3.68	4.96	6.22	7.87	7.79

These above-mentioned results for proton conductivities of various composite membranes at high temperatures are also presented in graphical form in [Figure 5-6 to 5-9](#). It can be seen clearly from the graphs that composite membranes containing Y-zeolite with TPA and MCM41 with TPA illustrate a noteworthy difference between the conductivities as compared to the membranes containing Y-zeolite with MPA and MCM41 with MPA. This is due to the high proton conductivity of TPA and high water retention abilities of Y-zeolite. Apart from this, various other factors which could be responsible to these results have already been discussed in the results of composite solid powder. Hence, the results for proton conductivity at room temperature as well as at high temperatures are according to expectations and are quite in conformity. Therefore, impedance spectroscopy results of prepared composite membranes exhibit potential findings as far as proton conductivity of composite membranes at room as well as high temperature is concerned.

Researchers in the past have also reported conductivity trends for high temperature ranges. In one such study, Alberti et al. have reported the conductivity trends for composite membranes of SPEEK with $ZrPO_4$ at high temperature upto 140 °C [81]. Composite membranes were prepared using 10 and 20 wt. % $ZrPO_4$ into SPEEK polymer matrix. A highest conductivity of the order of 10^{-2} S/cm was reported in case of 20 wt. % loading of $ZrPO_4$. The conductivity of zirconium phosphate is known to be strongly dependent upon degree of crystallinity, since its electrical properties result from surface conduction, while heteropolyacids are known to possess highest protonic conductivities among solid acids.

The membranes exhibited good conductivities at room temperatures and a sharp decrease in conductivity was observed at higher temperatures. This particular drop in conductivity was attributed to the dehydration of membranes at high temperatures. However, in our case, this sort of problem was not encountered and the membranes were found to be conductive at high temperatures as well as stable in those temperature ranges. This may be due to the reason that we have used Y-zeolite and MCM41 support for heteropolyacids in preparing solid proton conductors. Zeolites are supposed not to dehydrate even at high temperatures which make these solid proton conductors as one of the promising candidates as ideal inorganic material for high temperature application composite membranes. Another reason may be due to the changes in experimental conditions under which these measurements were carried out. The hydrophilic character of the solid proton conductor particles allows water to diffuse into another hydrophilic polymer matrix in a similar way as grafted sulfonic groups allow SPEEK membranes to be acidified [63]. Graphical depiction of proton conductivity in the range of 60-140 °C is shown in [Figure 5-10](#) [81].

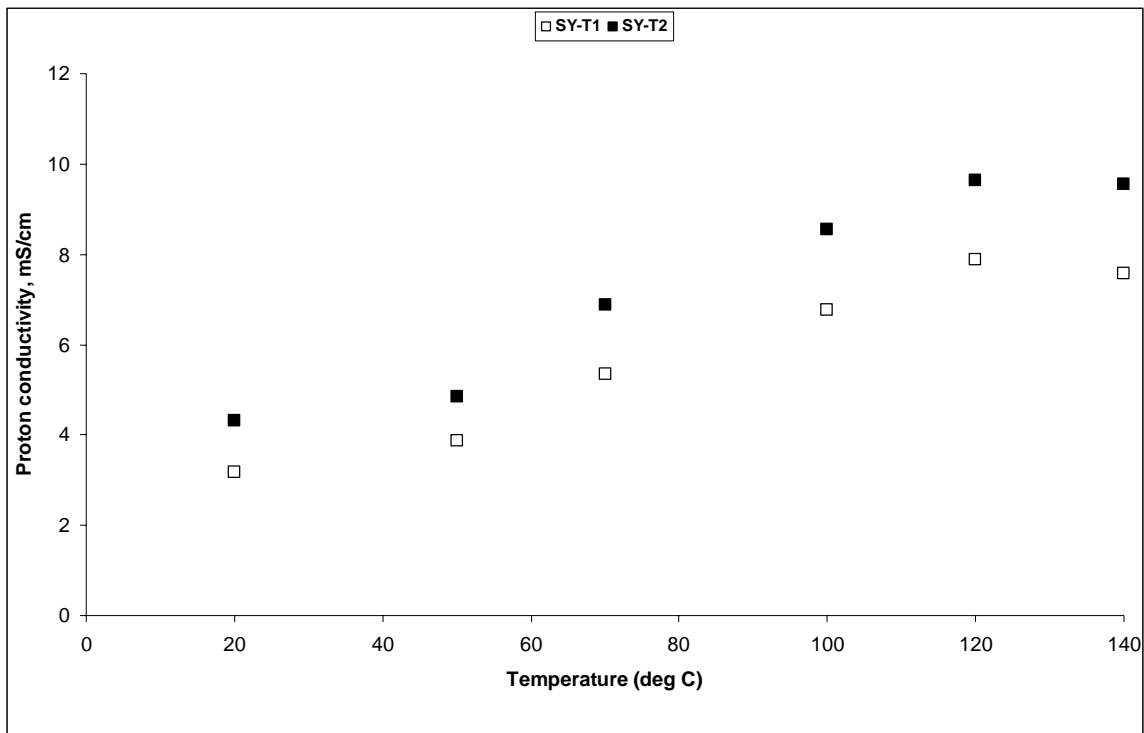


Figure 5-6 Proton conductivity plots for SPEEK(60 %)+[Y-zeolite+40 % TPA](40 %) and SPEEK(60 %)+[Y-zeolite+50 % TPA](40 %) at varying temperatures from 20 to 140 °C.

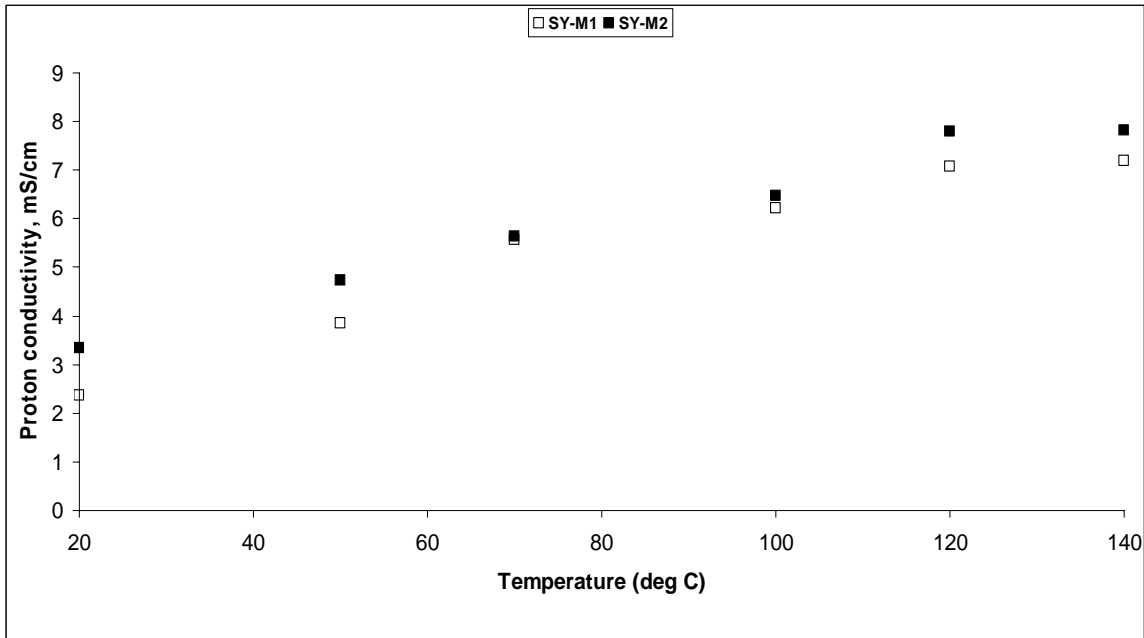


Figure 5-7 Proton conductivity plots for SPEEK(60 %)+[Y-zeolite+40 % MPA](40 %) and SPEEK(60 %)+[Y-zeolite+50 % MPA](40 %) at varying temperatures from 20 to 140 °C.

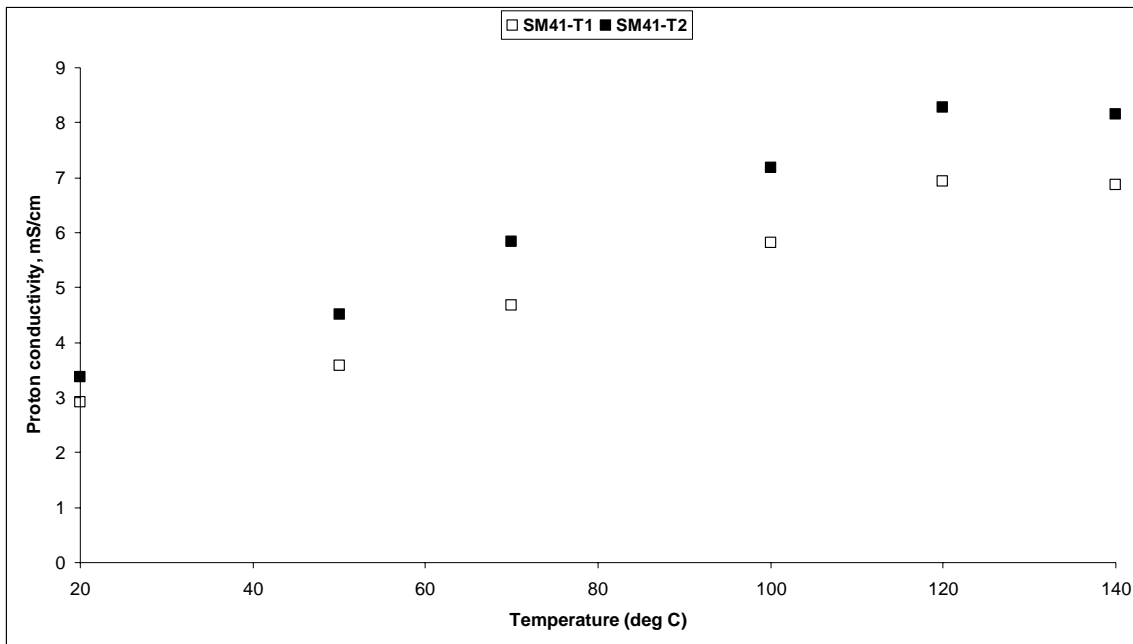


Figure 5-8 Proton conductivity plots for SPEEK(60 %)+[MCM41+40 % TPA](40 %) and SPEEK(60 %)+[MCM41+50 % TPA](40 %) at varying temperatures from 20 to 140 °C.

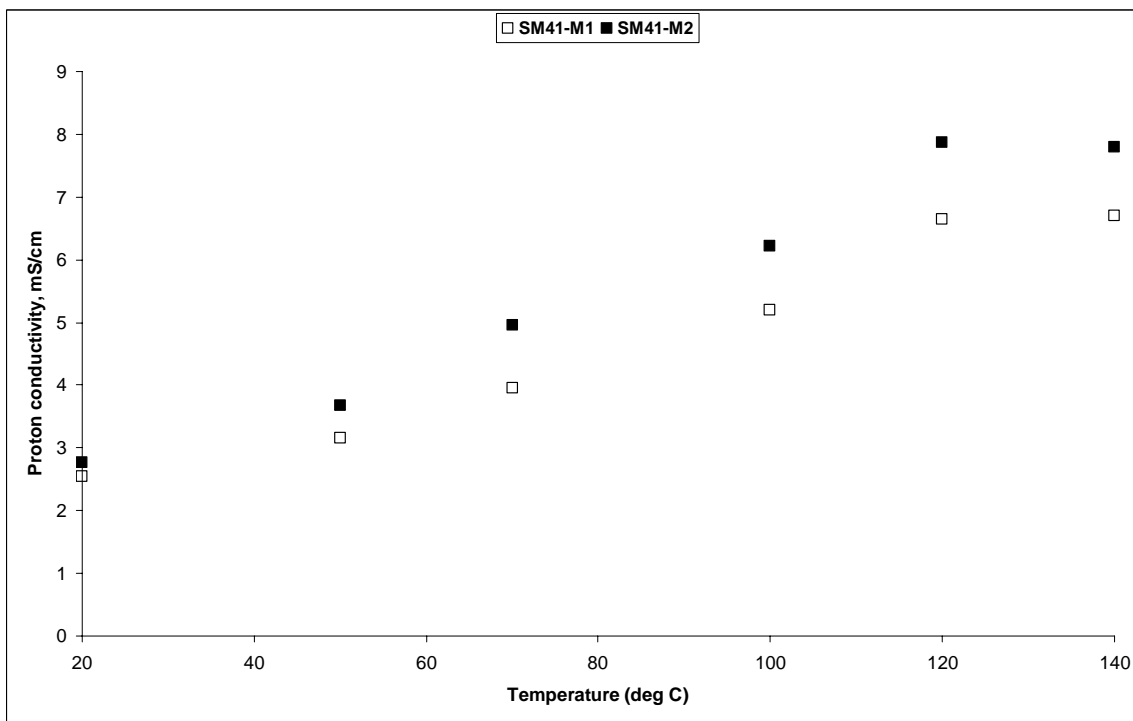


Figure 5-9 Proton conductivity plots for SPEEK(60 %)+[MCM41+40 % MPA](40 %) and SPEEK(60 %)+[MCM41+50 % MPA](40 %) at varying temperatures from 20 to 140 °C.

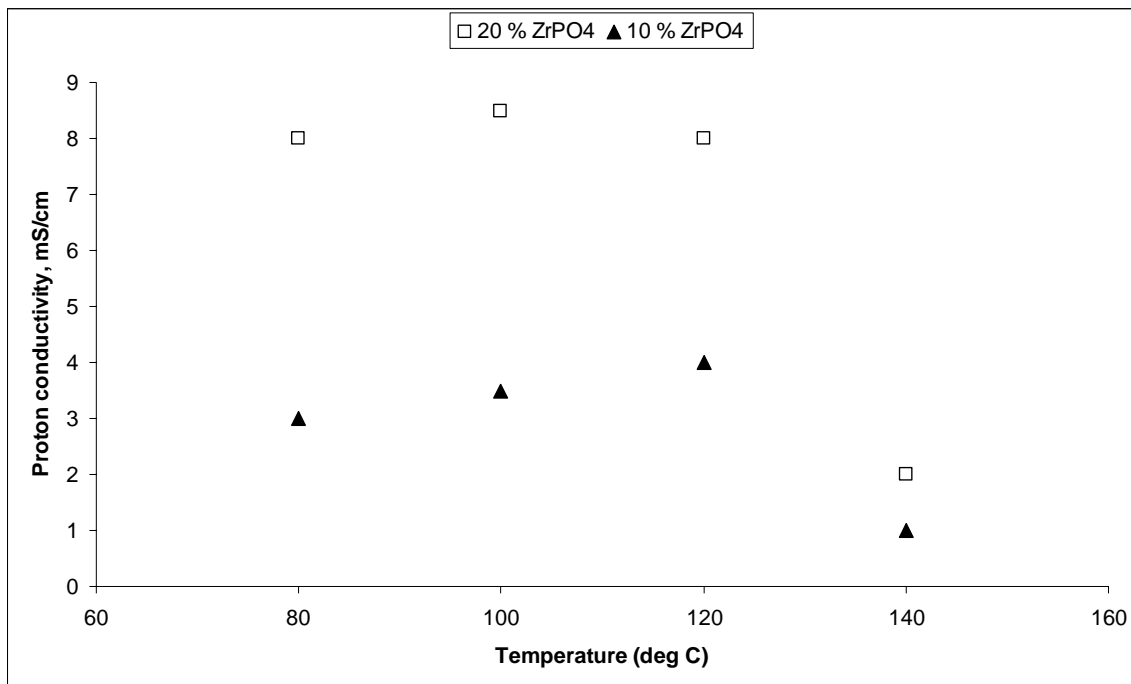


Figure 5-10 Proton conductivity plots for SPEEK with 10 and 20 wt. percent of ZrPO₄ at varying temperatures from 80 to 140 °C [81].

5.1.2. Water uptake measurements

In general, for ionomeric membranes, the proton conductivity depends on the number of available acid groups and their dissociation capability in water, which is accompanied by generation of protons. Water molecules dissociate acid functionality and facilitate proton transport, so the water uptake is an important parameter in studying PEMs. Swelling is also a key factor for the mechanical integrity of membranes. Excessively high levels of water uptake can result in membrane fragility and dimensional change leading to failures in mechanical properties, and in extreme cases, solubility in water at elevated temperatures. So, water uptake is an important phenomenon for the membranes to be used in fuel cells.

SPEEK polymer with ion exchange capacity (IEC) of 1.6 meq/gm was used to prepare composite membranes even though SPEEK with other IEC was available but with lower conductivity compared to SPEEK1.6. The physical and chemical properties of SPEEK depend on the concentration of sulfonic groups and the nature of counter ions. Sulfonation modifies the chemical character of PEEK, reduces the crystallinity and consequently affects solubility. Though SPEEK with high degree of sulfonation exhibits high conductivity, it also suffers from the problem of swelling when soaked in water. High water uptakes of membranes are desired but excessively high amount of water result in flooding of cathode in fuel cell, which consequently results in a drop of cell performance.

All of the membranes were immersed in distilled water for 48 hours prior to conduct water uptake measurements on them. This made sure that membranes were saturated with distilled water and there were no more weight changes of composite membranes. Membranes were then kept in a vacuum oven at 120 °C for 4 hours. All of the membranes experimented in the similar fashion and measured for differences in the weights prior to and after the experiments. The water uptake values were calculated using equation 3.5.3. The water uptake values of composite membranes of different composition are given in [Tables 5-5 and 5-6](#). It can be observed that by the introduction of both the solid proton conductors i.e. Y-zeolite loaded with TPA and MPA as well as MCM41 loaded with TPA and MPA into SPEEK polymer, the water uptake increase gradually. It increases marginally for low amounts of solid loading but jumps to very high values at 40 wt. % loading of solid proton conductors into polymer matrix. The main purpose of sulfonated polyether ether ketone (SPEEK) is to enhance acidity and hydrophilicity as it is known that the presence of water facilitates proton transfer and increases the conductivity of solid electrolytes.

Table 5-5 water uptake percentages for composite membranes from SPEEK with TPA & MPA loaded Y-zeolite

Sample Name	Thickness of the sample, cm				Percentage water uptake in 4 hours			
	Wt. % of SPC in composite membrane				Wt. % of SPC in composite membrane			
	10%	20%	30%	40%	10%	20%	30%	40%
S	0.014				65.574			
SY-T1	0.020	0.018	0.017	0.012	71.565	78.291	83.337	93.132
SY-T2	0.019	0.019	0.016	0.022	76.785	83.678	92.555	98.727
SY-M1	0.016	0.012	0.017	0.018	68.523	72.345	78.336	84.198
SY-M2	0.014	0.010	0.010	0.010	69.890	75.505	81.414	88.398

Table 5-6 Water uptake percentages for composite membranes from SPEEK with TPA & MPA loaded MCM41

Sample Name	Thickness of the sample, cm				Percentage water uptake in 4 hours			
	Wt. % of SPC in composite membrane				Wt. % of SPC in composite membrane			
	10%	20%	30%	40%	10%	20%	30%	40%
S	0.014				65.574			
SM41-T1	0.020	0.017	0.010	0.016	67.882	70.193	71.457	78.193
SM41-T2	0.014	0.012	0.020	0.012	62.427	71.749	79.456	82.227
SM41-M1	0.012	0.014	0.014	0.011	67.775	60.328	69.678	74.228
SM41-M2	0.010	0.010	0.010	0.010	68.743	75.278	78.302	83.516

Another reason for the increase of the water uptake by the introduction of the solid proton conductors may be the presence of keggin structure of heteropolyacids which itself contains high amounts of water and still can take more water due to the specific keggin structure. The density of keggin structure is very high which may involve clustering or agglomeration. Clustered ionomers absorb more water; therefore a large increase in water uptake results due to the presence of ion rich regions where proton transfer is particularly fast [8].

In our work, water uptake results obtained for various composite membranes do not exactly conform to previous results reported in literature [27]. One of the major reasons for the results which are reported previously, those composite membranes were prepared from pure heteropolyacids incorporated into SPEEK polymer while in our case the heteropolyacids are loaded onto Y-zeolite as well as MCM41 prior to their incorporation into SPEEK polymer matrix. It may be possible that interactions between keggin structures of heteropolyacids and Y-zeolite and/or MCM41 framework accounts for an optimum water uptake of these prepared composite membranes. The hydrophilic character of the solid proton conductor particles allows water to diffuse into another hydrophilic SPEEK polymer matrix in a similar way as grafted sulfonic groups allow SPEEK membranes to be acidified. When the membrane absorbs higher amount of water, the number of exchange sites available per cluster increases, indicating that the proton conductivity of the membrane increases.

Figures 5-11 to 5-14 show the graphical variations in water uptake for various composite membranes containing different amounts of solid inorganic powders. It is quite clear from the plots that as the amounts of solid inorganic material in the composite membrane increase, the water uptake of composite membranes also increase. This is probably a reflection of the fact that the voidage in the membranes increase due to these solid inorganic materials. A measurement of the pores size distribution and voidage would be a nice corroboration of these plots. It is also clear from the plots that the water uptake is significantly higher for the composite membranes containing Y-zeolite with heteropolyacids. Hence, the water uptake study corroborates the findings of proton conductivity measurement.

In previous studies, Nafion[®] membranes were modified with chabazite to get composite membranes [41]. Water uptake of the composite membranes were enhanced but at the expense of conductivity as conductivity decreased to significantly low levels as compared to parent Nafion[®] membrane. The water uptake at high temperature also decreased due to Nafion[®] dehydration at high temperatures. In our case, membranes retained good conductivities at temperatures above 120 °C with no apparent decrease in water uptake values. So, the composite membranes developed in this work appears to be possessing desired water uptake values.

The water uptake of sulfonated polymers is known to generally have a profound effect on proton conductivity and mechanical properties. Higher water uptake generates a more solvated species, which is needed for high conductivity, but unfortunately, greater water

content produces mechanically less stable membranes which might be due to the high porosities of membranes responsible for high water uptakes. Previous studies using copolymers with variable sulfonic acid concentrations confirm the tradeoff between high conductivity and good mechanical properties [55]. Incorporation of HPA into the sulfonated copolymer significantly reduced the water swelling behavior, without influencing the proton conductivity at room temperature.

Water uptake is an important phenomenon as far as composite membranes for fuel cell applications is concerned. Researchers have got mixed success as far as water uptake results are concerned. In our work, water uptake of the composite membranes increases as the wt. % of solid inorganic powders into the polymer matrix increased which conforms to the ideal conditions stated in the literature. However researchers in the past have reported contradictory trends with the water uptakes of composite membranes with increasing percentages of solid inorganic material into the polymer matrix. In one such study, Kim et al. have reported the manufacture of composite membranes from poly(arylene ether sulfone) and HPA [55]. Water uptake values dwindled with increasing percentages of HPA into polymer matrix. Trends reported are shown in [Figure 5-15](#). In another significant contribution, Zaidi et al. has reported proton conductivity results with increasing percentages of water uptake for composite membranes from SPEEK and BPO₄ [48]. Results reported here demonstrate increasing trends as the amount of BPO₄ increase in composite membranes. Highest conductivities were reported for at 40 wt. % loading of BPO₄ in SPEEK. [Figure 5-16](#) shows the trends reported for these composite membranes.

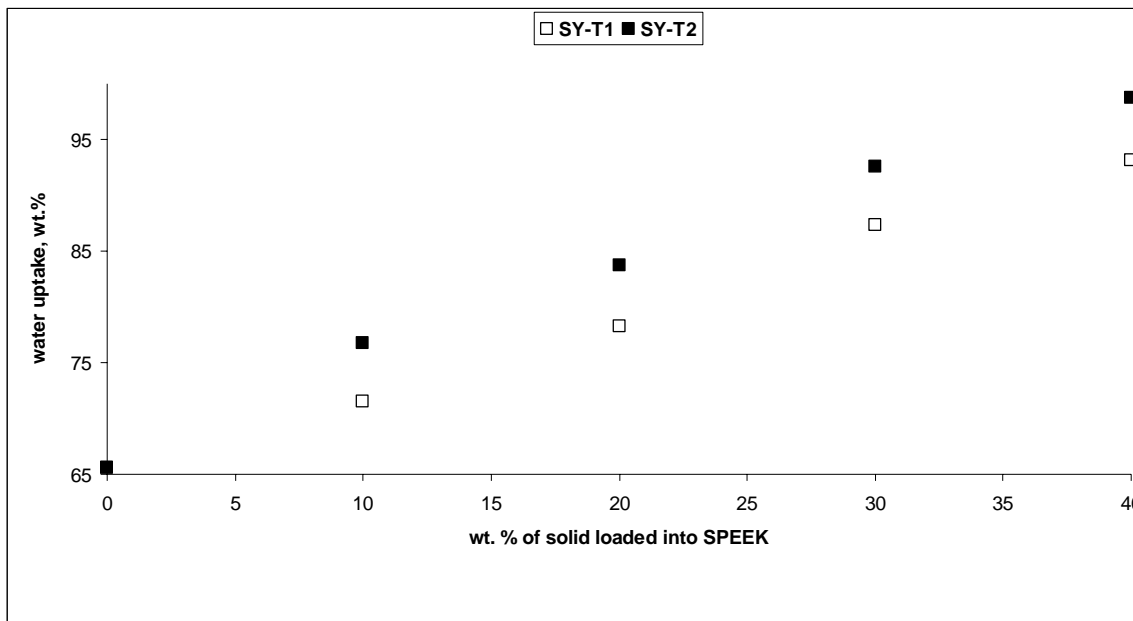


Figure 5-11 Water uptake plots for SPEEK+[Y-zeolite+40 % TPA] and SPEEK+[Y-zeolite+50 % TPA]

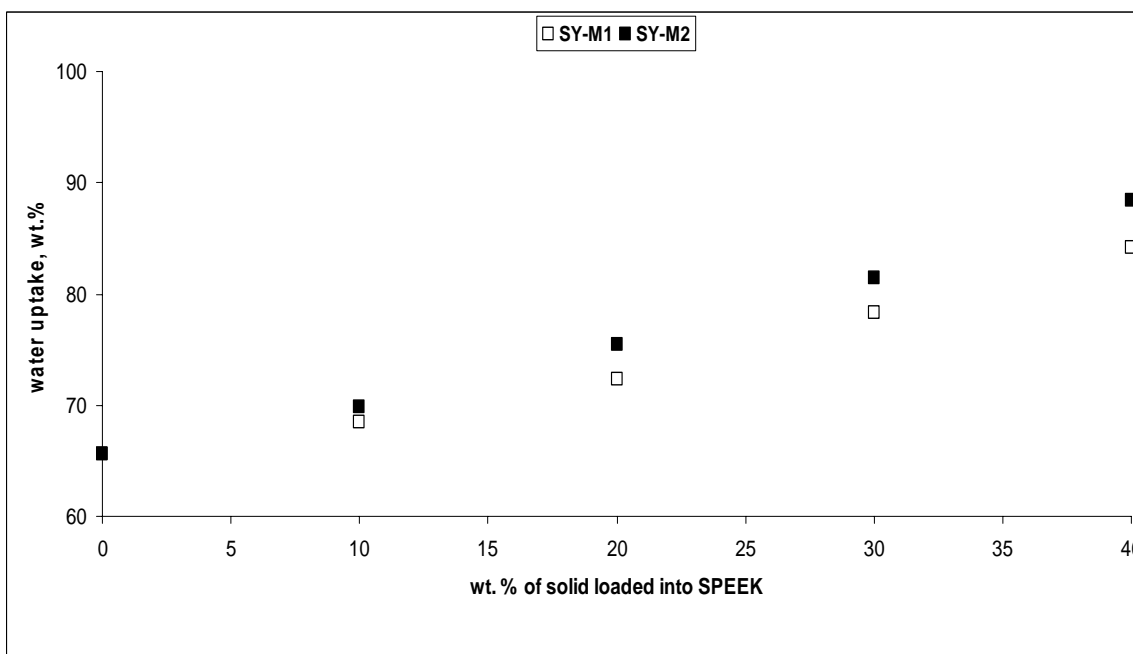


Figure 5-12 Water uptake plots for SPEEK+[Y-zeolite+40 % MPA] and SPEEK+[Y-zeolite+50 % MPA]

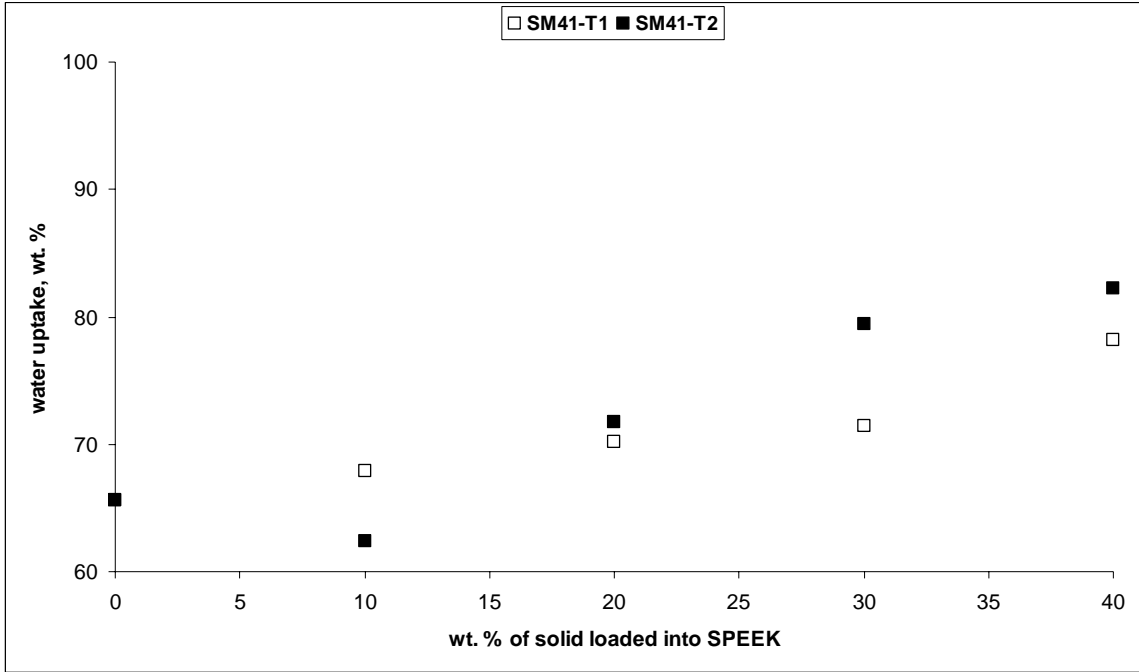


Figure 5-13 Water uptake plots for SPEEK+[MCM41+40 % TPA] and SPEEK+[MCM41+50 % TPA]

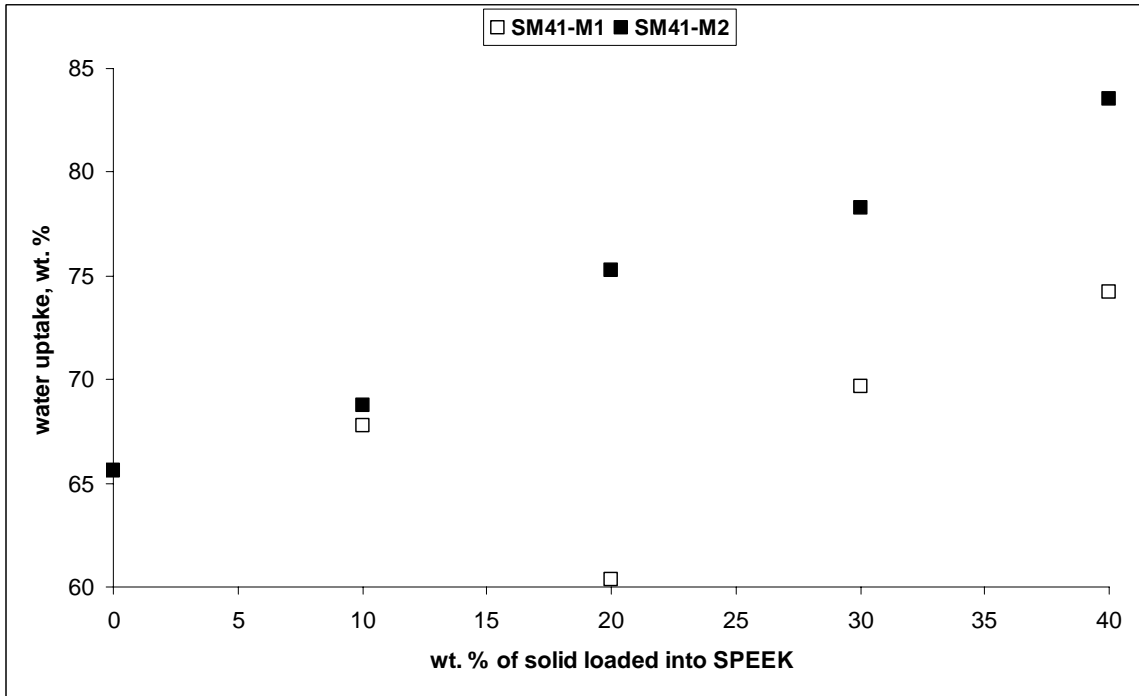


Figure 5-14 Water uptake plots for SPEEK+[MCM41+40 % MPA] and SPEEK+[MCM41+50 % MPA]

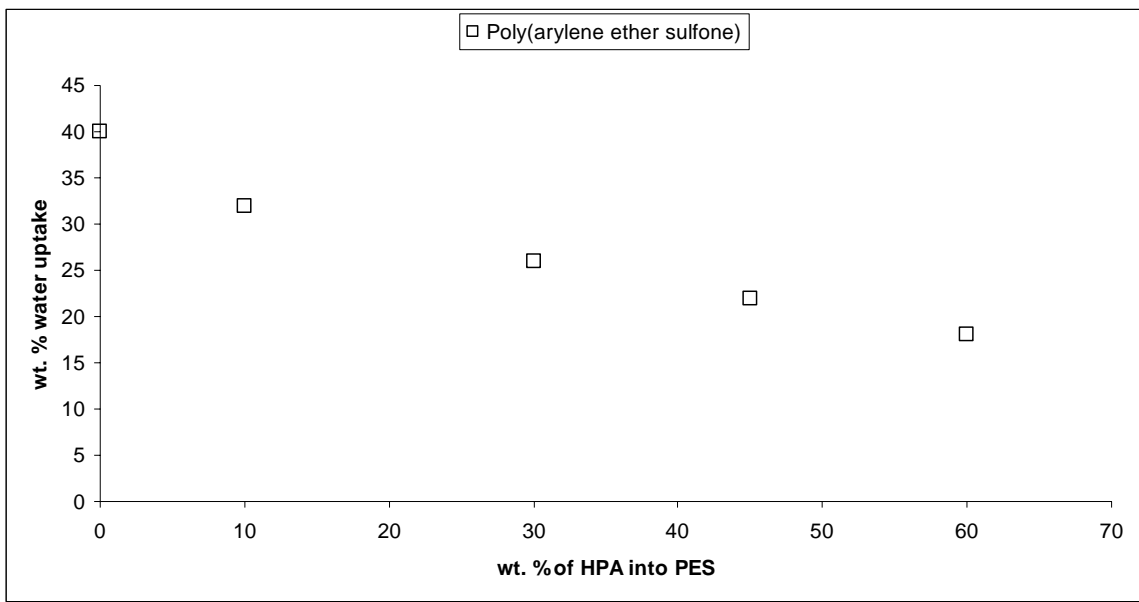


Figure 5-15 Water uptake plots for poly(arylene ether sulfone) (PES) with various percentages of HPA

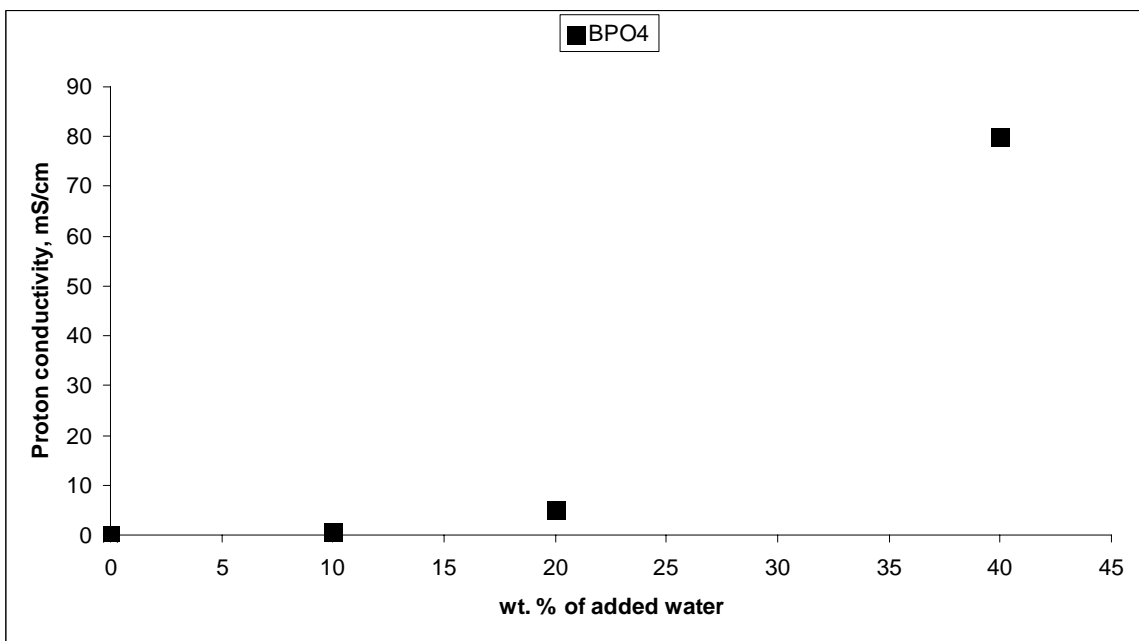


Figure 5-16 Proton conductivity plots with various water uptake percentages for SPEEK with various percentages of BPO₄

5.1.3. FTIR Analysis

As stated earlier, FTIR spectroscopy is an experimental tool used for detecting changes in the coordination and configuration of molecular species in a system. The underlying reason is that electromagnetic radiation in the infrared region has the same frequency as molecular vibrations. Figure 5-17 to Figure 5-20 represents the FTIR spectra of pure SPEEK samples with various composite membranes. Figure 5-17 shows the infrared spectra of the pure SPEEK polymer, solid inorganic powder of Y-zeolite with TPA and composite membrane of SPEEK blended with TPA/Y-zeolite solid powder while Figure 5-18 shows the IR spectra of the pure SPEEK polymer, solid inorganic powder of Y-zeolite with MPA and the composite membrane of SPEEK with MPA/Y-zeolite solid inorganic powder. The spectrum for SPEEK is almost the same as reported earlier in the literature [66]. Characteristic peaks of SPEEK at 1925 and 2028 cm^{-1} are well distinguished with other peaks obtained. For Y-zeolite with 50 wt. % TPA, two profound peaks were observed, two out of which were also observed in the composite membrane spectrum. In the IR spectrum of the composite membrane, the characteristic peaks of the keggin anion were also observed but with a faded intensity. In addition, we have observed a small shift of (W-O_b-W) band from 1925 cm^{-1} in pure SPEEK to 1909 cm^{-1} in the composite membrane with 50 wt. % TPA [76,77].

The broadband in SPEEK samples appearing at 1774 cm^{-1} was assigned to O–H vibration from sulfonic acid groups interacting with molecular water. The aromatic C–C band at 1902 cm^{-1} for SPEEK was observed to split due to new substitution upon loading of solid inorganic powder. A new absorption band at 1842 cm^{-1} in SPEEK was assigned to

sulfur–oxygen symmetric vibration O=S=O. The new absorptions at 1814, 1836, and 1848 cm^{-1} which appeared upon loading of solid powder were assigned to the sulfonic acid group in SPEEK [80], as their intensities with respect to the backbone carbonyl band at 1762 cm^{-1} increased with loading.

When the heteropoly acids loaded Y-zeolite and MCM41 were blended with SPEEK, these HPAs could act as the proton carrier and modify proton conductivity of these membranes. In prepared composite membranes, there could be a number of hydrogen bonds among $\text{H}_3\text{PW}_{12}\text{O}_{40}$, SPEEK and water. The volume of $\text{PW}_{12}\text{O}_{40}^{-3}$ is so big that anions cannot move as a result of the strength of hydrogen bonds, but protons can transfer along these hydrogen bonds. Thus, the addition of solid proton conductors not only provides more protons but also facilitates their transport, for aggregation of the Keggin anions of PWA can form proton channels.

In case of molybdophosphoric acid loading onto Y-zeolite, FTIR confirmed the presence of solid proton conductor in the SPEEK polymer matrix. In the IR spectrum of the composite membranes with MPA, a small shift of (Mo-O_b-Mo) band from 1956 cm^{-1} in solid inorganic powder of Y-zeolite with 50 wt. % MPA to 1964 cm^{-1} in the composite membrane with 50 wt. % solid inorganic powder loading. The frequency shift of about 16 cm^{-1} in case of TPA and shift of about 8 cm^{-1} in case of MPA loading reveals that the keggin structure of TPA and MPA interacts with Y-zeolite mostly through corner-shared oxygen (O_b). So from the IR spectra of the solid composite membranes, it is found that the keggin structure characteristic of the heteropoly anions ($\text{PX}_{12}\text{O}_{40}^{-3}$) is present in these

composite membranes which is strongly responsible for the high proton conductivity of heteropolyacids.

Figure 5-19 shows the infrared spectra of the pure SPEEK, MCM41 with 50 wt. % TPA (M41-T2) and composite membranes of SPEEK with M41-T2 powders. It can be observed that the characteristic peaks of tungstophosphoric acid is observed in the M41-T2 powder at 1625 cm^{-1} which shows the presence of characteristic keggin anion even in the synthesized composite powder. Though the pattern of the composite membrane is not as obvious as that of SPEEK and the solid inorganic powder but the characteristic peak shoulder of SPEEK and characteristic band spectrum of solid inorganic powder is observed. Solid composite powder material of MCM41 with 50 % TPA shows distinctive, strong IR bands in the range of $1650\text{--}1700\text{ cm}^{-1}$ while pure SPEEK shows a weak shoulder at about 1901 cm^{-1} . This strong IR band ranges of the solid inorganic material can be attributed to heteropoly anion which is mainly responsible for the high proton conductivity of the composite membranes [41,78].

It appears that the molecular structure of heteropolyacids is retained after adsorption on the solid proton conductor surface. The most important features for the inorganic modification in composite membranes are related to the adsorption properties of water on the surface. In this regard, the broad band in the O–H stretching vibration region at $2000\text{--}2400\text{ cm}^{-1}$ appears to be mainly composed by two overlapping peaks occurring in the ranges: $2040\text{--}2140$ and $2200\text{--}2340\text{ cm}^{-1}$. It is observed that the main band of peaks ($2200\text{--}2340\text{ cm}^{-1}$) shift to lower frequencies as the amount of the solid proton conductor

in composite membrane increases, which may be attributed to surface acidic characteristics of the solid proton conductors. It is well known that the O–H stretching vibration frequency of surface acidic groups increases as a function of the acidic character, whereas, the stretching frequency of O–H in water, in its non-bonded state, occurs at 2351 cm^{-1} (ν symmetric) and 2356 cm^{-1} (ν asymmetric) [79]. Formation of strong H-bonds with surface groups for the physically adsorbed water shifts the stretching frequencies to much lower energies. Thus, we identify the high frequency peak as due to H-bonded physically adsorbed water and the shoulder at lower frequency to the surface acid–base (O–H) functionalities in the solid proton conductors. Hence, increase in surface acidic character is deduced due to loading of solid proton conductors in SPEEK polymer matrix, and this surface acidic character is one of the major factors which are responsible for high proton conductivities [79].

Figure 5-20 shows the IR spectra of the pure SPEEK, MCM41 with 50 wt. % MPA (M41-M2) and composite membranes of SPEEK containing M41-M2 solid powders. Pattern obtained for M41-M2 as well as for composite membranes containing M41-M2 is found to be amorphous but certain peaks are also found in the composite membranes. In this case, however, the characteristic band of SPEEK is barely visible due to the faded intensity of the peaks which may be attributed to the weaker interactions of MPA with MCM41. These weaker interactions may be due to the weaker keggin structure of MPA compared to TPA. Nevertheless, observation of all the spectra confirms the presence of solid inorganic material into the SPEEK polymer matrix.

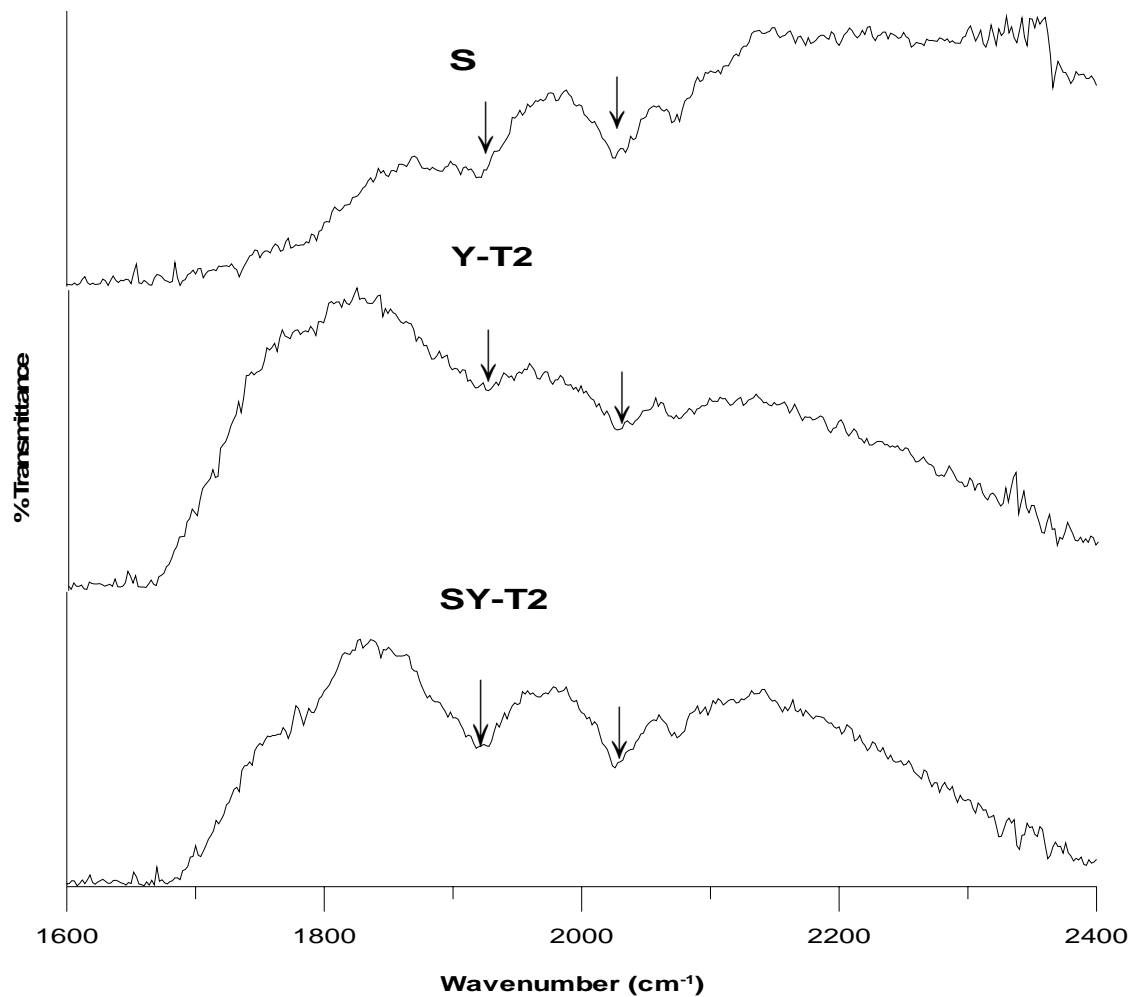


Figure 5-17 FTIR data comparison for (a) pure SPEEK; (b) Y-zeolite+50%TPA and (c) SPEEK(60%)+[Y-zeolite+50%TPA](40%).

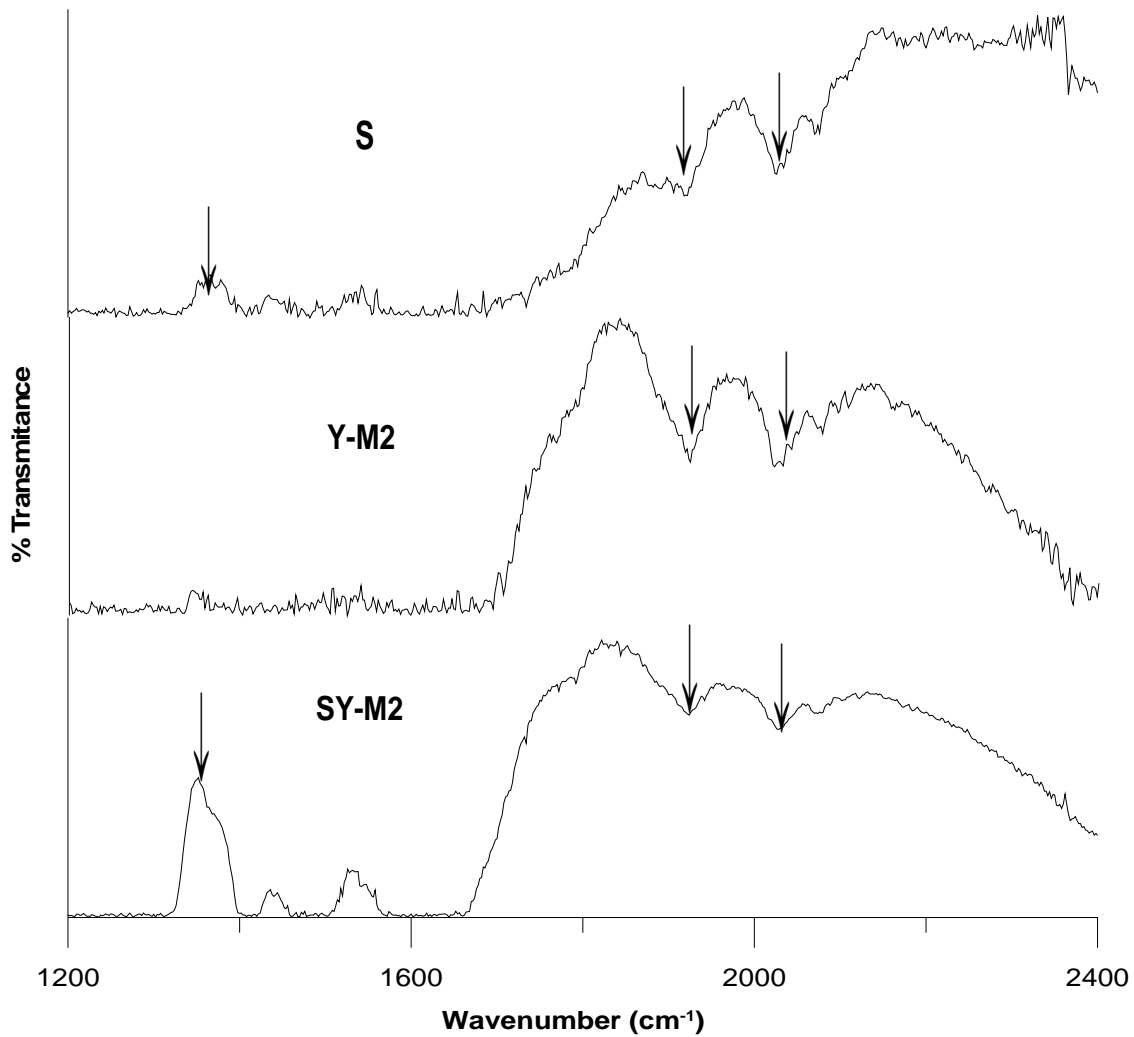


Figure 5-18 FTIR data comparison for (a) pure SPEEK; (b) Y-zeolite+50%MPA and (c) SPEEK(60%)+[Y-zeolite+50%MPA](40%).

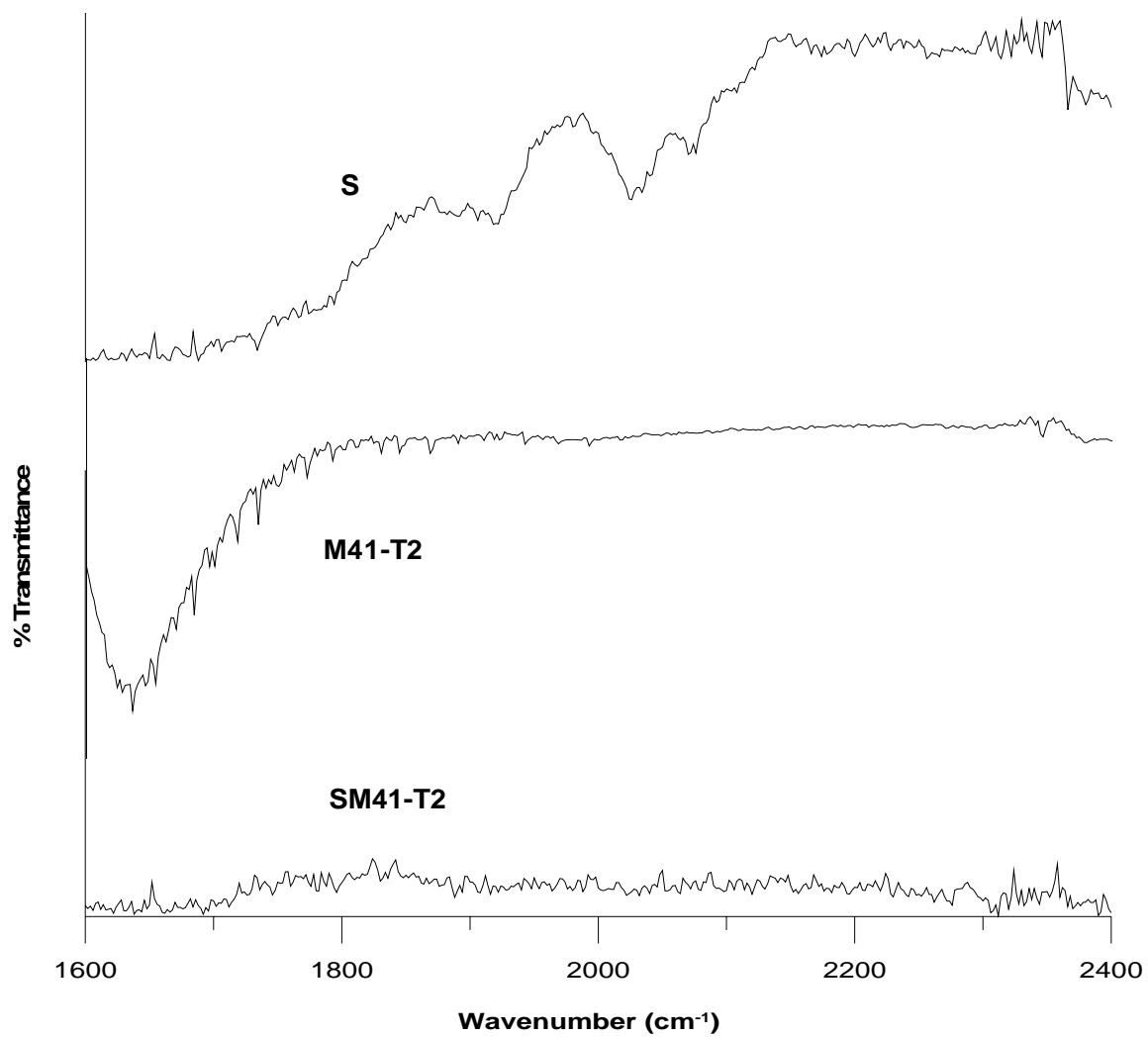


Figure 5-19 FTIR data comparison for (a) pure SPEEK; (b) MCM41+50%TPA and (c) SPEEK(60%)+[MCM41+50%TPA](40%).

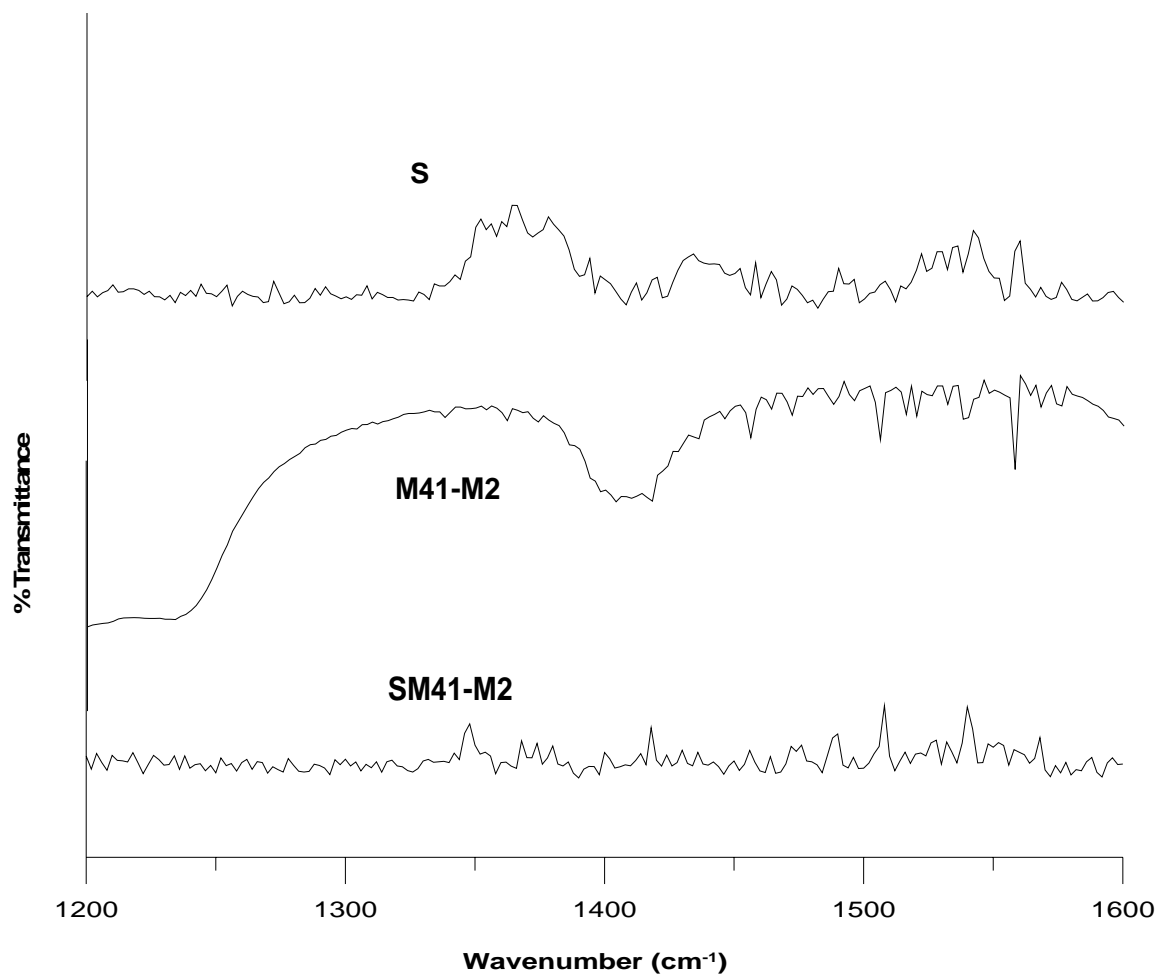


Figure 5-20 FTIR data comparison for (a) pure SPEEK; (b) MCM41+50%MPA and (c) SPEEK(60%)+[MCM41+50%MPA](40%).

5.1.4. X-Ray Diffraction Analysis

Most of the materials are crystalline and hence show symmetry and regularity. This can be made visible by X-ray diffraction producing patterns characteristic of each material. The ground sample is actually made up of thousands of small crystal (crystallites). The random orientation of these crystallites in the specimen ensures that every possible reflecting plane is presented parallel to the specimen surface by at least some crystallites. X-ray powder diffraction (XRD) patterns of pure SPEEK, Y-zeolite with TPA and MPA and that of composite membranes containing these solid proton conductors are shown in [Figure 5-21](#) and [Figure 5-22](#). Although the intensities are changed due to the influence of SPEEK polymer as well as Y-zeolite, the characteristic diffraction peaks of pure TPA and Pure MPA were still observed in the patterns of composite membranes containing 30 wt. % of solid inorganic materials respectively. It can be observed with these figures that pure polymer shows mostly amorphous nature except few peaks, which confirms the semi-crystalline nature of SPEEK polymer, while solid powder material i.e. Y-zeolite with both TPA and MPA shows highly crystalline nature. However, XRD pattern of composite membranes suggests assorted nature of spectra, which in turn signify the presence of SPEEK polymer as well as solid proton conductors.

The XRD patterns of composite membranes with 30 wt. % each of Y-zeolite containing 50 wt. % each of tungstophosphoric acid (TPA) and molybdophosphoric acid (MPA) show the amorphous states, but they are different from that of pure SPEEK whose most intense peak exists at about 44.8° , while in case of solid inorganic powder of Y-zeolite with 50 wt. % TPA, the most intense peak exists at about 17.6° [78]. Diffraction patterns

of composite membranes with 50 wt. % TPA show its most intense peak at about 42° which indicates the characteristic peak of SPEEK polymer. Apart from this the characteristic shoulder of TPA is also observed in the composite membranes which imparts enhanced conductivities to the composite membranes. The above observation is also strengthened by the impedance spectroscopy of the composite membranes in which composite membranes are found to be highly proton conductive. Again, in case of MPA loading on Y-zeolite, the most intense peak of Y-zeolite with 50 wt. % MPA occurs at about 24° . Again for the case of MPA loading into Y-zeolite, characteristic peaks of both SPEEK polymer as well as molybdophosphoric acid were found and hence confirm the findings of infrared spectra and impedance spectroscopy.

X-ray diffraction patterns of pure SPEEK and with 40 wt. % solid inorganic powders of MCM41 with TPA and MPA are shown in [Figures 5-23](#) and [Figure 5-24](#). From the figures, it is evident that pure SPEEK is semi crystalline [76], while solid inorganic powder with 50 wt. % TPA is amorphous. However, the diffraction pattern of composite membranes containing MCM41 with 40 wt. % solid inorganic powders is not totally amorphous and shows partial crystallinity with intense peaks of SPEEK. Since MCM41 powder is not crystalline at the atomic level so no reflections at higher angles are observed. Actually the patterns obtained for MCM41 with 50 % TPA represents poor crystallinity of the material and indicates a distortion of the long range ordering of the mesoporous structure and/or badly built hexagonal arrays. This is perhaps the result of the incorporation of aluminum into the silicate walls, causing structural irregularity. On the other hand, XRD patterns of MCM41 with 50 wt. % of MPA ([Figure 5-24](#)) shows

strongest peak at about 28° with other peaks at about 10.8 , 15.96 , 22 , 30.8 and 35.64° respectively. A relatively significant crystallinity is obtained in the case of MCM41 with 50 wt. % MPA. This may be due to the specific interactions between MCM41 and MPA, since MPA is far smaller in size as compared to TPA. Smaller size in case of MPA makes its keggin structure small as compared to TPA while the specific interactions may be due to the corner-shared oxygen (O_c) present in the heteropoly anion. Nevertheless, interaction due to edge-shared (O_e) oxygen atoms can not be ruled out completely. Hence, the XRD findings support the results discussed in proton conductivity study and FTIR analysis.

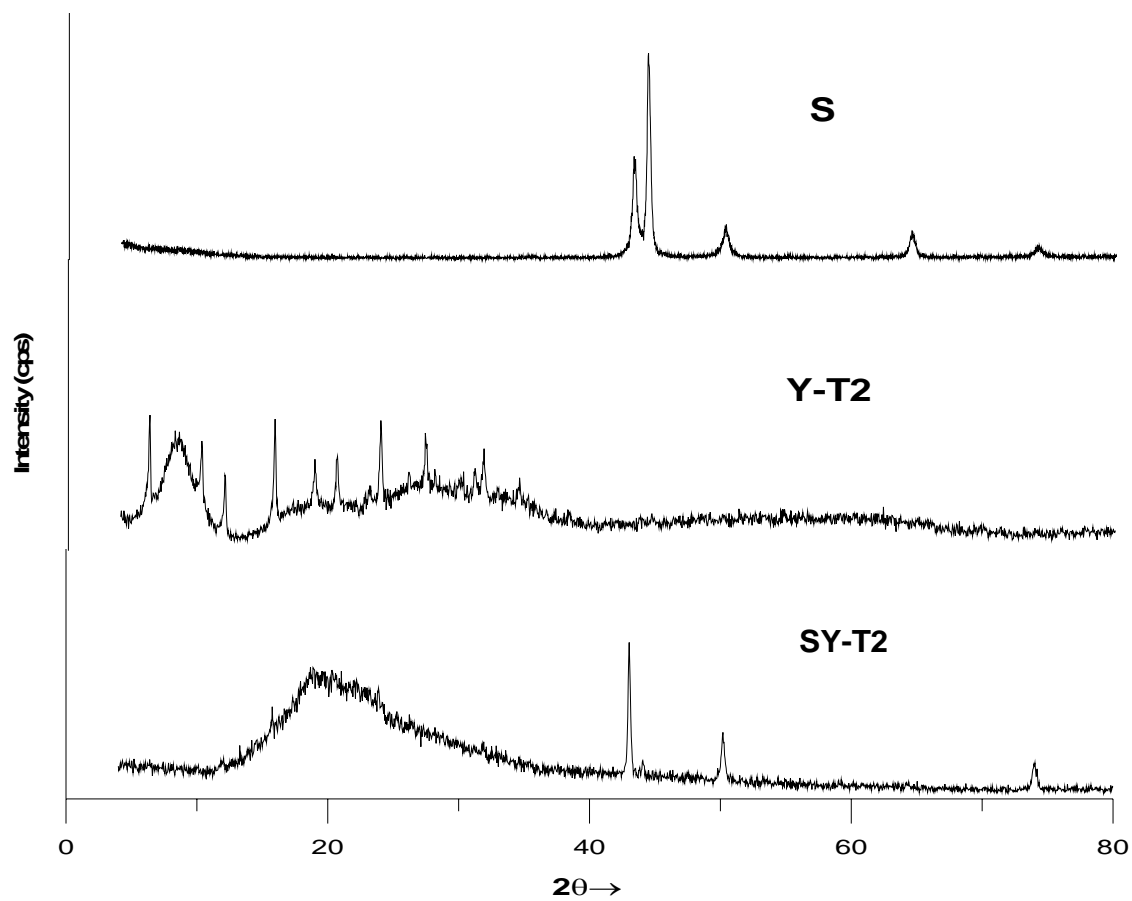


Figure 5-21 XRD data comparison for (a) Pure SPEEK; (b) Y-zeolite+50 % TPA and (c) SPEEK+[Y-zeolite+50 % TPA](30%).

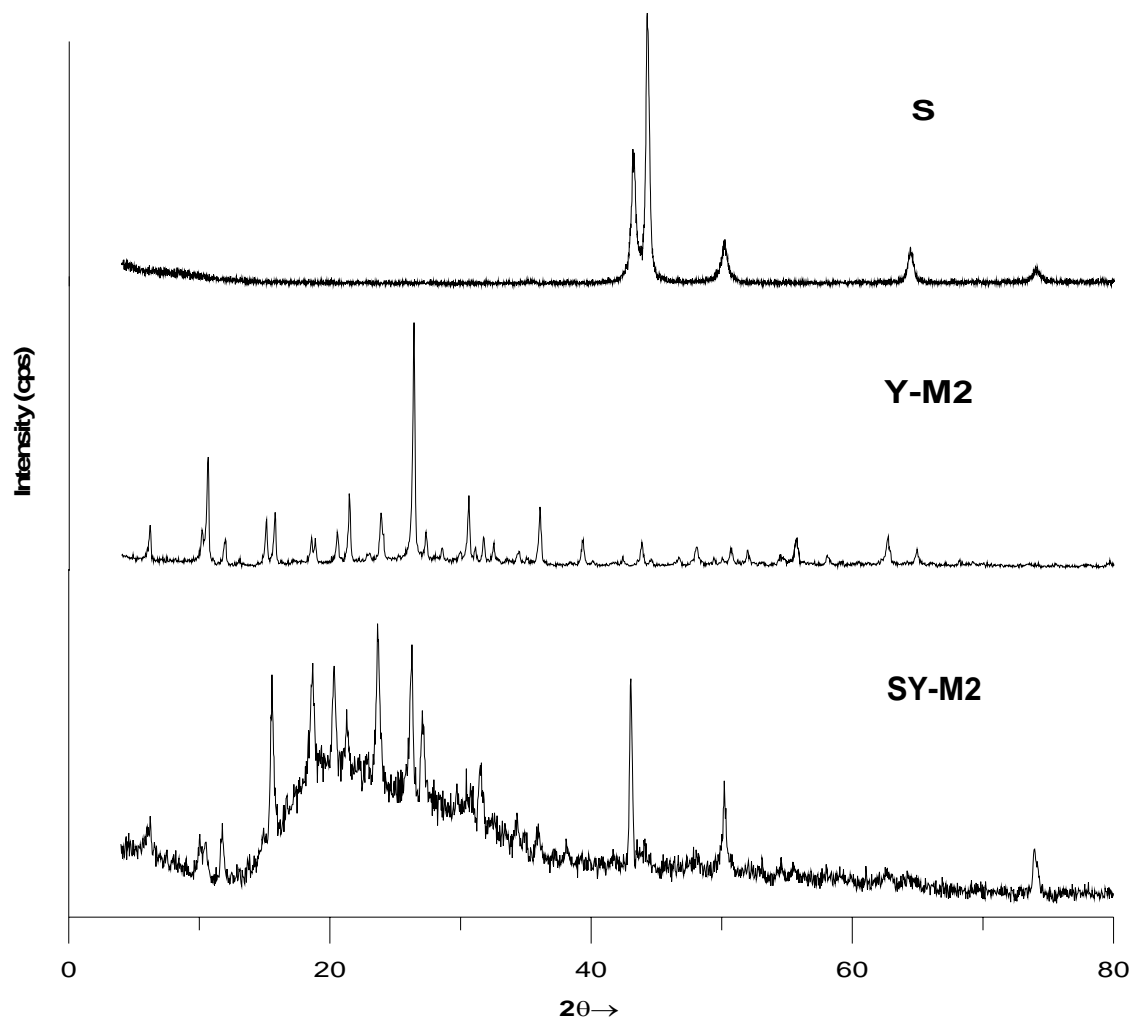


Figure 5-22 XRD data comparison for (a) Pure SPEEK; (b) Y-zeolite+50 % MPA and (c) SPEEK+[Y-zeolite+50 % MPA](30%).

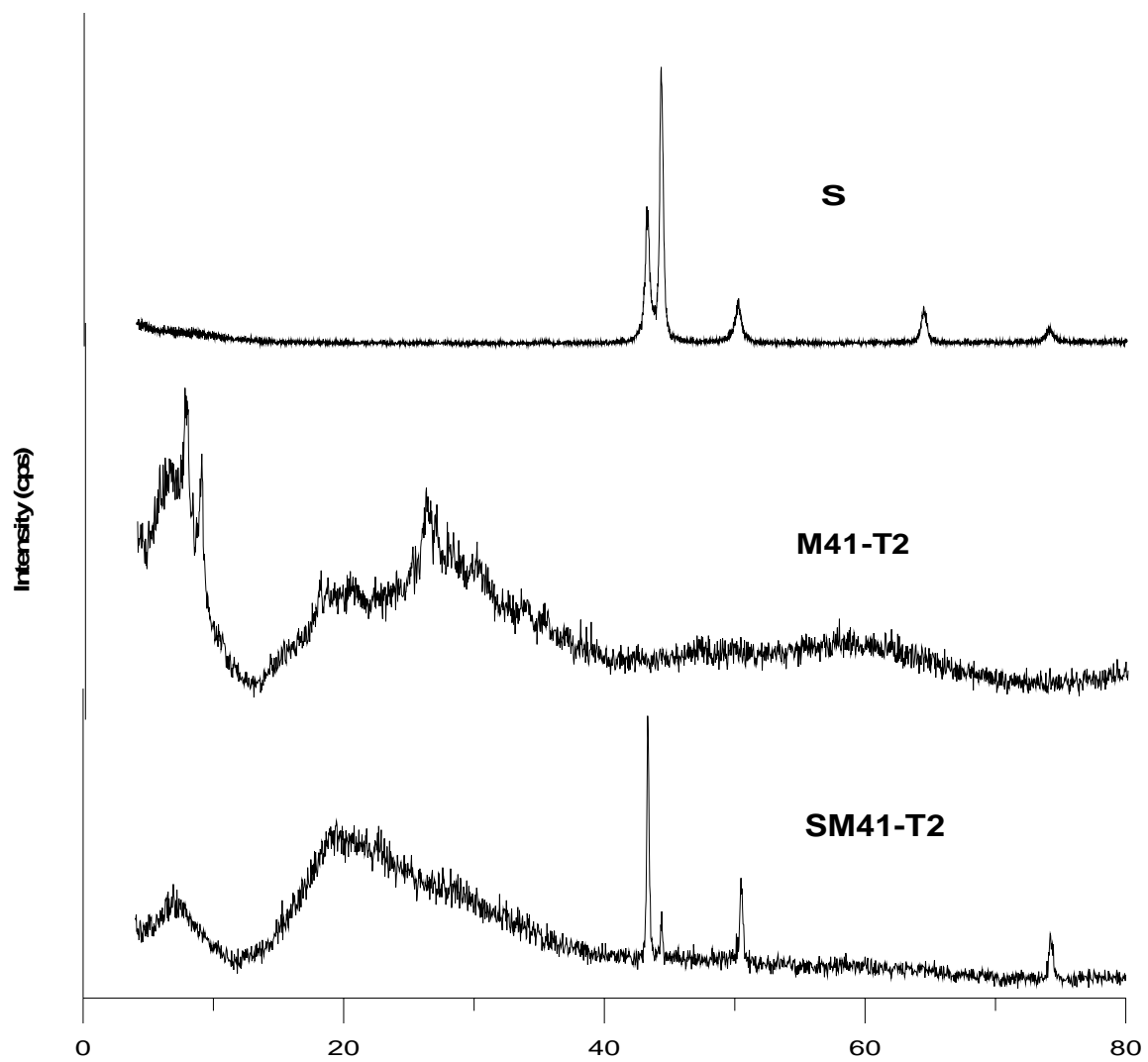


Figure 5-23 XRD data comparison for (a) Pure SPEEK; (b) MCM41+50 % TPA and (c) SPEEK+[MCM41+50 % TPA](40%).

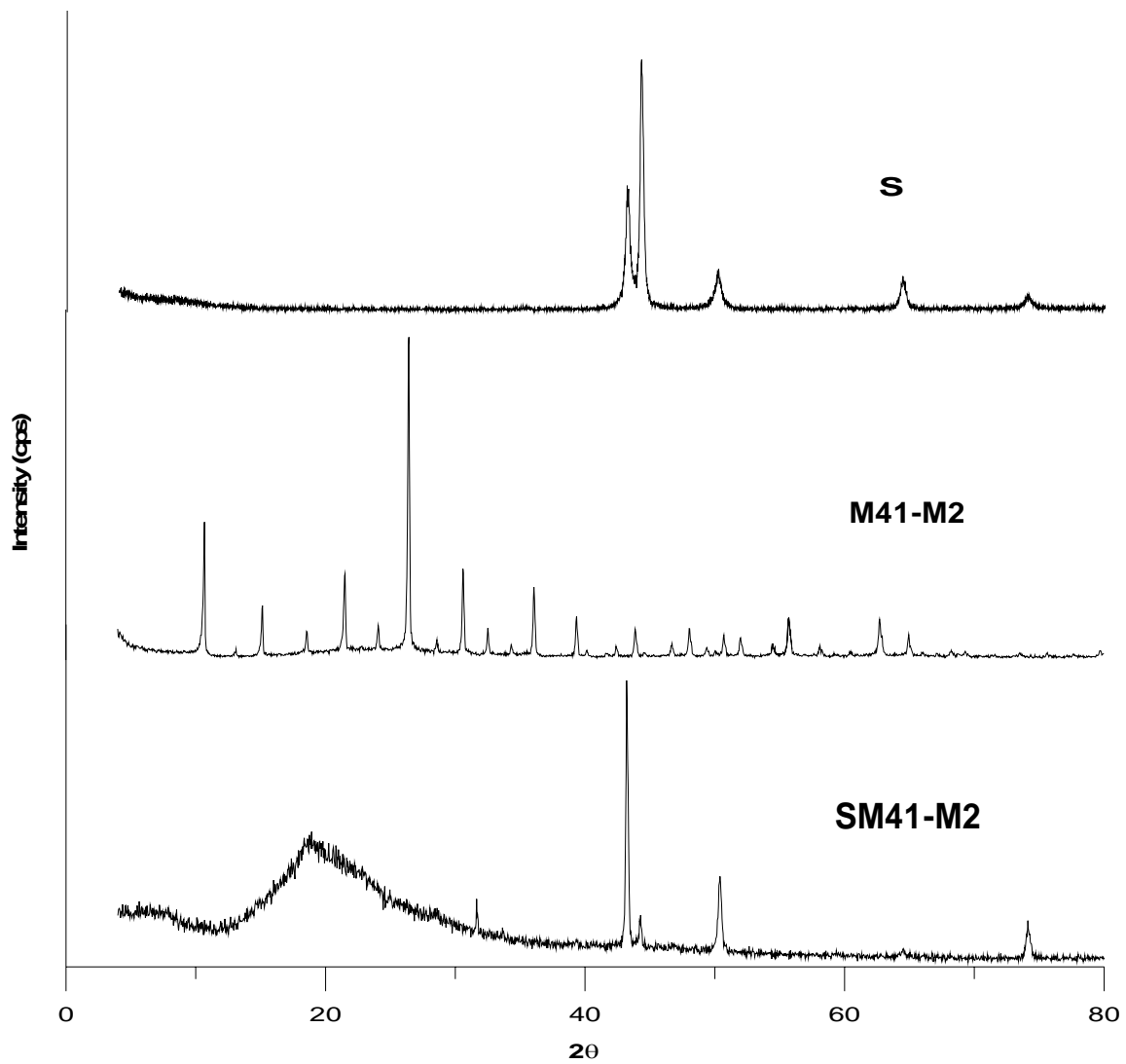


Figure 5-24 XRD data comparison for (a) Pure SPEEK; (b) MCM41+50 % MPA and (c) SPEEK+[Y-zeolite+50 % MPA](30%).

5.1.5. Scanning Electron Microscopy

The morphology of the pure SPEEK membranes and composite membranes prepared from SPEEK with solid inorganic powders has been studied by scanning electron microscopy. Cryogenic fractured images of pure SPEEK, and some composite membranes with various weight percent amount of solid inorganic powders are shown in [Figure 5-25](#). It can be seen that pure SPEEK membrane is almost uniform except some stains near the surface ([Figure 5-25: a](#)). At 30 wt. % loading of solid inorganic powder of Y-zeolite with tungstophosphoric acid (TPA) into SPEEK shows layered morphology ([Figure 5-25: b](#)), while at 40 wt. % loading of solid inorganic powder of Y-zeolite with molybdophosphoric acid (MPA) demonstrate uniform dispersion of inorganic material into SPEEK polymer matrix with no apparent agglomeration except at few sites ([Figure 5-25: c](#)). [Figure 5-25: d & e](#) show the SEM images for the membranes of SPEEK containing MCM41 with heteropolyacids. Almost semi layered morphology with few big discordant spots was observed for the membranes containing solid inorganic powder of tungstophosphoric acid (TPA) loaded onto MCM41 ([Figure 5-25: d](#)). The big keggin structure of TPA may be the main reason for these occasional occurrences of discordant sites present in the micrograph. However, composite membrane of SPEEK with MPA loaded onto MCM41 showed semi-layered morphology with no apparent spots as in case of TPA onto MCM41 ([Figure 5-25: e](#)). Hence, the micrographs strongly back the findings of the other characterization techniques i.e. FTIR and XRD analysis.

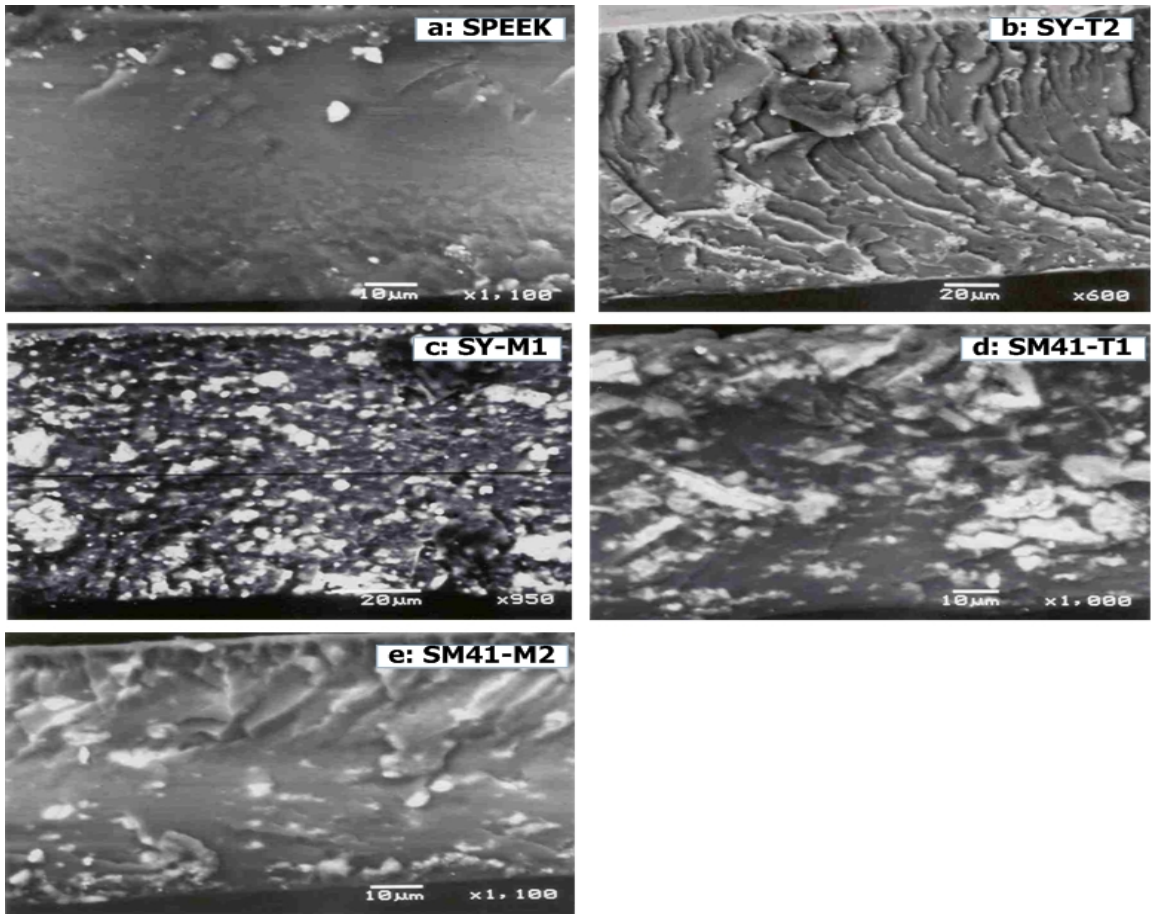


Figure 5-25 SEM images of pure SPEEK (a), SY-T2 (b), SY-M1 (c), SM41-T1 (d) and SM41-M2 (e)

Conclusions

The objective of this thesis work was the development of highly conductive composite membranes by embedding solid proton conducting solids in polymer matrices. The goals of the study were successfully achieved. The efforts of this research work resulted in the development of new inorganic solid proton conductors and a series of novel composite membranes. Conductivity of prepared solids and composite membranes has been studied. The conclusions of this thesis are divided into two sections: the development and study of solid inorganic proton conductors and the development of the polymer composite membranes based on sulfonated polyether ketone (SPEEK) and the proton conducting solids.

6.1. Development of proton conducting solids

Solid proton conductors from heteropolyacids (HPAs) namely tungstophosphoric acid (TPA) & molybdophosphoric acid (MPA) loaded Y-zeolite and MCM41 have been successfully synthesized.

1. Proton conductivities of prepared solid proton conductors were carried out using Impedance Spectroscopic (IS) technique. Samples with highest loadings of HPAs onto Y-zeolite as well as MCM41 demonstrated highest conductivity values. However, solid proton conductors from HPA loaded Y-zeolite was found to be

more conductive as compared to solid proton conductors from HPAs loaded MCM41. Conductivity values of prepared solid powders further increased to considerable levels with various water percentages. Highest conductivity with 40 wt. % water was found to vary from 0.652 to 10.91 mS/cm.

2. Synthesized materials were found to be crystalline, however MCM41 containing solid proton conductors were found to be less crystalline as compared to Y-zeolite containing solid proton conductors. X-ray diffraction technique confirmed crystallinity of the solid materials.
3. Flow studies of the solid proton conductors showed negligible leaching of the heteropolyacids from Y-zeolite as well as MCM41. Total amounts of HPAs leached out were found in the range of 7-19% of the initial amount loaded on Y-zeolite as well as MCM41. Flow study analysis was done using atomic absorption spectrometric (AAS) technique.
4. Crystallinity of the materials and presence of heteropolyacids through various functional groups were confirmed by FTIR analysis. Characteristic peaks of Y-zeolite as well as MCM41 with heteropolyacids were confirmed by FTIR analysis.
5. Scanning electron micrograph (SEM) technique showed that the heteropolyacids were loaded almost uniformly onto Y-zeolite and MCM41 with almost negligible areas of agglomeration.

6.2. Development of composite membranes

Composite electrolyte membranes were prepared by loading of prepared solid proton conductors into sulfonated polyether ether ketone (SPEEK) polymer matrix using solution casting technique. Prepared composite membranes were characterized using various characterization techniques.

1. Prepared composite membranes were found to be uniform and mechanically stable upto 40 wt. % loading of inorganic material into the polymer matrix.
2. Composite membranes were prepared by embedding different proportions of solid proton conductors; TPA & MPA loaded Y-zeolite as well as MCM41. The conductivity of the composite membranes was found to be increased as the loading of solid inorganic material was increased form 10 wt. % to 40 wt. % and also with temperature. The maximum conductivity of these SPEEK/solid proton conductors was found to be of the order of 10^{-2} S/cm. Membranes also remained stable in the temperature range of 90-140 °C.
3. Water uptake studies of the prepared composite membranes illustrated considerably high water uptake values, which is responsible for high proton conductivity of the membranes. High water uptake also prevents membrane dehydration at high operating temperatures due to the water retention in the membrane.
4. FTIR analysis of membranes also confirmed the presence of solid inorganic proton conductors in SPEEK polymer matrix, though with faded intensity of characteristic peaks of individual pure materials.

5. XRD analysis of the prepared composite membranes also confirmed the solid inorganic material loading into polymer matrix. Though SPEEK is non-crystalline but the loading of solid proton conductors shows partial crystallinity, which is also indicative of the presence of inorganic material in the polymer structure.
6. Scanning electron micrograph (SEM) analysis of composite membranes demonstrated quite good dispersion of solid material into the polymer structure.

Recommendations

Fuel cells attract worldwide attention as a cleaner source of energy and hold promise for a pollution free ambience. A tremendous research activity worldwide in the fuel cell polymer membrane development is going on especially for transportation and portable applications. A number of groups worldwide are putting their efforts to introduce the best possible membrane material for PEM fuel cell as well as DMFC. The results obtained in this research for the development of composite membranes are very vital and promising. Different series of highly conductive and thermally stable composite membranes developed in this work need to be evaluated for their performance in an experimental fuel cell. The following recommendations can be suggested for future work:

1. Materials e.g. Y-zeolite used in this study has been used as procured from CATAL, UK. Professor Inui in his personal communication suggests that It would have produced far better results if tailored Y-zeolite is prepared with high silica alumina ratio.

2. BET surface area studies will impart in-depth knowledge about the surface area as well the voidage of the prepared materials, then and only then it can be concretely declared that how much surface area loaded heteropolyacids occupy and what exactly the situation is with Y-zeolite as well as MCM41 after loading of heteropolyacids.
3. Evaluation of performance of prepared composite membranes in H₂/O₂ PEM fuel cells.
4. Evaluation of performance of prepared composite membranes in direct methanol fuel cells.
5. Study the long term stability and aging mechanism of the prepared composite membranes for both H₂/O₂ PEM and direct methanol fuel cells.
6. Study the methanol permeation and diffusion experiments on the composite membranes to find out the methanol permeation/diffusion through the membranes.

APPENDIX A

PROTON CONDUCTIVITY MEASUREMENTS

Proton conductivity is an important factor of membranes to be used in fuel cells. Proton conduction decides the amount of electricity and effectiveness of any fuel cell device. Proton conduction through the membrane takes place when there are generations of protons and electrons because of two electrode reactions at anode and cathode of the fuel cell. Protons are been transferred from anode to cathode in order to produce the electricity. The amount of protons transferred by the membrane per unit area and per unit thickness is called the proton conductivity of the membrane.

Basically there are many techniques available to measure the conductivity of membranes or of the solid powders, primarily based on impedance spectroscopy. The techniques based on impedance spectroscopy use either AC impedance method or the DC impedance method. Actually by these methods, we calculate the resistance offered by the membrane or the powder employed between the two electrodes of the conductivity measurement cell. This resistance is then plugged into the following equation to get the conductivity of the membrane or the powder, whatever the case may be.

$$C = \frac{L}{RA} \quad (A)$$

where C represents conductivity, L is the thickness of the membrane or the powder layer, R is the resistance and A is the area through which the conduction of protons is taking place.

Protonic conductivity plays a key role in important processes as diverse as the photosynthesis in green plants and the production of electricity in hydrogen fuel cells [26]. The highest reported protonic conductivities in inorganic solids at temperatures near ambient are those of the heteropolyacids which have been reported by Zaidi et al. [8]. Solid heteropoly compounds (HPC) have been shown to be good protonic conductors. Proton conductivity, mostly on palletized samples is reported in the literature [27] for $\text{H}_3\text{PW}_{12}\text{O}_{40}\cdot n\text{H}_2\text{O}$. Polycrystalline samples with large grain boundaries will short circuit the bulk conductivity to fast conduction rates. Moreover, in most of the cases the temperature dependence of conductivity is studied over a limited temperature region only [28].

Salient Points during Conductivity measurements

1. All of the conductivity measurement data were collected through software called PowerSine using electrochemical impedance spectroscopy (EIS) technique.
2. The frequency range employed during the experiments was $0.1\text{-}1.2\times 10^5$ Hz, in which upper limit of frequency corresponds to real resistance offered by powder or membrane sample respectively.
3. The oscillating voltage during the experiments was set at $\pm 10\text{mV}$.
4. The data obtained through PowerSine software was then analyzed by fitting the R(QR) model in another software called Zsimpwin in order to calculate the real resistance offered by the particular sample, where R outside the bracket depicts the real resistance offered by the sample, Q corresponds to the leaking capacitor and R inside the bracket represent the open circuit resistance.

5. The thickness L and area A of every sample was noted down prior to conducting the experiment. Thickness and area for powder samples remained constant because of Teflon spacer used for holding the powder samples, while L and A varied for various membrane samples.
6. Resistance R , thickness L and area A was then put in Equation (A) to obtain the proton conductivity of the sample.

APPENDIX B

RECIPE FOR PREPARATION OF HETEROPOLYACIDS LOADED SOLID PROTON CONDUCTORS

Materials used:

1. 99.995% purity grade heteropolyacids procured from Fluka
2. Y-zeolite from CATAL, UK
3. distilled water
4. 10% V/V HCl solution

Apparatus Used:

1. 200 ml beaker
2. Ultrasonic treatment equipment
3. A mercury thermometer
4. Magnetic stirrer with heater

Preparation Procedure:

- 1) First of all we weighed the materials as given above i.e. Y-zeolite and/or MCM41 and heteropolyacids according to weight percentages on a high precision weighing machine on ambient conditions.
- 2) Then we took 50 ml of distilled water in a beaker and dissolved in it the already weighed heteropolyacids.

- 3) Then, 0.5 ml of 10 % V/V HCl solution was poured into the beaker; in order not to let the HPA decompose in the solution and ensuring complete miscibility of respective heteropolyacids in distill water.
- 4) Already weighed amounts of Y-zeolite or MCM41 were then put into the beaker and the contents were given an ultrasonic treatment for half an hour to ensure optimum mixing.
- 5) Now the beaker was put onto a heating plate magnetic stirrer with a thermometer installed in it. The contents were continuously heated and stirred at a constant temperature of 80 °C.
- 6) The sample was continuously stirred and heated with the above specified conditions, until dried by evaporation.
- 7) The dried material so obtained was then put into a programmable air flowing oven (automatic) at 200 °C for 6 hours for removing excess moisture present (if any) and bottled.

References

1. K. Kordesch, G. Simader, "Fuel cells and their applications" *New York: VCH Publishers, Inc.*, (1996).
2. M. A. J. Cropper, S. Geiger, D. M. Jollie, "Fuel cells: A survey of current developments" *J. Power Sources*, 131(1-2) (2004) 57-61.
3. S. M. Haile, "Fuel cell materials and components", *Act. Materil.*, 51 (2003) 5981-6000.
4. S. M. J. Zaidi, S.D. Mikhailenko, S. Kaliaguine, "Development of composite membranes for DMFC", *4th International Symposium on New Materials for Electrochemical Systems, Montreal, Quebec Canada* (2001).
5. P. Jannasch, "Recent developments in high-temperature proton conducting polymer electrolyte membranes", *Current Opinion Coll. Inter. Sci.*, 8 (2003) 96-102.
6. A. S. Arico, S. Srinivasan, V. Antonucci, "DMFCs: From fundamental aspects to technology development", *Fuel Cells* 1(2) (2001)133-161
7. S. M. J. Zaidi, S.D. Mikhailenko, S. Kaliaguine, "Electrical properties of sulfonated polyether ether ketone/polyetherimide blend membranes doped with inorganic acids", *J. Polymer Sci.: part B: Polymer Physics*, 38 (2000) 1386-1395.
8. S. M. J. Zaidi, "Development of proton conducting composite membranes for fuel cell applications", *PhD Thesis*, University of Laval, Department of Chemical Engineering, Quebec Canada (2000).
9. S. R. Mukai, T. Masuda, I. Ogino, Hashimoto, K., "Preparation of encaged heteropolyacid catalyst by synthesizing 12-molybdophosphoric acid in the supercages of Y-type Zeolite", *Applied Catalysis A: General* 165 (1997) 219-226.

10. Hoogers, G., "Fuel cell technology handbook", CRC Press, Florida, USA (2003) 337 pages.
11. N. Walsby, "Preparation and characterization of Radiation-Grafted membranes for fuel cells", *Academic dissertation*, University of Helsinki, Department of Chemistry, Helsinki Finland (2001).
12. G. Hormandiger, "Fuel cells in transportation", *Licentiate's Thesis*, University of London, Imperial College of Science, Technology & Medicine, Centre for Environmental Technology, London (1995).
13. W. L. Harrison, "Synthesis and characterization of sulfonated poly (arylene ether sulphone) copolymers via direct copolymerization: candidates for proton exchange membrane fuel cells", *PhD Dissertation*, Virginia polytechnic institute and state university, Department of Chemistry, Blacksburg Virginia (2002).
14. V. Gogel, L. Jorissen, J. Kerres, J. Garche, "New membranes for direct methanol fuel cells", *J. Power Sources*, 105 (2002) 267-273.
15. A. B. Hart, G. J. Womack, "Fuel cells: Theory and application", *Chapman and Hall Ltd.*, London (1974) 372 pages.
16. A. Dyer, "An Introduction to Zeolite molecular sieves", John Wiley & sons, New York, USA (1988) 149 pages.
17. M. Lassinantti, "Synthesis, characterization and properties of Zeolite films and membranes", *Licentiate's Thesis*, Lulea Tekniska Universitet, Institutionen för Kemi och metallurgi, Luleå Sweden (2001).
18. N. Ohler, "Properties and reactivity of keggin structures", Review: Catalysis, U.C. Berkeley, Dept. of Chemical Engineering, California USA (2002) spring.

19. S. M. J. Zaidi, S.D. Mikhailenko, S. Kaliaguine, "Electrical conductivity of boron orthophosphate in presence of water", *J. Chem. Soc., Faraday Trans.*, 94(11) (1998) 1613-1618.
20. S. Kaliaguine, S. D. Mikhailenko, J. B. Moffat, "Electrical impedance studies of the ammonium salt of 12-tungstophosphoric acid in the presence of liquid water", *Solid State Ionics* 99 (1997) 281-286.
21. S. Chandra, N. Lakshmi, "Proton conducting composites of heteropolyacid hydrates (phosphomolybdic and phosphotungstic acids) dispersed with insulating Al_2O_3 ", *Phys. Stat. sol. (a)*, 186 (3) (2001) 383-399.
22. S. Chandra, N. Lakshmi, "Ion transport in some solid state proton conducting composites studied from volta cell e.m.f. and complex impedance spectroscopy", *Bull. Mater. Sci.*, 25 (3) (2002) 197-201.
23. D. H. Park, S. S. Park, S. J. Choe, "Photoacoustic spectroscopic study on cobalt incorporation onto the surface of mesoporous molecular sieves", *Bull. Korean Chem. Soc.*, 20 (6) (1999) 715-719.
24. D. H. Park, C. F. Cheng, J. Klinowski, "Optimization of synthetic parameters for mesoporous molecular sieve MCM-41 using surfactant CTAC1", *Bull. Korean Chem. Soc.*, 18 (4) (1997) 379-384.
25. R. A. Khan, "Metal incorporation in MCM-41 for hydrodesulfurization", *MS Thesis*, King Fahd University of Petroleum & Minerals, Department of Chemical Engineering, Dhahran Saudi Arabia (2002).
26. K. D. Kreuer, "Hydrocarbon Based Membranes for PEM Fuel Cells", *Handbook of Fuel Cell Technology*. John Wiley & Sons. September 7 (2001).

27. S. M. J. Zaidi, S. D. Mikhailenko, G. P. Robertson, M. D. Guiver, S. Kaliaguine, "Proton conducting composite membranes from polyether ether ketone and heteropolyacids for fuel cell applications", *J. Memb. Sci.*, 173 (2000) 17-34.
28. K. Paulraj, S. J. Ethilton, D. P. Padiyan, "Protonic conductivity and photoconductivity studies on $H_3PW_{12}O_{40} \cdot 21H_2O$ single crystals", *Cryst. Res. Technol.*, 35 (1) (2000) 87-94.
29. A. E. Steck, "Membrane Materials in Fuel Cells", 1st *International Symposium on New Materials For fuel Cell Systems. Montreal, Canada* (1995) 74.
30. K. D. Kreuer, "On the development of proton conducting polymer membranes for hydrogen and methanol fuel cells", *J. Memb. Sci.*, 185 (2001) 29-39.
31. O. Savadogo, "Emerging membranes for electrochemical systems: (I) solid polymer electrolyte membranes for fuel cell systems", *J. New Mat. Electrochem. Systems*, 1 (1998) 47-66.
32. W. C. Choi, J. D. Kim, and S. I. Woo, "Modification of proton conducting membrane for reducing methanol crossover in a direct methanol fuel cell", *J. Power Sources*, 96 (2001) 411-414.
33. C. Yang, S. Srinivasan, A. S. Arico, P. Creti, V. Baglio, V. Antonucci, "Composite Nafion/Zirconium phosphate membranes for direct methanol fuel cell operation at high temperature", *Electrochemical and Solid State Letters*, 4(4) (2001) A31-A34.
34. P. Costamagna, C. Yang, A. B. Bocarsly, S. Srinivasan, "Nafion[®] 115/zirconium phosphate composite membranes for operation of PEMFCs above 100 °C", *Electrochim. Act.*, 47 (2002) 1023-1033.

35. K. T. Adjemian, S. J. Lee, S. Srinivasan, J. Benziger, A. B. Bocarsly, "Silicon oxide Nafion composite membranes for proton-exchange membrane fuel cell operation at 80-140 °C", *J. Electrochem. Soc.*, 149 (3) (2002) A256-A261.
36. D. H. Jung, S. Y. Cho, D. H. Peck, D. R. Shin, J. S. Kim, "Performance evaluation of a Nafion/silicon oxide hybrid membrane for direct methanol fuel cell", *J. Power Sources*, 106 (2002) 173-177.
37. P. Dimitrova, K. A. Friedrich, U. Stimming, B. Vogt, "Modified Nafion-based membranes for use in direct methanol fuel cells", *Solid State Ionics*, 150 (2002) 115-122.
38. P. Staiti, "Proton conductive membranes constituted of silicotungstic acid anchored to silica-polybenzimidazole matrices", *J. New Mat. Electrochem. Systems*, 4 (2001) 181-186.
39. O. Savadogo, B. Tazi, "New cation exchange membranes based on Nafion and heteropolyacids with and without thiophene", *J. New Mat. Electrochem. Systems*, (submitted) (2003).
40. V. Ramani, H. R. Kunz, J. M. Fenton, "Investigation of Nafion[®]/HPA composite membranes for high temperature/low relative humidity PEMFC operation", *J. Memb. Sci.*, 232 (2004) 31-44.
41. V. Tricoli, F. Nannetti, "Zeolite-Nafion composites as ion conducting membrane materials", *Electrochim. Act.*, 48 (2003) 2625-2633.
42. B. Holmberg, H. Wang, J. Norbeck, Y. Yan, "Synthesis and Characterization of Zeolite Y Nanocrystals for Nafion Zeolite Y Composite Proton Exchange

- Membranes”, *AIChE, Spring National Meeting*, March 10-14 (2002) New Orleans, Los Angeles, USA.
43. P. G. Pickup, M. C. Lefebvre, J. Halfyard, Z. Qi, J. Nengyou, “Modification of Nafion proton exchange membranes to reduce methanol crossover in PEM fuel cells”, *Electrochemical and solid state letters*, 3(12) (2000) 529-531.
44. F. Liu, B. Yi, D. Xing, J. Yu, H. Zhang, “Nafion/PTFE composite membranes for fuel cell applications”, *J. Memb. Sci.*, 212 (2003) 213-223.
45. J. Shim, H. Y. Ha, S. A. Hong, I. H. Oh, “Characteristics of the Nafion ionomer-impregnated composite membrane for polymer electrolyte fuel cells”, *J. Power Sources*, 109 (2002) 412-417.
46. G. Deluga, B. S. Pivovar, D. S. Shores, “Composite membranes in liquid feed direct methanol fuel cells”, *DOE/NRL workshop*, University of Minnesota Oct. 6-8 (1999).
47. Z. G. Shao, X. Wang, I. Hsing, “Composite Nafion/polyvinyl alcohol membranes for the direct methanol fuel cell”, *J. Memb. Sci.*, 210, 147-153 (2002).
48. S. M. J. Zaidi, S. D. Mikhailenko, S. Kaliaguine, “Sulfonated polyether ether ketone based composite polymer electrolyte membranes”, *Catalysis Today* 67 (2001) 225-236.
49. L. Li, J. Zhang, Y. Wang, “Sulfonated poly(ether ether ketone) membranes for direct methanol fuel cell”, *J. Memb. Sci.*, 226 (2003) 159-167.
50. V. Silva, B. Ruffmann, H. Silva, H. Mendes, A. Madeira, S. P. Nunes, “Zirconium oxide modified sulfonated polyether ether ketone membranes for direct methanol fuel cell applications”, *Materials 2003-II International Materials Symposium*, Caprica Portugal (2003) April 14-16.

51. B. Ruffmann, H. Silva, B. Schulte, S. P. Nunes, "Organic/inorganic composite membranes for application in DMFC", *Solid State Ionics*, 162-163 (2003) 269-275.
52. J. H. Chang, J. H. Park, G. G. Park, C. S. Kim, O. O. Park, "Proton conducting composite membranes derived from sulfonated hydrocarbon and inorganic materials", *J. Power Sources*, 124 (2003) 18-25.
53. S. P. Nunes, B. Ruffmann, E. Rikowski, S. Vetter, K. Richau, "Inorganic modifications of proton conductive polymer membranes for direct methanol fuel cells", *J. Memb. Sci.*, 203 (2002) 215-225.
54. M. L. Ponce, L. Prado, B. Ruffmann, K. Richau, R. Mohr, S. P. Nunes, "Reduction of methanol permeability in polyetherketone-heteropolyacid membranes", *J. Memb. Sci.*, 217 (2003) 5-15.
55. Y. S. Kim, F. Wang, M. Hickner, T. A. Zawodzinski, J. E. McGrath, "Fabrication and characterization of heteropolyacid ($H_3PW_{12}O_{40}$)/directly polymerized sulfonated poly(arylene ether sulfone) copolymer composite membranes for higher temperature fuel cell applications", *J. Memb. Sci.*, 212 (2003) 263-282.
56. L. Li, L. Xu, Y. Wang, "Novel proton conducting composite membranes for direct methanol fuel cell", *Mater. Lett.*, 57 (2003) 1406-1410.
57. R. He, Q. Li, G. Xiao, N. J. Bjerrum, "Proton conductivity of phosphoric acid doped polybenzimidazole and its composites with inorganic proton conductors", *J. Memb. Sci.*, 226 (2003) 169-184.
58. X. F. Xie, H. Guo, Z. Q. Mao, J. M. Xu, "Organic/inorganic nanocomposites for direct methanol fuel cell", *AICHE, Spring National Meeting*, March 10-14 (2002) New Orleans, Los Angeles, USA.

59. D. J. Jones, L. T. Bouckary, J. Roziere, "Hybrid polyetherketone membranes for fuel cell applications", *Fuel Cells*, 2 (1) (2002) 1-6.
60. D. J. Jones, B. Baur, J. Roziere, L. Tchicaya, G. Alberti, M. Casciola, L. Massinelli, A. Peraio, S. Besse, E. Ramunni, "Electrochemical characterization of sulfonated polyetherketone membranes", *J. New Mat. Electrochem. Systems*, 3 (2000) 93-98.
61. B. Bonnet, D. J. Jones, J. Roziere, L. Tchicaya, G. Alberti, M. Casciola, L. Massinelli, B. Bauer, A. Peraio, E. Ramunni, "Hybrid organic-inorganic membranes for a medium temperature fuel cell", *J. New Mat. Electrochem. Systems*, 3 (2000) 87-92.
62. W. R. Bowen, T.A. Denova, H. Yin, "The effect of sulfonated Polyether ether ketone additives on membrane formation and performance", *Desalination*, 145 (2002) 39-45.
63. D. J. Jones, J. Roziere, "Recent advances in the functionalization of polybenzimidazole and polyetherketone for fuel cell applications", *J. Memb. Sci.*, 185 (2001) 41-58.
64. M. Y. Jang, Y. Yamazaki, "Preparation, characterization and proton conductivity of membrane based on zirconium tricarboxybutylphosphonate and polybenzimidazole for fuel cells", *Solid State Ionics*, 167 (2004) 107-112.
65. Z. G. Shao, P. Joghee, I. M. Hsing, "Preparation and characterization of hybrid Nafion-silica membrane doped with phosphotungstic acid for high temperature operation of proton exchange membrane fuel cells", *J. Memb. Sci.*, 229 (2004) 43-51.

66. H. Y. Chang, C. W. Lin, "Proton conducting membranes based on PEG/SiO₂ nanocomposites for direct methanol fuel cells", *J. Memb. Sci.*, 218 (2003) 295-306.
67. J. Kerres A. Ullrich, F. Meier, T. Haring, "Synthesis and characterization of novel acid-base polymer blends for application in membrane fuel cells", *Solid State Ionics*, 125 (1999) 243-249.
68. J. Kerres, A. Ullrich, T. Haring, M. Baldauf, U. Gebhardt, W. Preidal, "Preparation, characterization and fuel cell application of new acid base blend membranes", *J. New Mat. Electrochem. Systems*, 3 (2000) 129-139.
69. P. Pintauro, H. Yoo, R. Wycisk, J. Lee, R. Carter, "Direct methanol fuel cell performance with multilayered polyphosphazene membranes", *AIChE, Spring National Meeting*, March 10-14 (2002) New Orleans, Los Angeles, USA.
70. C. Manea, M. Mulder, "New polymeric electrolyte membranes based on proton donor-proton acceptor properties for direct methanol fuel cells", *Desalination*, 147 (2002) 179-182.
71. F. G. Wilhelm, I. G. M. Punt, N. F. A. Van der vagt, H. Strathmann, M. Wessling, "Cation permeable membranes from blends of sulfonated Polyether ether ketone and polyether sulfone", *J. Memb. Sci.*, 199 (2002) 167-176.
72. Y. Wang, H. Wu, S. Wang, "A methanol barrier polymer electrolyte membrane in direct methanol fuel cells", *J. New Mat. Electrochem. Systems*, 5 (2002) 251-254.
73. Y. Gao, G.P. Robertson, M.D. Guiver, X. Jian, "Synthesis and characterization of sulfonated poly(pthalazinone ether ketone) for proton exchange membrane materials", *J. Polymer Sci.: part A: Polymer Chemistry*, 41 (2003) 497-507.

74. B. Libby, "Composite multi-layered membranes for direct methanol fuel cells", *PhD Thesis*, University of Minnesota, Dept. of Chemical Engg. & Materials Science, Minneapolis (2001).
75. D. T. On, S.M.J. Zaidi, S. Kaliaguine, "Stability of mesoporous aluminosilicate MCM-41 under vapor treatment, acidic and basic conditions", *Micro. and Mesop. Mater.*, 22 (1998) 211-224.
76. P. Staiti, S. Freni, S. Hocevar, "Synthesis and characterization of proton-conducting materials containing dodecatungstophosphoric and dodecatungstosilic acid supported on silica", *J. Power Sources* 79 (1999) 250-255.
77. A. S. Arico, V. Baglio, A. D. Blasi, V. Antonucci, "FTIR spectroscopic investigation of inorganic fillers for composite DMFC membranes", *Electrochem. Commun.* 5 (2003) 862-866.
78. Q. Wu, S. Tao, H. Lin, G. Meng, "Preparation and conductivity of solid high-proton conductor silica gels containing 12-tungstogermanic heteropoly acid", *Mater. Sci. & Engg.* B68 (2000) 161-165.
79. C. Danumah, S. Vaudreuil, L. Bonneviot, M. Bousmina, S. Giasson, S. Kaliaguine, "Synthesis of macrostructured MCM-48 molecular sieves", *Micro. and Mesop. Mater.*, 44-45 (2001) 241-247.
80. G. P. Robertson, S. D. Mikhailenko, K. Wang, P. Xing, M. D. Guiver, S. Kaliaguine, "Casting solvent interactions with sulfonated poly(ether ether ketone) during proton exchange membrane fabrication", *J. Memb. Sci.*, 219 (2003) 113-121.
81. G. Alberti, M. Casciola, E. D'Alessandro, M. Pica, "Preparation and proton conductivity of composite ionomeric membranes obtained from gels of amorphous

zirconium phosphate sulfophenylenphosphonates in organic solvent", J. Mater. Chem., 14 (2004) 1910-1914.

AUTHOR'S VITAE

Name	Mohammad Irfan Ahmad
Father's Name	Abdul Rahman Khan
Mother's Name	Kherun Nisha
Place of Birth	Bahadurgarh in Ghaziabad district of UP in INDIA
Date of Birth	January 1 st 1980
Religion	Islam
Nationality	Indian
Education	Bachelor of Technology (B. Tech.) in Chemical Engineering Zakir Hussain College of Engineering & Technology (ZHCET) Aligarh Muslim University (AMU) Aligarh, INDIA August, 2001. Master of Science (MS) in Chemical Engineering King Fahd University of Petroleum & Minerals (KFUPM) Dhahran, Saudi Arabia April, 2004.
Research Interests	Development and characterization of solid proton conductors, polymer science and engineering, polymeric materials and characterization, development of composite polymeric membranes for fuel cell applications, catalysis, microporous and mesoporous materials.
